Effect of alkaline activator composition on the geopolymer properties produced from South African power station fly ash

Tshiamo Geneke

orcid.org/0000-0002-8279-3619

Dissertation submitted in fulfilment of the requirements for the degree
Master of Engineering in Chemical Engineering
at the North West University

Supervisor:	Professor JR Bunt
Co-supervisor:	Professor H Annegarn
Co-supervisor:	Professor SJ Piketh

Examination:	November 2021
Student number:	37109219

DECLARATION OF AUTHORSHIP

I, Tshiamo Geneke, declare that this report is a presentation of my own original work.

Whenever contributions of others are involved, every effort was made to indicate this clearly, with due reference to the literature.

No part of this work has been submitted in the past, or is being submitted, for a degree or examination at any other university or course.

Signed on this 30th day of November 2021

Tshiamo Geneke

ACKNOWLEDGEMENTS

Thank you to the following people for their contributions in this study:

My supervisor, Prof John Bunt, and co-supervisors, Prof Harold Annegarn and Prof Stuart Piketh, for the guidance and support.

My industrial mentor, Dr Kelley Reynold-Claussen, for providing me with most of the materials I've used for the study as well as personally communicated information that I was able to use in the study.

Prof Yunus Ballim and Janina Kaffee for assisting me in completing my compressive strength tests using facilities at Wits University.

Dr Ratale Matjie for your expert insights and help with interpreting my results.

Thank you to my sponsors, Eskom EPPEI, for the financial support that has enabled me to complete the study.

Lastly, a big thank you to my parents for the love and support that carried me through the study. I could not have done this without you both.

ABSTRACT

Eskom produce ~36 million tons of ash annually, of which 90 % is fly ash. Only 7 % of the ash is valorised; much lower than the global average of ~75 %. Geopolymer production from fly ash, as a Portland cement substitute, presents an opportunity to upcycle this underutilised resource.

Geopolymers require significantly lower energy inputs compared to cement production and on average emit 0.45 kg of CO_2 per kg produced whereas cement production emits 1 kg of CO_2 per kg produced. To date there has been limited research on geopolymers using South African fly ash as a feed stock. Specifically, the formulations of alkaline activator (a sodium silicate and sodium hydroxide mixture) required to produce geopolymers of the required strength and durability at competitive cost needs to be determined.

The overall aim is to develop a cost-effective geopolymer formulation using South African power station fly ash as a housing building material. The significance of this investigation is that it could valorise an underutilised waste stream from coal combustion, with significant reductions in energy and greenhouse gas emissions compared to Portland cement. Phase one determined the sodium silicate to sodium hydroxide ratio required to produce the target geopolymer strength (30 MPa) and crystalline properties. The variables studied were sodium hydroxide concentrations, curing age (3, 7 and 28 days) and curing temperature (21 and 80 ºC).

The ultimate compressive strength was found to increase by 32 % with sodium hydroxide concentrations increasing from 10 M to 15 M. A sodium silicate to sodium hydroxide ratio of 2.5 performed notably better than a ratio of 1.5. Curing at the elevated temperature significantly increased geopolymer strength compared to curing at ambient temperature. The optimum geopolymer formulation was made using 15 M sodium hydroxide, the highest sodium silicate to sodium hydroxide ratio (2.5) and cured at 80 ºC for 6 hours and achieved a compressive strength of 23 MPa.

XRF, XRD, TGA and FTIR analyses were used to characterise the geopolymers. The XRD results show a decrease in amorphous phase content from 60% in the fly ash to an average of 52 % in the geopolymers. This is primarily caused by the decrease in mullite as it is the aluminosilicate source that is decomposed by the sodium hydroxide. The Si: Al ratio, calculated from the XRF results reveal that the geopolymer with the highest compressive strength, has the highest ratio while the geopolymer with the lowest

ratio. The TGA showed an 8 – 10% weight loss between 0 and ~200ºC associated primarily with water loss.

Drying shrinkage, expansion on rewetting and soundness are required tests according to SANS 1215 for concrete masonry units. The drying shrinkage results average 600 microstrain which is out of specification by a factor of 10 and is most likely caused by a high water content. Expansion on rewetting and soundness test results, however, were well within specification.

An economic evaluation was conducted to compare with cement brick prices in industry. The geopolymer cost calculations were based on operating cost which included cost of the materials used and the cost of electricity for oven curing. The geopolymers cost between R1.50 and R1.79 per brick while cement bricks cost R2.00 per brick on average. This shows that the geopolymers are cost effective when compared to cement bricks.

Keywords: Geopolymer, fly ash, alkaline activator, cement, coal

TABLE OF CONTENTS

LIST OF FIGURES

LIST OF TABLES

LIST OF ABBREVIATIONS

SS:SH	Sodium silicate to sodium hydroxide ratio
XRD	X-Ray Diffraction
XRF	X-Ray Fluorescence
FTIR	Fourier-Transform Infrared Spectroscopy
TGA	Thermogravimetric Analysis
OPC	Ordinary Portland Cement
F_{ck}	Target mean strength
sg	Specific gravity
ρ	Density
MP	Mpumalanga
LP	Limpopo
FS	Free State

CHAPTER 1: INTRODUCTION

1.1 Overview

Chapter 1 introduces the study outlining the background of energy usage globally as well as the use of coal as a source of electricity in South Africa. This is followed by the motivation where the opportunity for using fly ash, a by-product in coal electricity generation, as a raw material in geopolymer manufacture is considered. The problem statement, aim and objectives of the study are presented in Section 1.3 followed by a general outline of the study in Section 1.4.

1.2 Background

In 2015, the global electricity consumption reached 22 471 TWh as shown in Figure 1 (International Energy Agency 2019). The industrial, residential and commercial sectors are the largest consumers of electricity globally and respectively account for 42 %, 27 % and 22 % of the global electricity consumption respectively (International Energy Agency 2019).

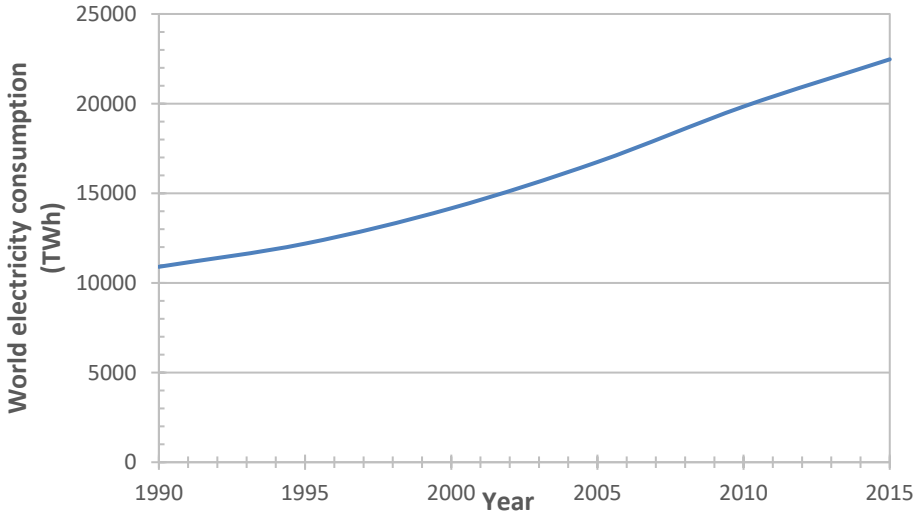

Figure 1: World electricity consumption (International Energy Agency 2019)

Approximately 5 270 Mton of fuel is used annually to meet the global demand (International Energy Agency 2016). The electricity generation mix by fuel from 1990 to 2015 is shown in Figure2, which indicated that coal accounts for 37 % of the total fuel supply.

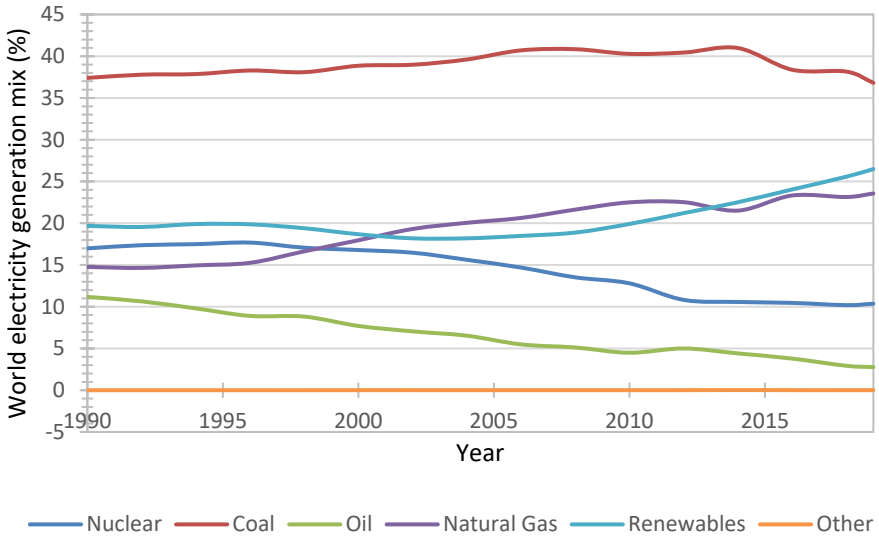

Figure 2: World electricity generation mix by fuel (International Energy Agency 2021)

South Africa currently ranks as the seventh largest producer of coal in the world (Index Mundi 2020), while contributing 3.5% towards the world's coal reserves (Ratshomo and Nembahe 2015). The coal reserves in the country are currently estimated at 53 billion tons (Eskom 2016). Due to abundant reserves, the lack of comparable alternatives and relative ease to transport, store and use (Ratshomo and Nembahe 2015), coal is the primary source of energy in South Africa. As shown in Figure 3, coal accounts for 92% of the country's electricity supply. Eskom, the state-owned and primary electricity producer in South Africa, estimates that the country's coal reserves will last about 200 years at the current consumption rate. Other than being used as the primary energy source in electricity production, coal mining in South Africa plays a key role in the country's chemicals industry and especially in the steelmaking industry (Ratshomo and Nembahe 2015). The distribution of saleable coal to different industries in South Africa is illustrated in Figure 4. Although the country is seeking to diversify energy sources, coal is expected to continue to play a major role in the foreseeable future (Department of Mineral Resources and Energy (DMRE) 2019).

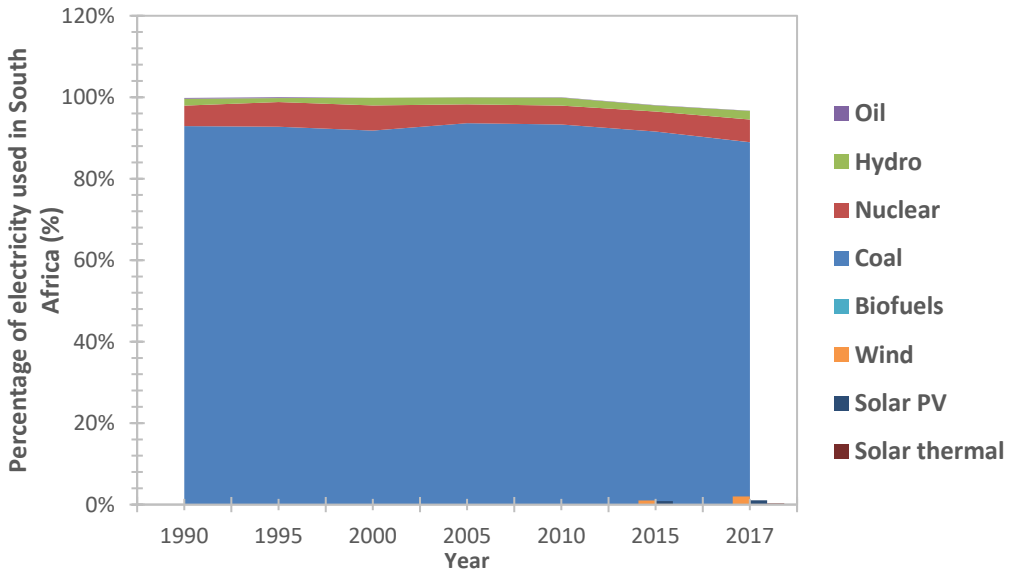

Figure 3: Electricity source percentage in South Africa (International Energy Agency 2019)

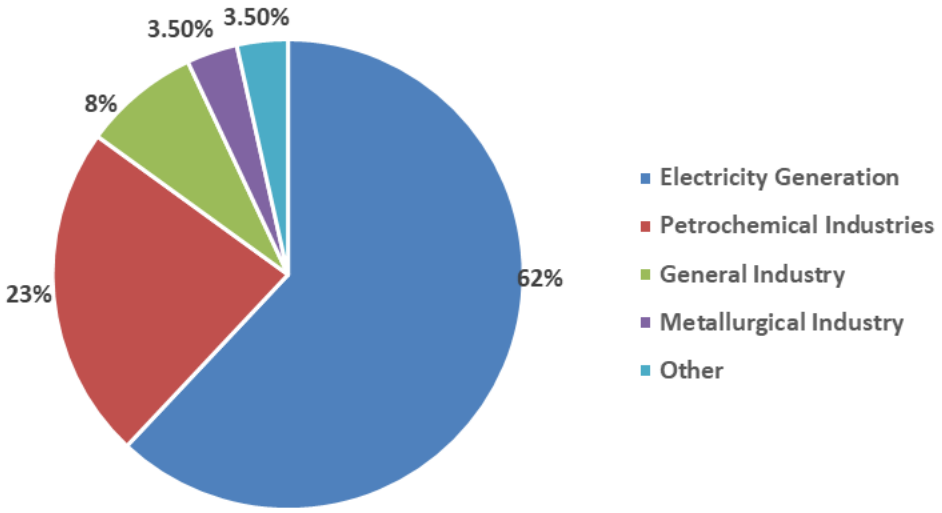

Figure 4: Saleable coal distribution in South Africa (International Energy Agency 2019)

The transition away from coal has been met with much resistance. In 2018, the National Union of Metalworkers of South Africa (Numsa) submitted a court interdict to restrict the signing up of renewable energy power producers citing the negative impacts that moving away from coal energy would have on job security (Fakir 2018) as coal mining accounts for 0.5% of the total employment in South Africa (McSweeney and Timperley 2018). South Africa is also economically dependent of coal mining as it is the 5th largest exporter of coal in the world, making up 12% of the country's exports, and is the backbone of the mining industry that

contributes to 8% of the GDP (McSweeney and Timperley 2018). The potential economic loss from these industries discourages a shift to renewable energy use.

As a result of the country's rich coal deposits and its accessibility, electricity is primarily produced from coal (Department of Energy 2020). Such a strong dependence on coal results in the coal energy supply industry accounting for 80% of emissions in South Africa (McSweeney and Timperley 2018). Consequently, South Africa ranks as the 14th largest CO_2 atmospheric emissions contributor and has the 7th largest fleet of coal fired plants in the world despite the fact that it has a smaller economy compared to the other top emitters (International Energy Agency 2017). South Africa's high carbon intensity is illustrated in Figure 5 compared to the two largest CO_2 emission contributors, namely, China and the United States. The South African economy has an energy consumption per unit of GDP that is more than double the global average, making it a highly energy-intensive economy (McSweeney and Timperley 2018).

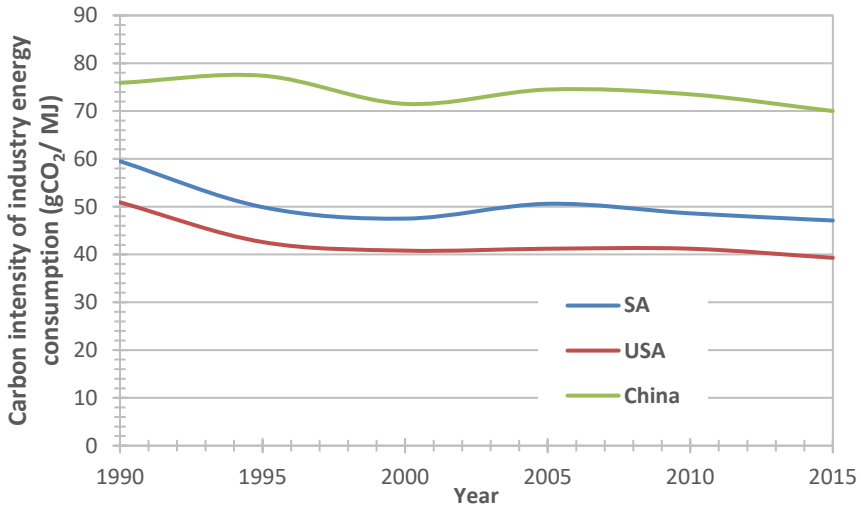

Figure 5: Carbon intensity SA vs China and USA (International Energy Agency 2019)

1.3 Motivation

Apart from CO_2, the combustion of coal for electricity production is also plagued by the formation of other pollutants, of which fly ash remains a major concern. In 2001, 68 million tons of fly ash were produced globally (Federal Highway Administration 2017) and production increased to 1.2 billion tons of fly ash in 2016 (Zierold and Odoh 2020). On average Eskom produces approximately 36 million tons of ash from 120 million tons of coal consumed, of which 90% is fly ash (Eskom 2021). Eskom only sells about 7% of the ash produced (Department of Environmental Affairs 2018), while the top 10 producing countries of fly ash utilise on average

75% of the fly ash produced (Dhadse, Kumari and Bhagia 2008). Furthermore, the performance of the fly ash emissions control devices at South Africa's ageing coal-powered power stations are not sufficient in many cases to meet the particular matter (PM) emissions standards as stipulated in the 2013 amendments to the National Environmental Management: Air Quality Act no. 39 of 2004.

In developing countries such as South Africa, emissions from the domestic burning of solid fuels such as wood and coal for cooking and space heating purposes in dense, low-income settlements further contributes to reducing the ambient air quality. Furthermore, many such dense, low-income settlements are in close proximity to the coal-fired power plants. In terms of poor air quality, these communities are therefore the most heavily impacted (Staden 2019). One possible solution that can contribute to lowering the emissions from such activities, and thereby improve the local ambient air quality in these communities is to develop efficient coal stoves that can be incorporated in low cost- and thermally efficient dwellings. This objective forms part of the national carbon offset program (Department of National Treasury 2014), which aims to offset fly ash and other pollutant emissions from Eskom's coal-fired power stations, thereby limiting the impact of these emissions, by reducing domestic emissions resulting from the burning of solid fuels. The widespread implementation of such energy and thermally efficient dwellings coupled with low emissions coal stoves would not only improve the local ambient air quality of in the targeted settlements but also the living conditions of the residents.

The construction of cost-effective and thermally efficient dwellings relies mostly on the availability of novel, low-cost building materials. One possible solution would be geopolymer-based building materials that can be manufactured using fly ash captured from the flue gas streams of coal-fired power stations. In this respect, structurally sound and thermally resistant geopolymer building materials can be applied in two ways in such energy and thermally efficient dwellings. The first is as an insulator or refractory in the novel semi-continuous coal stoves that are being developed (Meyer 2020) to allow safe and efficient operation. The second way in which a fly ash based geopolymer can be used in energy efficient dwellings is as a low-cost building material that also functions as an insulator to help regulate indoor temperatures. In 2015, it was reported that approximately 14.1 % of the South African population lived in informal dwellings while 6.9 % lived in traditional dwellings (Statistics South Africa 2016). Informal dwellings are defined as structures that have not been built according to approved plans. The dwellings are often constructed using materials such as plastic, cardboard,

untreated wood and corrugated iron (Socio-Economic Rights Institute of South Africa 2018). As a result of the use of these cheap and in some cases highly flammable materials, 46.2 % of fires in the country between 1995 and 2004 were in informal settlements. These makeshift settlements are therefore also poorly insulated, which necessitates the combustion of large quantities of coal, wood and other solid fuels in the dilapidated and inefficient coal stoves often used by the residents to keep warm during the winter months.

According to the latest statistics of 2015, 14.4 % of South African households lived in Reconstructed and Development Programme (RDP) houses (Statistics South Africa 2016) which are state-funded houses that are provided to low-income families (GroundUp 2017). Although these RDP houses generally offer much improved conditions compared to other makeshift dwellings, 14.2 % of RDP households reported weak or very weak walls and 13.8 % reported weak or very weak roofs (Statistics South Africa 2016).

These challenges present an opportunity to research the use of fly-ash, which is currently underutilised in South Africa, as a raw material to produce fly ash based geopolymer that can function as a refractory and building material to construct cost-efficient and thermally efficient dwellings. A co-benefit of using fly ash to produce geopolymers that can be applied as low-cost building materials, is that it can contribute to lowering the CO_2 emissions related to the production of cement. Cement production is energy intensive and a large contributor to global warming and climate change due to its significant carbon footprint. In 2017, China, the largest cement producer in the world, produced more than 1 500 million tons of CO_2 from cement making (Rodgers 2018). About a kilogram of CO_2 is emitted for each kilogram of cement produced, which translates to approximately 3 to 4 billion tons of global CO_2 emission annually (Chandler 2019). Although much is being done to manage the toxicity of the industry, such as substituting fuels, the carbon dioxide emissions released in the process are unavoidable primarily due to the use of limestone as a raw material. The production of fly ash based geopolymers generally have an emissions range of 0.1 to 0.8 kg of CO_2 per kg of geopolymer produced depending on the mixture used (Wang, Aravinthan and Omar 2009). Using fly ash for the manufacture of geopolymers that can compete with cement is therefore advantageous to also offset CO_2 emissions from coal-derived electricity production.

1.4 Problem statement, Aim and Objectives

1.4.1 Problem statement

The development of robust fly ash based geopolymers is limited by the lack of understanding of the geopolymerisation process and the issue of long-term durability of the geopolymer once produced. The alkaline activator used in the process is one aspect that has hindered the implementation of geopolymers derived from fly ash. For example, the optimal alkaline activator to fly ash ratio varies depending on the fly ash composition and physical properties. Consequently, the composition and relative amount of the alkaline activator used can influence the geopolymerisation process and the resulting geopolymer properties. In this respect, sodium silicate plays a critical role in the kind of geopolymer matrix that is formed, the applications that the geopolymer can be used for and, by virtue of it being the costliest component in the process, also affects the cost efficiency of the process.

1.4.2 Aim

This study represents a first step towards developing a geopolymer formulation based on South African power station fly ash that would be suitable for the production of cost-effective geopolymer building and refractory material. Accordingly, the aim of this study is to develop an effective sodium silicate-based alkaline activator that would enable the environmentally friendly and cost-effective production of high quality geopolymer building materials based on South African power station fly ash.

1.4.3 Objectives

The following objectives have been identified to assist in achieving the aim of this study. These are namely to:

a) Characterise the fly ash.
b) Asses the effects of the composition of the alkaline activator by varying the sodium hydroxide to sodium silicate ratio on the formed geopolymers and compare the geopolymer properties to that reported in the literature as well as to current industry standards.
c) Identify an optimal alkaline activator to fly ash ratio that results in a geopolymer that is cost-efficient and durable.

1.5 Scope and limitations

This study focuses on finding a geopolymer mix design that results in a geopolymer that is comparable to cement bricks. The factors that were varied are curing conditions and time and the sodium silicate to hydroxide ratio.

The dry materials, fly and aggregates were kept constant for each geopolymer according to optimal ratios from literature. The fly ash used was from one coal power station, Eskom Kriel, as the ash at this station typically has fly ash with a high calcium source content and would likely produce a better performing geopolymer than fly ash with low calcium content. Since the curing oven used was permanently set to 80°C, this is the only oven curing temperature that was investigated. Curing plays an important role in the properties of a geopolymer thus further experiments on this is a limitation on the study.

1.6 Study outline

The outline, illustrated in Figure 6, starts with Chapter 1 which introduces the study, giving background on the study and the motivation thereof. In Chapter 2 the literature relevant to the study is assessed. This includes the literature on the geopolymerisation process, geopolymer formulations from other studies and the reported characterisation results of geopolymers. The methodology used in the study is covered in Chapter 3. The compressive strength results are reported and discussed in Chapter 4 as well as the characterisation results relating to the chemistry of the geopolymers. The economic evaluation is reported in Chapter 5. Finally, Chapter 6 concludes the study highlighting the recommendations for future studies.

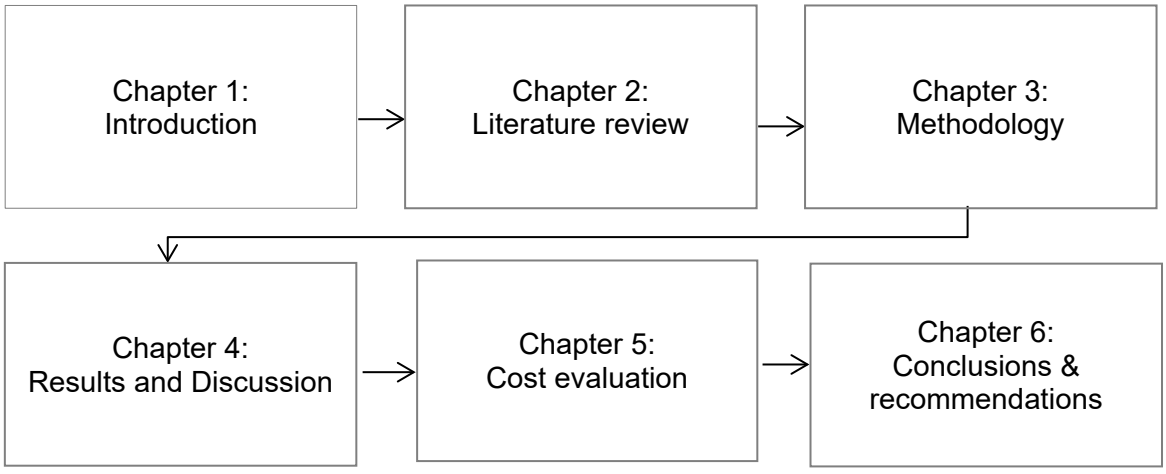

Figure 6: Flow of the study

CHAPTER 2: LITERATURE REVIEW

2.1 Overview

This section of the study reviews the literature that is relevant to the geopolymerisation process. First, the geopolymerisation process is discussed, where a brief background on the origins of the process and the reactions that take place are given. Following this, the function that the starting materials, fly ash and the alkaline activator, play in making a fly-ash based geopolymer is presented. Six geopolymer formulations are assessed in order to select the best experimental route for the study and finally, the results from the previous studies of geopolymer product characterization techniques are reported on.

2.2 Geopolymerisation process

In 1975, Joseph Davidovits proposed a binder produced by mixing sodium silicate, sodium hydroxide and an aluminosilicate (Davidovits 2008) and these binders were termed 'geopolymers.' A geopolymer is a type of amorphous aluminosilicate cementitious material (Mustafa Al Bakri, et al. 2011) that has similar binding performances as Portland cement (Zhuang, et al. 2016) and geopolymerisation is the process of alkali activation on the aluminosilicate to create a geopolymer.

Geopolymerisation depends on the ability of the aluminium ion to induce chemical changes on the silica backbone of the aluminosilicate (Mustafa Al Bakri, et al. 2011). The reaction produces a three-dimensional polymeric chain and ring structure containing Si-O-Al-O bonds (Patankar, Ghugal and Jamkar 2014).

The reactions that occur during geopolymerisation are complex and not well understood. However, a simplified version of the process can be summarised as follows (Zhuang, et al. 2016):

a) The fly ash decomposes and the Si and Al atoms dissolve by the action of hydroxide ions (alkali activation).
b) The silica and alumina species nucleate and form aluminosilicate oligomers.
c) Through oligomerisation, the polysialate framework is formed. The sialate network consists of SiO_4 and AlO_4 tetrahedral linked by sharing oxygen atoms.
d) The framework polymerizes and a geopolymer paste is formed.
e) The paste cures and the geopolymer concrete is produced.

The reactions observed are shown in the reaction equations given in Equation (1) and (2) (Singh 2018):

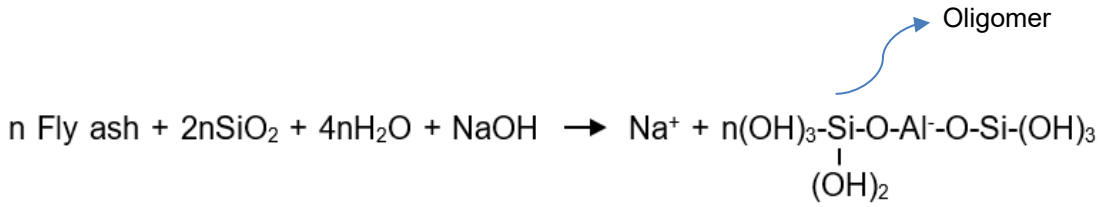

(1)

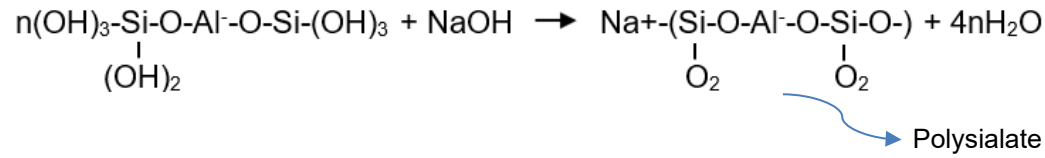

(2)

2.2.1 Curing and thermal resistance

Curing at elevated temperatures is a necessary step in producing strong geopolymers since fly generally has low reactivity. When curing at room temperature, fly ash does not decompose well, restricting the ability of the geopolymerisation process to continue (Zhuang, et al. 2016). Curing between 60 and 90 °C increases the reactivity of the fly ash and allows for the geopolymerisation process to be complete, while excessive curing at temperatures higher than 80 °C breaks down the granular structure of the geopolymer and results in dehydration and shrinkage which decreases the compressive strength (Zhuang, et al. 2016).

Curing for long periods of time (6 hours – 28 days) promotes the formation of a denser geopolymer. Higher temperatures during curing increase the compressive strength since water is removed resulting in fewer pores and a denser structure (Zhuang, et al. 2016).

When the geopolymer is exposed to elevated temperatures, shrinking occurs as water vaporises from the structure (Zhuang, et al. 2016). Geopolymers have a smaller temperature gradient than OPC concrete. The average residual strength of OPC under 650 °C and 1 000 °C is 52 % and 16 % while geopolymer residual strengths at the same temperatures are 82 % and 29 % respectively (Zhuang, et al. 2016), resulting in only minor surface cracking occurring of geopolymer concrete at 800 – 1 000 °C.

2.3 Starting materials

2.3.1 Fly ash

The overall process of generating electricity from coal, and fly ash as a result, is as follows: First, coal is burnt in a boiler to produce steam. Under high pressure, the steam flows into a

turbine that spins to create electricity. Finally, the steam is cooled and condenses into water which is then returned to the boiler where it will be reused. The coal is burnt by blowing air into the boilers combustion chamber which instantly ignites it. The ignition generates heat and a mineral residue. Boiler tubes extract the heat and the flue gas produced upon burning condenses. This causes the mineral residue to form two types of ash: fly ash and bottom/ slag ash. The slag ash falls to the bottom of the chamber while the fly ash, which is a finer alumina-silicate solid particle residue, remains in the flue gas and is removed by particulate emission control devices.

As shown in Equation 1, fly ash can be used as the aluminosilicate source in geopolymerisation. The composition of fly ash depends on the coal that is combusted, however the general components include SiO_2, AlO_3, CaO and Fe_2O_3 (Zhuang, et al. 2016). The silica content in fly ash varies between 40 to 60 wt % while the alumina content ranges between 20 and 30 % (Mustafa Al Bakri, et al. 2011). Being a by-product, it is highly likely for fly ash to contain toxic elements. The trace elements typically observed are titanium, vanadium, manganese, cobalt, arsenic, strontium, molybdenum, lead and mercury (Zhuang, et al. 2016).

Fly ash is characterised based on the calcium oxide contents (Zhuang, et al. 2016). Accordingly, two classes exist: Class C and Class F. Class C fly ash has a high calcium oxide content (between 20 wt% to 50 wt%) while Class F has a low content (less than 10 wt%). The class of the fly ash plays a role in the type of geopolymer that is produced since a high calcium source fly ash shortens the setting time of the geopolymer paste resulting in a less porous geopolymer which ultimately creates a stronger product.

Other significant properties of the fly ash to consider are the Si: Al ratio and fineness, since these properties affect the strength of the geopolymer (Patankar, Ghugal and Jamkar 2014). The Si: Al ratio of the fly ash also affects the porosity of the final structure (Zhuang, et al. 2016).

Fly ash samples from three provinces in South Africa: Mpumalanga (MP), Limpopo (LP) and Free State (FS) are presented in Table 1 to assess the composition of fly ash in the country. These three provinces respectively account for 81%, 11% and 6% of the coal deposits in the country (Garside 2020).

The predominant compounds in the ash are SiO_2, Al_2O_3 and CaO which average 52.5, 26.8 and 6.10 wt% respectively. The low calcium oxide content in the ash makes the ash a Class F type. Mpumalanga ash reaches 10.1 and 13.0 wt% of CaO, which affects the compressive

strength of the geopolymer positively. The average Si: Al ratio of the ash is 5.34. According to (Mustafa Al Bakri, et al. 2011), ash with this Si: Al ratio will result in a geopolymer that can doubly function as a building material and fire-resistant material.

Table 1: Typical South African ash XRD results

	(A. C. Collins 2019)			(Ribberink 2018)			
Sample	**1 (MP)**	**2 (MP)**	**3 (MP)**	**4 (FS)**	**5 (LP)**	**6 (MP)**	**Average**
SiO_2	63.2	41.6	55.2	57.2	58.5	55.3	52.5
Al_2O_3	28.5	25.2	25.9	30.4	27.2	29.0	26.8
CaO	1.5	13.0	5.1	4.3	3.4	5.4	6.1
Fe_2O_3	2.0	5.7	5.5	3.6	6.5	5.5	4.8
K_2O	0.7	1.1	0.4	0.7	0.8	0.7	2.9
SO_3	1.5	7.6	4.3	0.3	0.5	0.4	2.8
TiO_2	1.5	1.8	1.3	1.5	1.3	1.6	1.5
MgO	0.8	3.2	1.8	1.0	1.0	1.3	1.7
P_2O_5	0.1	0.3	0.1	0.3	0.4	0.4	0.3
MnO	-	0.1	0.1	1.0	0.1	0.1	0.3
SrO	-	0.3	0.1	-	-	-	0.2
BaO	-	0.2	0.1	-	-	-	0.2
Na_2O	-	-	-	0.4	0.1	0.1	0.1
Cr_2O_3	0.1	-	0.0	-	-	-	0.0
Si: Al	**6.1**	**4.5**	**5.8**	**5.1**	**5.8**	**5.2**	**5.3**

The amount of silicon and aluminium ions were calculated by multiplying the molecular percentages of each in the SiO_2 and Al_2O_3 respectively by the amount shown in the table. The silicon was then divided by the aluminium to get the Si: Al ratio.

2.3.2 Alkaline activator

The activator normally consists of an alkaline hydroxide and an alkaline silicate. The type and concentration of the alkaline solution influences how many Si^{4+} and Al^{3+} ions are released from the fly ash (Zhuang, et al. 2016). The higher the concentration of the solution is, the higher the compressive strength of the resulting geopolymer. Studies have shown that the optimum hydroxide to silicate ratio ranges between 0.67 to 2.50, however, a ratio of 2.50 is most commonly used (Mustafa Al Bakri, et al. 2011).

In the alkali activation process, shown in Equation 1 above, the molecules on the surface form a gel (Mustafa Al Bakri, et al. 2011) due to the reaction of Si^{4+} and Al^{3+} with Ca^{2+}. Three types

of gels may form in the presence of water: calcium silicate hydrate gel ($CaO\text{-}SiO_2\text{-}H_2O$), calcium aluminate hydrate gel ($CaO\text{-}Al_2O_3\text{-}H_2O$) or calcium aluminium silicate gel ($CaO\text{-}Al_2O_3\text{-}SiO_2\text{-}H_2O$) depending on the composition of the fly ash that is used and the conditions of reaction (Zhuang, et al. 2016), however, calcium aluminium silicate gel is most often formed (Mustafa Al Bakri, et al. 2011). The formation of $CaO\text{-}Al_2O_3\text{-}SiO_2\text{-}H_2O$ and $CaO\text{-}Al_2O_3\text{-}H_2O$ leads to a shorter setting time, a decrease in geopolymer porosity (Zhuang, et al. 2016) and subsequently an increase in the compressive strength of the geopolymer.

2.3.3 Alkaline hydroxide

The type and concentration of the alkaline hydroxide used affects the degree of decomposition of the fly ash and release of Si^{4+} and Al^{3+} which in turn influences the final structure of the geopolymer. NaOH is typically used for the process, however KOH and the combination of the two are also used (Mustafa Al Bakri, et al. 2011).

NaOH generally leaches more Si^{4+} and Al^{3+} ions than KOH, accelerating the geopolymerisation reaction and produces a rougher textured geopolymer (Mustafa Al Bakri, et al. 2011). Si^{4+} and Al^{3+} ions are more soluble in NaOH than KOH (Zhuang, et al. 2016) which makes NaOH a more preferred alkaline source. On the other hand, since the K^+ is generally larger than the Na^+, it leads to a higher degree of polymerization (Singh 2018).

The concentration of the solution must be no less than 10 mol/L (Zhuang, et al. 2016), otherwise the decomposition of the fly ash does not occur. Higher concentrations would also result in faster polycondensation, while the compressive strength of the resulting geopolymer has been shown to be directly proportional to the concentration of sodium hydroxide (Patankar, Ghugal and Jamkar 2014).

2.3.4 Alkaline silicate

The alkaline silicate acts as part of the activator in the alkaline solution. It has been shown that reactions occur much faster when a soluble silicate (Na_2SiO_3 or K_2SiO_3) is added compared to when only alkaline hydroxides are used (Mustafa Al Bakri, et al. 2011). The formation of gel is observed as soon as the solution contacts the fly ash.

The silicate introduces more Si atoms into the solution which increases the Si: Al ratio. A high ratio increases the number of -Si-O-Si- bonds, as opposed to the -Si-O-Al- and -Al-O-Al- bonds that can be formed (Zhuang, et al. 2016), which are the strongest bonds. The stronger bonds therefore result in a higher compressive strength in the geopolymer. A high Si: Al ratio also

results in a lower porosity and a finer pore system (Zhuang, et al. 2016). The decrease in porosity increases the weight and compressive strength of the geopolymer, while increasing the thermal conductivity. The application of the geopolymer depends on the Si: Al ratio in the polysialate. A low ratio (between 1 and 3) results in a rigid 3D network that can be used as a building material (Mustafa Al Bakri, et al. 2011), while ratios between 3 and 35 can be used for fire resistance and insulation applications as seen in Table 2.

Table 2: Application according to Si: Al ratio (Mustafa Al Bakri, et al. 2011)

Si: Al ratio	Application
1	Bricks, ceramics, fire protection
2	Low carbon dioxide concrete, toxic waste confinement
3	Heat resistance, foundry equipment, aeronautics tooling
>3	Sealants from 200ºC to 1 000ºC, aeronautics tooling
20 - 35	Fire and heat resistance

2.4 Geopolymer formulations

Various experimental geopolymer formulations have been presented on the production of fly ash based geopolymers. The primary property that most designs focus on is the compressive strength of the geopolymer. Although design mixes and results vary greatly, this part of the literature seeks to find the optimal geopolymer formulations from six proposed designs. The fly ash composition is discussed if included in the original research paper.

2.4.1 Formulation 1 (Jha and Budhamagar 2012)

This formulation was studied because it investigates the relationship between the sodium hydroxide concentration, the addition of sodium silicate and the curing time against the compressive strength. In geopolymer formulation 1 (F1), fifteen samples were tested. The mechanical property tested was compressive strength using a MARTO testing machine. The following parameters were varied: concentration of the sodium hydroxide, the amount of sodium silicate added and the curing time.

2.4.1.1 Sodium hydroxide concentration

The sodium hydroxide was added to the fly ash without the addition of sodium silicate. The solution and fly ash were blended manually for 2 minutes and the moulds are then allowed to cure in an oven for 4 hours at 40°C before being tested. Six samples in total were tested for this test, one for each NaOH concentration.

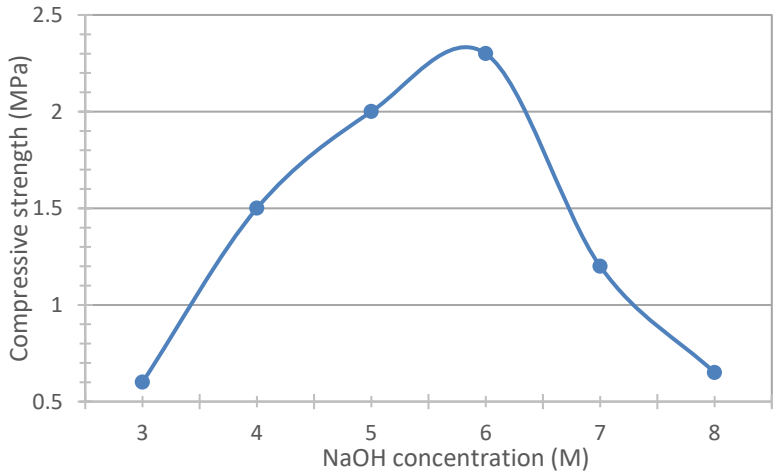

Figure 7: NaOH concentration vs compressive strength – F1 (Jha and Budhamagar 2012)

As seen in Figure 7 above, the compressive strength initially increases, peaks at 6 M and then decreases thereafter. The initial increase in compressive strength is attributed to the increase in OH^- ions which allow the silicate and aluminate to dissolve. When the concentration increases past 6 M, a highly alkaline environment reduces the connectivity of the silicate anions and results in poor polymerization. The unreacted NaOH reacted with carbon in the atmosphere to form sodium carbonate, further contributing to poor polymerisation.

The curing conditions of the geopolymers were generally low. Since the geopolymers were cured at 40 °C for 4 hours, it is possible that the geopolymers has not fully cured thus impacting the strength results shown. Additionally, the kind of fly ash, which was not mentioned in the paper, may have an effect on the results since the sodium hydroxide dissolves the ash.

2.4.1.2 Sodium silicate addition

The sodium silicate is treated with 6 M NaOH since this was the optimal concentration found in 2.4.1.1 above. The sodium hydroxide and sodium silicate are mixed together in a beaker before being blended with the fly ash. The mixture is then moulded and allowed to cure for 6 days in an oven at 40°C.

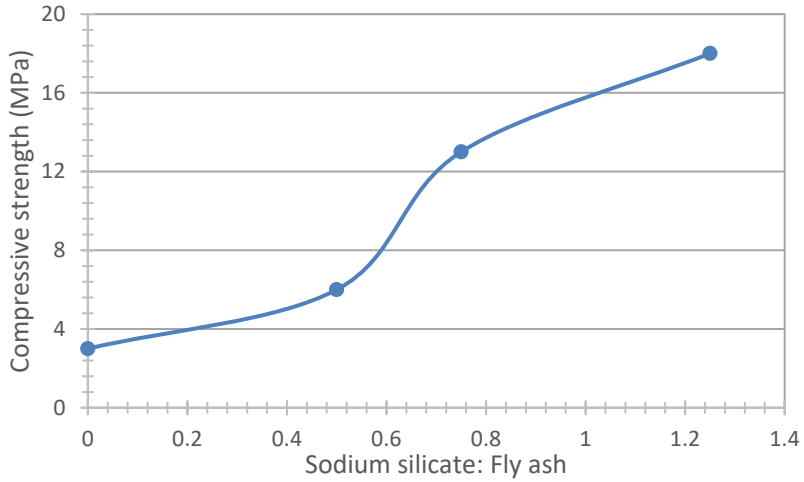

Figure 8: Sodium silicate: Fly ash ratio vs compressive strength - F1 (Jha and Budhamagar 2012)

As illustrated in Figure 8, in general the compressive strength increases as the mass ratio of sodium silicate to fly ash. The increase in compressive strength is attributed to the higher concentration of silicates aiding the ion-pair formation, which results in longer chain silicate oligomers and geopolymer precursors.

Between a sodium silicate to fly ash ratio of 0.5 and 0.7, there is a threshold value that results in a notable increase in compressive strength, while after a 0.8 ratio, the compressive strength plateaus and the benefit of increasing the ratio further lessens.

2.4.1.3 Curing time

A NaOH concentration of 6 M and the weight ratio of sodium silicate to fly ash of 1.25 were kept constant in analysing the effect of curing as these were previously tested to be the optimal conditions and all other factors were kept constant. After mixing, six moulds were allowed to cure for 5 to 15 days in an oven at 40°C for four hours after the removal of air bubbles by an ultrasonicator. Only one specimen was test for each data point.

The data in Figure 9 suggests an increase in compressive strength as curing time increases. A curing time increase at low temperatures is preferable due to the slow evaporation of the water in the geopolymer which prevents the geopolymer from cracking.

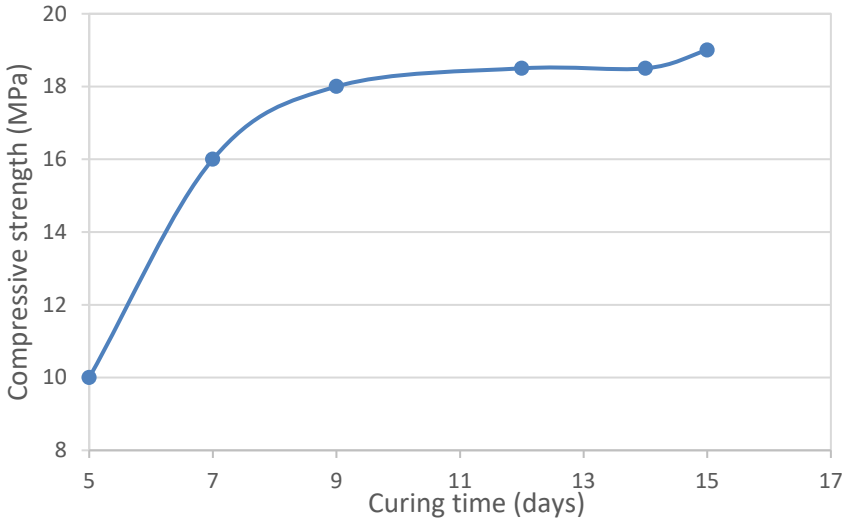

Figure 9: Curing time vs compressive strength - F1 (Jha and Budhamagar 2012)

2.4.1.4 Formulation 1 conclusions

- The optimal NaOH molarity is 6 M
- The highest sodium silicate: fly ash weight ratio tested, 1.2, gives the highest compressive strength
- The compressive strength increases as the curing time increases.

2.4.2 Formulation 2 (Bellum, et al. 2019)

In this paper, the mechanical properties investigated are compressive strength, split tensile and flexural strength at different curing conditions. The fly ash (Class F) and ground granulated blast furnace slag (GGBFS) were obtained from the National Thermal Power Corporation in India. The geopolymer produced is placed in an oven for 24-hour hours and cured under sunlight for 3, 7, 4 and 28 days. This formulation was investigated because the fly ash class is the same as that of South African ash (Class F) and other mechanical properties, flexural and split tensile strength, are investigated as opposed to just compressive strength. The formulation will also provide more information on the influence of GGBFS in geopolymers.

The Scanning Electron Microscope (SEM) images of the fly ash indicate a spherical shape with a particle size range of 14 to 23 µm while the GGBFS particles are tetrahedron with a particle size range of 2 to 6 µm. The specific gravity of the fly ash and GGBFS are both 2.1 g/cm^3.

The alkaline hydroxide was prepared by mixing NaOH pellets with distilled water (pH 7.11) for approximately 9 minutes. Different NaOH molarities are tested and these solutions are then mixed with the sodium silicate solution. The Na_2SiO_3/NaOH ratio is kept constant at 2.5.

The addition of fine and coarse aggregates was also tested and the specifications of these are shown in Table 3. Superplasticizer, a sulphonated naphthalene-based water reducer, was added at different percentages to improve workability.

Table 3: Fine and coarse aggregate parameters – F2

	Fine aggregates	Coarse aggregates
Specific gravity (g/cm^3)	2.48	6.97
Fineness modulus (%/%)	2.20	2.71
Maximum size (mm)		20

The ratios that were kept consistent throughout the experiments are shown in Table 4. 'Cementitious material' refers to the mixture of fly ash and GGBFS and is also referred to as ash 'binder'.

Table 4: Constant material proportions – F2

Materials	Ratio
Coarse: fine aggregates	2.33
Alkaline liquid: Cementitious material	0.35
Na_2SiO_3 : NaOH	2.50
Super plasticizer: Cementitious material	0.04

Three parameters were varied: NaOH molarity, curing time and fly ash to GGBFS percentage proportions. The NaOH molarities tested are: 6, 8, 10, 12 and 14 M. Cementitious material proportions were varied by the following fly ash: GGBFS ratios: 70:30, 60:40, 50:50, 40:60 and 30:70. These ratios were manufactured with NaOH molarities of 6, 8, 10, 12 and 14 M respectively. One specimen was tested for each data point.

2.4.2.1 Compressive strength

The maximum failure load was tested using a compressive test machine. This was divided by the area of the specimen to get the compressive strength as seen in Equation 3. The moulds

used were cubes of 150 mm which were placed in an oven for 24 hours at 70°C. Figure 4 illustrates the compressive strength against the differing molarities and curing times.

$$Compressive\ strength = \frac{Maximum\ failure\ load\ (N)}{Area\ of\ the\ specimen\ (mm^2)} \quad (3)$$

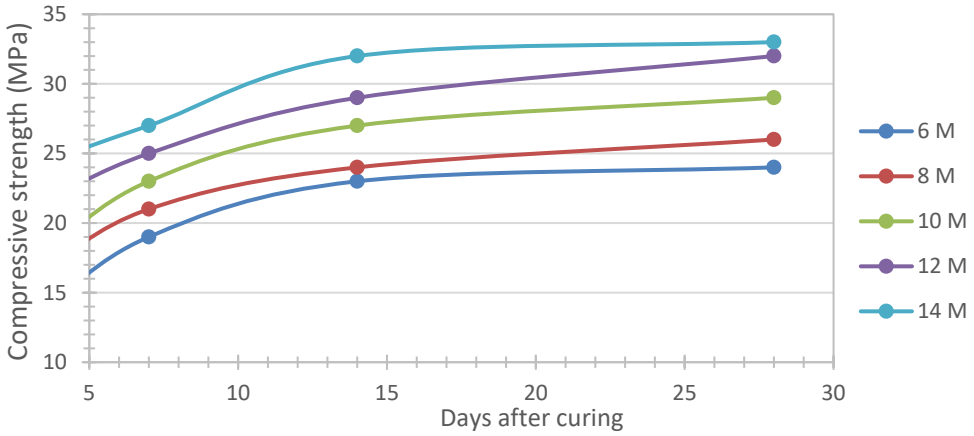

Figure 10: Curing time and NaOH molarity vs compressive strength - F2 (Bellum, et al. 2019)

Figure 10 shows that the influence of the NaOH concentration and curing time. Increasing the concentration from 6 to 14 M, improves the compressive strength by 35 % on average. A longer curing time also increases the compressive strength however after day 12 the curves plateau indicating that the benefit of curing for a longer period does not have must of a benefit.

The compressive strength for the sample at 24 days made with GGBFS to fly ash ratio of 60:40 and a NaOH concentration of 12 M is 32 MPa, while the sample with a ratio of 70:30 and concentration of 14 M is 33 MPa, which is a difference of 3 %. This shows that a decrease in the GGBFS content at a lower NaOH concentration can yield similar results to that of a specimen a higher GGBFS content and higher NaOH concentration.

2.4.2.2 Split tensile strength

The split tensile strength (Figure 11) was calculated using Equation 4. Cylindrical moulds with a diameter of 150 mm and length of 300 mm were used as moulds and the NaOH molarity and curing time was changed similarly to the compressive strength tests seen above. The graph illustrates that flexural strength increases as both NaOH and curing time increase.

$$Split\ tensile\ strength\ (MPa) = \frac{2P}{\pi DL} \quad (4)$$

where P = Maximum load applied (N), and D = Cylinder diameter (mm).

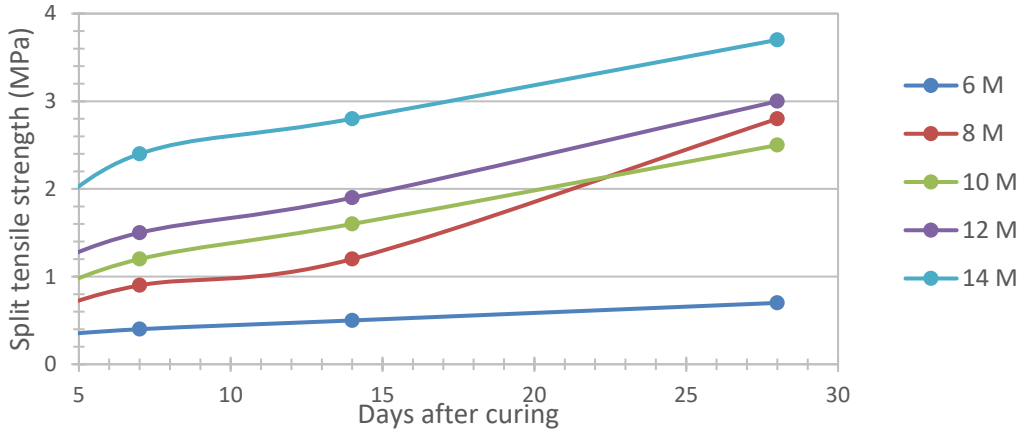

Figure 11: Curing time and NaOH molarity vs Split tensile strength - F2 (Bellum, et al. 2019)

Figure 11 shows the split tensile strength of the specimens. A higher concentration of NaOH and a longer curing time results in an improved split tensile strength. The graph shows that at 22 days after oven curing, the strength with a GGBFS to fly ash ratio of 40:60 and a NaOH concentration of 8 M exceeds the strength of the specimen with a ratio of 50:50 and concentration of 10 M and is 6 % less than the specimen with a GGBFS to fly ash ratio of 60:40 and a NaOH concentration of 12 M. This illustrates that the more GGBFS is contained in the geopolymers, the lower the split tensile strength will be despite the addition of a more concentrated NaOH.

2.4.2.3 Flexural strength

Flexural strength is a tensile strength test that measures the ability of a specimen to resist bending (Nevada Ready Mix 2021). The moulds for this test are 100 x 100 x 500 mm third point prisms/ beams. A flexural test machine is used to find the maximum force applied. The NaOH concentration and curing time is varied again and the flexural strength is determined as shown in Figure 12.

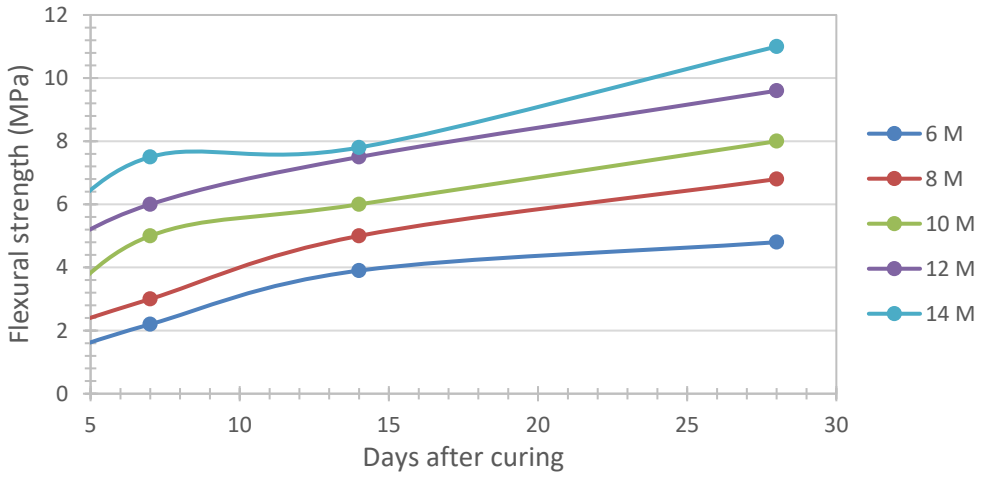

Figure 12: Curing time and NaOH molarity vs Flexural strength - F2 (Bellum, et al. 2019)

Figure 12, which illustrates the flexural strength of the geopolymers shown that an increasing in curing time and NaOH concentration also increases the flexural strength, similarly to the results seen for compressive and split tensile strength.

2.4.2.4 Formulation 2 conclusions

- The compressive, split tensile and flexural strength are highest after 28 days. Thus, a higher curing time result in a stronger geopolymer.
- The maximum compressive, split tensile and flexural strengths are obtained at a NaOH concentration of 14 M which is the highest NaOH concentration analysed.
- The increase in NaOH concentration from 8 M to 14 M results in compressive strength increase of 33%, 26% increase in split tensile strength and 42.5% increase in flexural strength.
- The lower GGBFS content manufactured with a low concentration NaOH increases the mechanical strength indicating that GGBFS decrease mechanical strength.

2.4.3 Formulation 3 (Ferdous, Kayali and Khennane 2013)

The fly ash was obtained from the Boral Company, Australia. The compounds of SiO_2, Al_2O_3 and Fe_2O_3 make up 93% of the fly ash composition (Table 5). The calcium oxide composition is 1.97%, and the fly ash is a Class F type. The values presented in this study are based on a total geopolymer volume of 1 m^3. Similarly to Formulation 2, this paper is selected because it uses Class F fly ash which is relevant to the study. This paper also included a step-by-step procedure for manufacturing the geopolymer which would give guidance for the study.

Table 5: Formulation 3 fly ash composition

Compound	SiO_2	CaO	Al_2O_3	MgO	Fe_2O_3	SO_3	TiO_2	Na_2O	K_2O
Oxide (%)	62.2	1.97	27.2	0.40	3.23	0.07	1.06	0.30	0.89

The properties of the materials used are illustrated in Table 6. The absorption capacity is the amount of water the oven-dried aggregates can absorb water (Sacramento State 2019) and the moisture content is the percentage of moisture in the aggregates before oven drying.

Table 6: Material properties - F3

Material	Specific gravity (g/cm^3)	Adsorption capacity (% of Oven Dry)	Moisture content (% of Oven Dry)
14 mm aggregates	2.65	0.675	0.254
10 mm aggregates	2.63	0.772	0.326
7 mm aggregates	2.59	1.38	0.445
Fine aggregate	2.06	1.17	0.202
Fly ash	1.52	-	-
Na_2SiO_3 solution	1.08	-	-

The alkaline liquid is a combination of Na_2SiO_3 and NaOH with a molarity of 16 M. The Na_2SiO_3 was obtained from IMCD Australia Limited and the sodium hydroxide was prepared by dissolving NaOH pellets in water. A carboxylic ether polymer-based superplasticiser (ADVA 142) was used to improve workability.

2.4.3.1 Formulation 3 is concluded in 9 steps:

Step 1: Fly ash and activator weight

For a geopolymer with a compressive strength of 45 MPa and a fly ash content of 320 kg/m^3, a low activator-to-fly ash ratio is observed: 0.76, as shown in Figure 13. In order to improve workability, superplasticiser and water are added. The added water and superplasticiser make up 1 % of the total amount of fly ash.

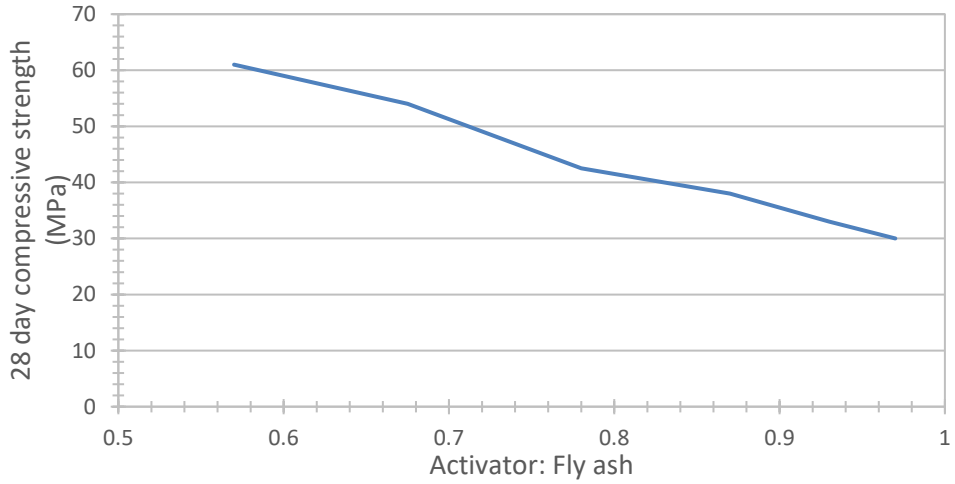

Figure 13: Activator to fly ash ratio – F3 (Ferdous, Kayali and Khennane 2013)

To account for the liquids added to increase workability, the activator to fly ash ratio is adjusted from 0.74 to 0.76. Therefore, 320 kg/m^3 of fly ash and 237 kg/m^3 of activator are used.

Step 2: Superplasticiser

The superplasticiser and water addition are 3.2 kg/m^3 (1 % of the fly ash content) each. The approximate rate of superplasticiser addition is 924 ml/100 kg of fly ash.

Step 3: Activator

The ratio of Na_2SiO_3 to NaOH is taken as 2.5 therefore each material is 169 and 68 kg/m^3 respectively since the total activator is 237 kg/m^3. The NaOH has a molarity of 16 and is prepared by mixing 44.4 % of NaOH pellets and 55.6 % of water. The required NaOH and water are 30 kg/m^3 and 38 kg/m^3 respectively. With the addition of the water required to improve workability (Step 2), the total water in the solution is 41.2 kg/ m^3. In order to keep the NaOH solution constant at 16 M, 33 kg/m^3 of NaOH pellets are added.

Step 4: Coarse and fine aggregates

The volume occupied by the material mentioned thus far are shown in Table 7. The total volume is 0.35 m^3. The total geopolymer composition is 1 m^3, therefore 0.65 m^3 of aggregates are required to obtain the desired strength.

Table 7: Volume occupied by materials – F3

Material	Fly ash	NaOH	Na_2SiO_3	Entrapped air	Total
Volume (m^3)	0.155	0.051	0.111	0.0329	0.35

The aggregates have a particle size of 14, 10, 7 mm and fine aggregates. They are added in percentages: 15, 35, 20 and 30 % respectively and have a combined specific gravity of 2.62 g/cm^3. The volume factor (% volume of the aggregates/ specific gravity/ 1 000) of the coarse aggregates is 0.0267 and 0.0117 for fine aggregates. The actual volume of the aggregates is therefore 69.6 and 30.4 % for coarse and fine aggregates instead of the 70 and 30% initially reported. The actual amount of coarse aggregate used is 0.452 m^3 (1185 kg/m^3) and 0.198 m^3 (508 kg/m^3) for fine aggregates.

The amount of aggregates required per 1 m^3 of geopolymer is shown in Table 8:

Table 8: Amounts of aggregates used

Aggregate	14 mm	10 mm	7 mm	Fine
Amount (kg/m^3)	254	593	339	508

Step 5: Aggregate absorption adjustments

The absorption of the aggregates must be taken into consideration as they alter the activator to fly ash ratio. The water taken up by the absorption in the aggregates is 17 kg/m^3, from the absorption capacities shown in Table 6. The total volume of the concrete is thus 1.003 m^3. The 0.3% offset is due to the inclusion of the superplasticiser.

Step 6: Volume adjustment

The volume of each material is adjusted by dividing the amount by 1.003. The original and adjusted volumes are shown in Table 9.

Table 9: Original vs adjusted volumes - F3

Constituents	**Original volume (m^3)**	**Adjusted volume (m^3)**
Coarse aggregates	0.4519	0.4505
Fine aggregates	0.1976	0.1971
Fly ash	0.1553	0.1549
Na_2SiO_3	0.1113	0.1110
NaOH	0.0510	0.0508
Superplasticiser	0.0030	0.0029
Entrapped air	0.0329	0.0328
Total	1.003	1.000

Step 7: Aggregate mixing

The amount of the aggregates after the adjustments in step 6 are shown in Table 10.

Table 10: Aggregates adjusted amounts

Aggregate	14 mm	10 mm	7 mm	Fine
Amount (kg/ m^3)	254	593	339	507

Step 8: Aggregate mixing in field conditions

Since the amount of aggregates changed, the absorption decreases to 12 kg from 17 kg, the activator to binder ratio becomes 0.76 and the Na_2SiO_3: NaOH ratio is 2.3 resulting in a geopolymer density of 2269 kg/ m^3. The ratio of fly ash: fine aggregate: coarse aggregate is 1: 1.59: 3.71.

Step 9: Water to solids ratio

The solids in the geopolymer are obtained from the Na_2SiO_3 (44.1% of the solution), NaOH (44.4% of the solution) and fly ash while the water is provided for only by the Na_2SiO_3 and NaOH solutions. The resulting water to geopolymer solids ratio is hence 0.32.

2.4.3.2 Formulation 3 conclusions

- The geopolymer has an inversely proportional relationship between the compressive strength and the water-to geopolymer solids ratio, as illustrated in Figures 14 and 15.

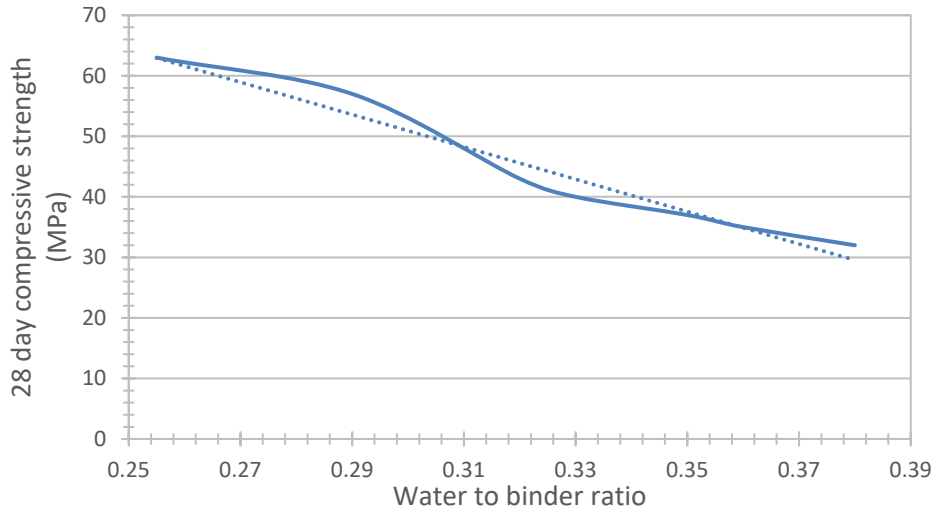

Figure 14: Compressive strength vs water to binder ratio (Ferdous, Kayali and Khennane 2013)

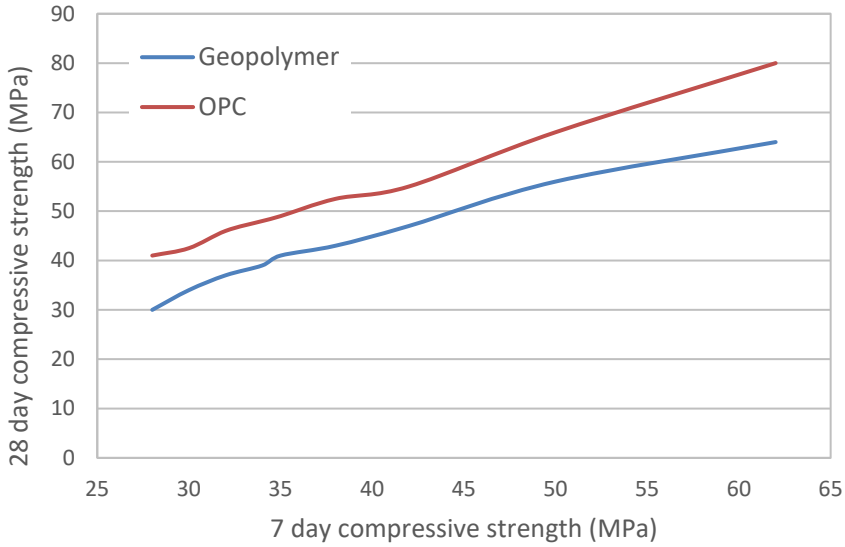

Figure 15: 7- to 28-day compressive strength results - F3 (Ferdous, Kayali and Khennane 2013)

- The water to geopolymer solids ratio increases as alkaline liquid to fly ash ratio increases given that the NaOH molarity and the Na_2SiO_3: NaOH ratio remains the same.

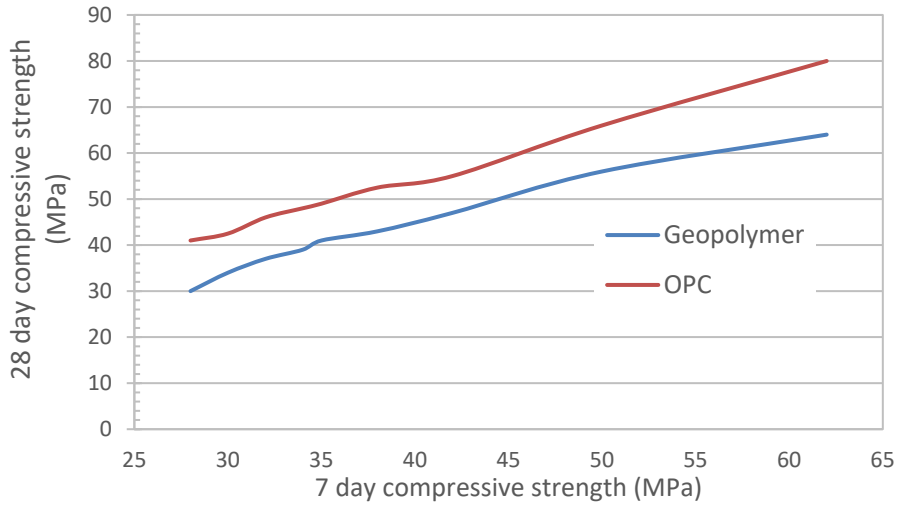

Figure 16: Geopolymer and OPC 7 vs 28 day compressive strength (Ferdous, Kayali and Khennane 2013)

- Although OPC compressive strength is higher than the geopolymers, the geopolymer achieved 87% of its 28-day strength in 7 days while OPC concrete achieves only 67%. This means that the geopolymer gains its strength quicker than OPC concrete (Figure 16).

2.4.4 Formulation 4 (Patankar, Ghugal and Jamkar 2015)

The study is selected because it is based on the fineness and amount of fly ash (Class F) required to meet a desired compressive strength, the amount of water needed for workability and the fine and coarse aggregate grading. It also provides a step-by-step procedure for the geopolymer manufactured which is comparable to Formulation 3.

The ratios that are kept constant are: the solution to fly ash ratio of 0.35, a water to geopolymer binder ratio of 0.35, which is chosen because it gives better results of workability and compressive strength, and a Na_2SiO_3 to NaOH ratio of 1. The geopolymers are heated at 60°C for 24 hours in cubes. Thereafter they are cooled to room temperature in the same oven and tested after 7 days.

The fly ash used is low calcium (Class F) and is sourced from an Indian thermal power plant. The Na_2SiO_3 (16.4% Na_2O, 34.4% SiO_2 and 49.7% H_2O) and NaOH (13 M) solutions are used as the alkaline activator. Locally available river sand is used as fine aggregates and 20- and 12.5 mm sized basalt stones are used as coarse aggregates.

Aggregates are an inert material and occupy a volume of 70 – 85% in the geopolymer. Fine and coarse aggregates are mixed in a manner that gives the least void in the geopolymer.

In preparation, the dry ingredients (aggregates and fly ash) are added first followed by the solution of Na_2SiO_3 and NaOH with extra water being added for workability purposes. All the ingredients are mixed together for 3 – 4 minutes. The mixture is then poured into 150 mm cubes and vibrated for 2 minutes to increase compaction. After 24 hours of casting, the cubes are placed in an oven.

The following steps were followed for proportioning on the basis of a 1 m^3 geopolymer product:

Step 1: Finding a target mean strength

The target mean strength (F_{ck}) is found using Equation 5:

$$F_{ck} = f_{ck} + 1.65 \times S \quad (5)$$

where f_{ck} = Characteristic compressive strength of geopolymer concrete = 30 MPa and S = Standard deviation (calculated using at least 30 samples) = 5.5

The target mean strength (MPa) is 38.25 MPa

Step 2: Amount of fly ash

The amount of fly ash required (405 kg/m^3) is determined by a target mean strength of 38.25 MPa, as calculated above, and a fly ash specific surface fineness of 430 m^2/kg using Figure 17.

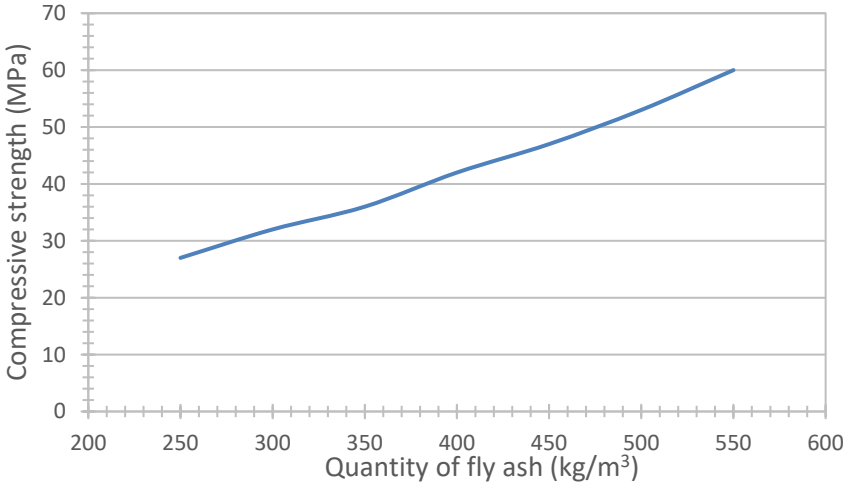

Figure 17: Quantity of fly ash vs Desired compressive strength – F4 (Patankar, Ghugal and Jamkar 2015)

Step 3: Amount of activator

The amount of alkaline activator required is obtained from the amount of fly ash used. The activator to fly ash ratio is 0.35, thus the required activator is 141.8 kg/m^3. Thereafter, the amount of Na_2SiO_3 and NaOH are found using the Na_2SiO_3: NaOH ratio of 1 resulting in a mass of 70.9 kg/m^3 each.

Step 4: Solid content in activator

The solid content in the Na_2SiO_3 and NaOH are calculated on the basis of the percentage of solids in each. These are 50.8% for Na_2SiO_3 and 38.5% for the NaOH thus, the respective masses are 35.7 and 27.3 kg/m^3.

Steps 5, 6 and 7: Water content

The amount of water used depends on the water needed in the alkaline solution and to increase workability. Since finer aggregates have a larger surface area and absorb more water, an additional amount of water must be added to produce a workable mix. It is therefore recommended that a water correction, similar to that of OPC cement, is applied on the basis of the absorption ability of finer aggregates.

Fly ash has a fineness of 430 m^2/kg and a medium degree of workability is desired. The total water added, as per Table 11, is therefore 110 kg/m^3. The water is adjusted by reducing it by 1.5% which results in a water content of 108.4 kg/m^3. The water content in the activator is 78.8 kg/m^3 and the additional water added for workability is therefore 29.5 kg/m^3.

Table 11: Water content for workability – F4 (Patankar, Ghugal and Jamkar 2015)

Degree of workability	Flow in percentage	Quantity of water required in kg/m^3			
		Specific surface fineness of fly ash in m^2/kg			
		< 300	300 - 400	400 – 500	> 500
Low	0-25	80	85	100	110
Medium	25-50	90	95	110*	120
High	50-100	100	110	120	135
Very high	100-150	120	130	140	160

Step 8: Selection of geopolymer wet density

The wet density of the geopolymer for a specific surface fineness of 430 m^2/kg is 2528 kg/m^3 as illustrated in Figure 18.

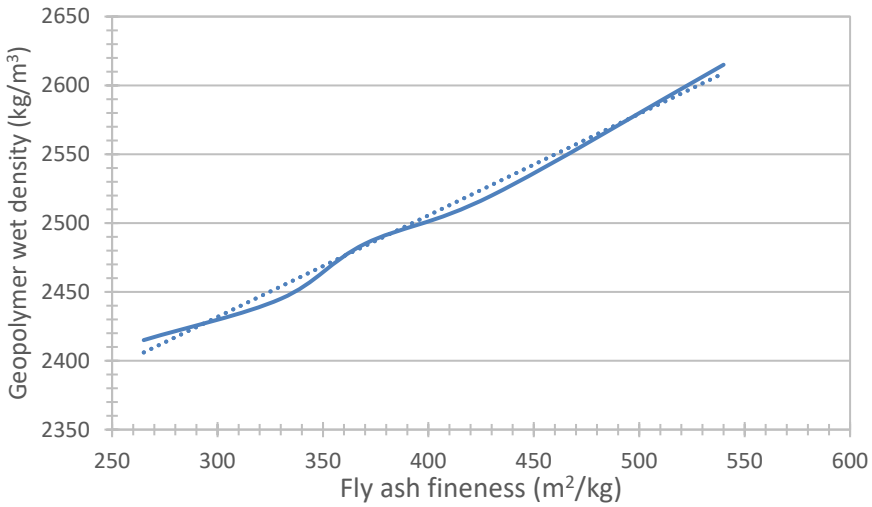

Figure 18: Fly ash fineness vs geopolymer wet density – F4 (Patankar, Ghugal and Jamkar 2015)

Step 9: Fine to coarse aggregate content

The fine to total aggregate content, for a fineness modulus of 3.35, is 35% as shown in Figure 19.

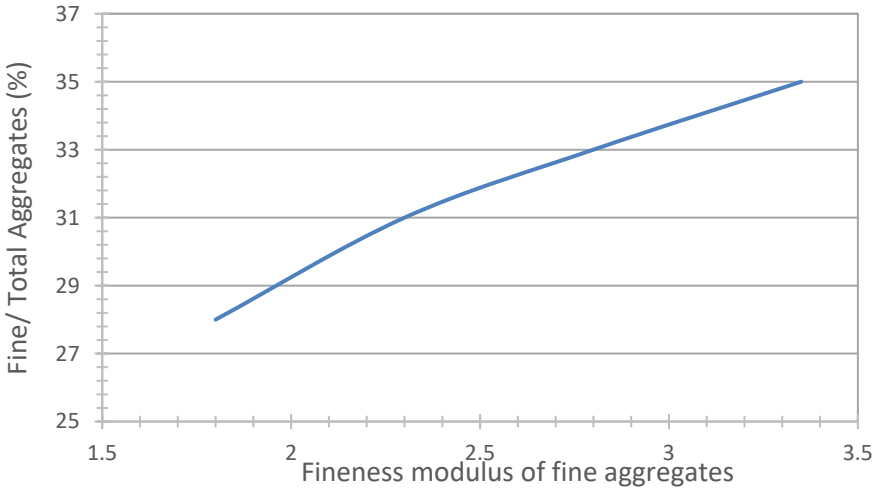

Figure 19: Fineness modulus vs fine to total aggregate ratio – F4 (Patankar, Ghugal and Jamkar 2015)

Step 10: Fine and coarse aggregate

The total aggregate required (1 953 kg/m^3) is the wet density of the geopolymer subtracted by the fly ash, alkaline activator and additional water added. Using the fine-to-total aggregate of 35%, from Step 9, the fine and total aggregates are 683 and 1 269 kg/m^3 respectively.

2.4.4.1 Formulation 4 conclusions

The resulting geopolymer was viscous, cohesive, a dark colour and glossy. Curing of the geopolymer for 24 days showed the highest compressive strength results. The results for the compressive strength with increasing curing time are illustrated in Figure 20.

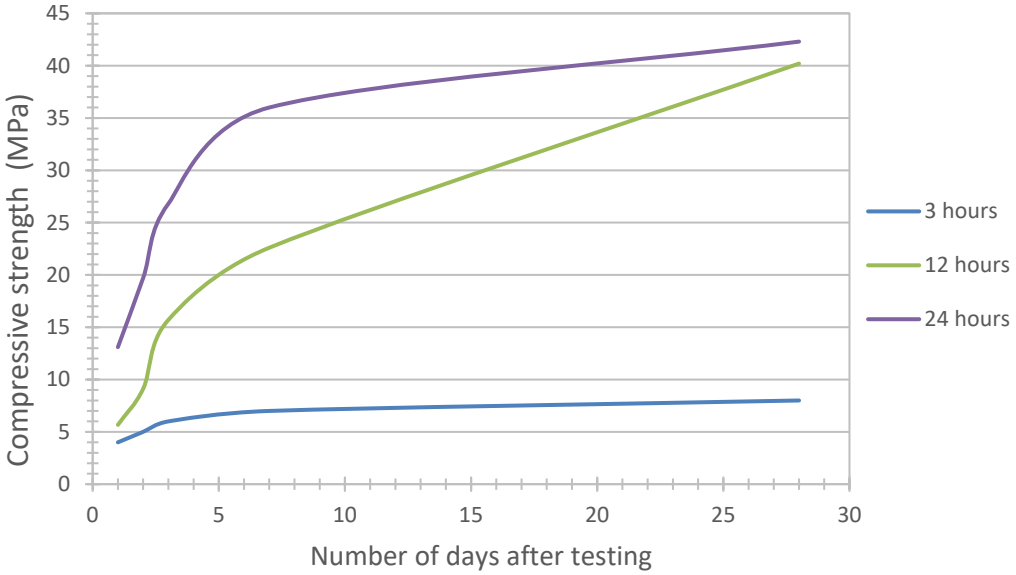

Figure 20: Curing time vs compressive strength - F4 (Patankar, Ghugal and Jamkar 2015)

- There was a slight differentiation in the target specification and the actual specification acquired. Compressive strength showed the highest variability with a difference of 2.86%, as shown in Table 12

Table 12: Target vs actual specifications – F4 (Patankar, Ghugal and Jamkar 2015)

Specification	Target	Actual	Difference
Workability (flow)	25 – 50%	44%	-
Mass density	2 528 kg/m^3	2 601 kg/m^3	2.81%
Compressive strength	38.3 MPa	37.2 MPa	2. 86%

2.4.5 Formulation 5 (Phoo-ngernkham, et al. 2018)

In Formulation 5, Class C fly ash with a specific gravity of 2.65 g/cm^3 and a mean particle size of 15.6 µm, from the Mae Moh power plant in northern Thailand is investigated. This formulation is selected because it uses Class C fly ash and shows the result of using a different type of ash class while manufacturing the geopolymer with comparable steps to Formulations 3 and 4. As stated above, a high calcium source fly ash resulting in a less porous geopolymer which ultimately creates a stronger product. The composition of the fly ash is shown in Table 13. Fine sand is sourced from a local riverbed and has a specific gravity of 2.52 g/cm^3 while the coarse aggregates are crushed limestone with average sizes of 7, 10 and 16 mm. The formulation was based on a geopolymer product of 1 m^3 and the effect of alkaline activator to fly ash ratio and concentration of NaOH was investigated against compressive strength after 28 days. 24 cylindrical samples were tested with a diameter of 100 mm and 200 mm height. Each of these were then cured at ambient temperature.

The sodium silicate solution is made up of 11.7% Na_2O, 28.7% SiO_2 and 59.7% H_2O and the concentration of the sodium hydroxide solution is varied. The sodium silicate to hydroxide ratio is kept constant at 1.

Table 13: Formulation 5 fly ash composition (Phoo-ngernkham, et al. 2018)

	SiO_2	Al_2O_3	Fe_2O_3	CaO	MgO	K_2O	Na_2O	SO_3	LOI
Composition (%)	31.3	14.0	15.6	25.8	2.94	2.93	2.83	3.29	1.30

The following steps were taken in the mix design:

Step 1 and 2: Coarse aggregate size and activator content

Three different sand particle sizes are investigated: 7 mm, 10 mm and 16 mm. The activator content is based on the aggregate size per the American Concrete Institute (ACI) standards and is determined by the maximum aggregate size as seen in Table 14. These values are only applicable when the fine aggregate has a 35% void content. The maximum coarse aggregate size chosen is 10 mm.

Table 14: Maximum aggregate size and activator content - F5 (Phoo-ngernkham, et al. 2018)

Maximum aggregate size (mm)	Maximum activator content (kg/m^3)	Void (%)
10	225	3
12.5	215	2.5
20	200	2

Step 3: Activator adjustment

The water content must be adjusted if the fine aggregate void is not 35% (see Equation 6).

$$Alkaline\ activator\ adjustment = \left[\left[1 - \frac{\rho_{fine\ aggregate}}{sg_{fine\ aggregate} \times \rho_{water}} \times 100\right] - 35\right] \times 4.75 \qquad (6)$$

where $\rho_{\text{fine aggregate}}$ = density of the fine aggregate (kg/m^3) = 1 585 kg/m^3, $sg_{\text{fine aggregate}}$ = specific gravity of the fine aggregates = 2.52, and ρ_{water} = density of water (kg/m^3) = 1 000 kg/m^3

The adjustment of the water content in the activator (kg/m^3) is thus 10 kg/m^3 and the activator content required is 225 kg/m^3 + 10 kg/m^3 = 235 kg/m^3

Step 4: Selection of the activator to fly ash ratio

From Figure 21, it can be observed that a compressive strength of just below 30 MPa is achieved using 10 M NaOH when the activator to fly ash ratio is 0.5.

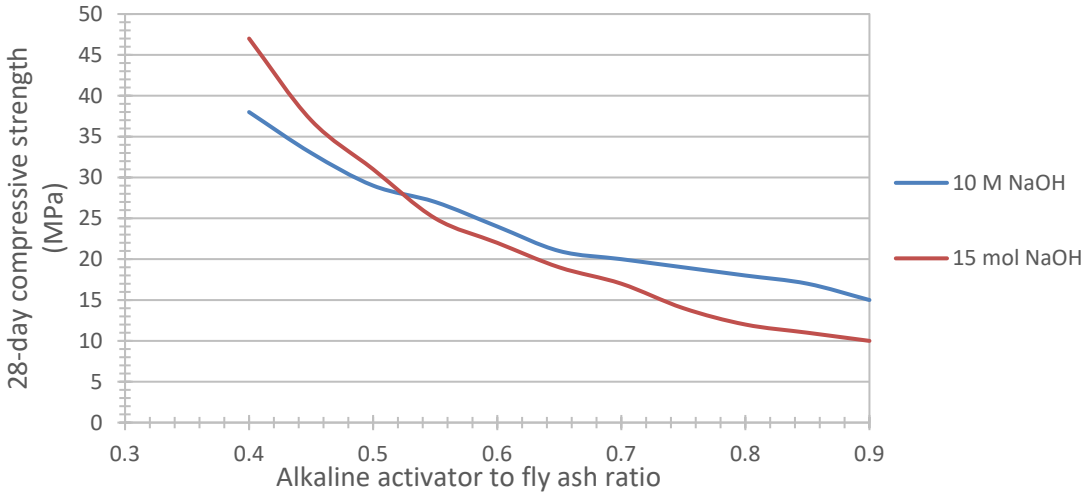

Figure 21: Activator to fly ash ratio vs compressive strength - F5 (Phoo-ngernkham, et al. 2018)

Step 5: Fly ash content

The fly ash content is calculated using Equation 7.

$$Fly\ ash\ content = \frac{Activator\ content}{Activator\ to\ fly\ ash\ ratio} \quad (7)$$

where *Activator content* = amount of activator used = 235 kg/m^3, and *Activator to fly ash ratio* = 0.5

The resulting fly ash content is 470 kg/m^3

Step 6: Activator composition

Using a sodium silicate to sodium hydroxide ratio of 1, the silicate and hydroxide content is 117.5 kg/m^3 for both solutions.

Step 7: Aggregate content

The fine and coarse aggregate content is found using Equations 8 and 9 respectively.

$$M_{fine\ aggregate} = 0.3 \times sg_{fine\ aggregate} \times \left[1 - Vol_{fly\ ash} - Vol_{hydroxide} - Vol_{silicate} - Vol_{air}\right] \times 1\,000 \quad (8)$$

$$M_{coarse\ aggregate} = 0.7 \times sg_{coarse\ aggregate} \times \left[1 - Vol_{fly\ ash} - Vol_{hydroxide} - Vol_{silicate} - Vol_{air}\right] \times 1\,000 \quad (9)$$

where $sg_{\text{fine aggregate}}$ = specific gravity of the fine aggregate = 2.25,

$sg_{\text{coarse aggregate}}$ = specific gravity of the coarse aggregate = 2.25,

$Vol_{\text{fly ash}}$ = Volume of the fly ash = 0.177 m^3,

$Vol_{\text{hydroxide}}$ = Volume of the sodium hydroxide = 0.0832 m^3, and

Vol_{silicate} = Volume of the sodium silicate = 0.0791 m^3.

The fine aggregates are therefore 477 kg/m^3, while the coarse aggregates are 1164 kg/m^3.

Step 8: Superplasticiser content

The superplasticiser content is 1% of the fly ash content (Equation 10).

$$SP\ dosage = \frac{fly\ ash\ content}{100} \quad (10)$$

Where *fly ash content* = 470 kg/m^3.

The amount of superplasticiser added is therefore 4.7 kg/m^3

Formulation 5 conclusions

- The objective of the study was to make a geopolymer that had a characteristic compressive strength of 30 MPa. The moulds were tested and a compressive strength of 31.1 MPa was achieved after 28 days of curing. This mix design therefore meets the target strength was 30 MPa. The difference in desired and target strength is 3.54%.

2.4.6 Formulation 6 (Pavithra, et al. 2016)

Low calcium Indian fly ash and aggregates are added to the alkaline activator and the influence of activator to fly ash ratio on compressive strength is observed. This formulation is selected as it also makes use of Class F fly ash and a step-by-step mix design which can be compared to the other Formulations.

The following steps were taken:

Step 1: Alkaline activator content

An activator content of 200 kg/m^3 is the basis of the study as this produces a geopolymer with better strength, workability and highest cost efficiency.

Step 2: Strength

The desired strength of the geopolymer is 38 MPa. This strength is achieved when the activator to fly ash ratio is 0.5 in Figure 22.

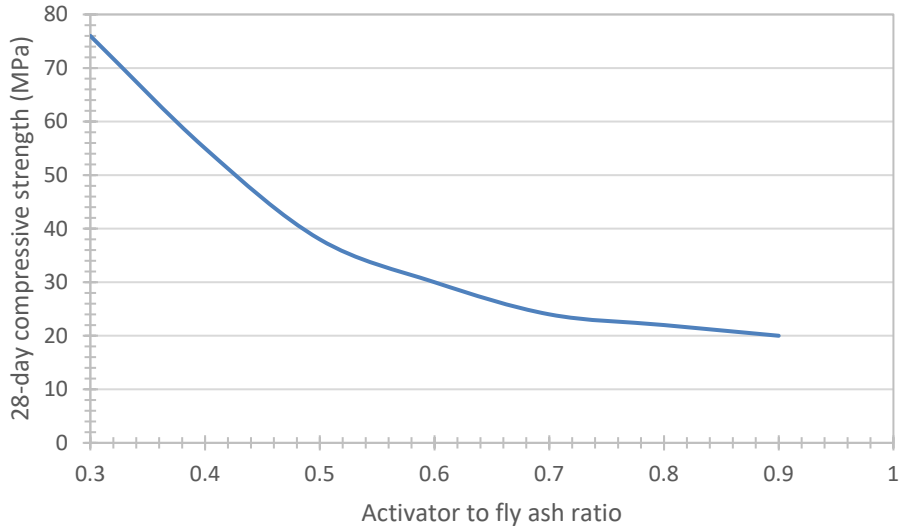

Figure 22: Activator to fly ash ratio vs compressive strength - F6 (Pavithra, et al. 2016)

Step 3: Fly ash to binder content

$$Amount\ of\ fly\ ash = \frac{Amount\ of\ activator}{Activator\ to\ fly\ ash\ ratio} \quad (11)$$

With an activator content of 200 kg/m^3 and activator to fly ash ratio of 0.5, the amount of fly ash required is 400 kg/m^3 (Equation 11).

Step 4: Activator composition

The Na_2SiO_3 to NaOH ratio is 1.5. Since the total amount of activator is 200 kg/m^3, the Na_2SiO_3 and NaOH content are 120 and 80 kg/m^3 respectively.

Step 5: Activator water content

The percentage of water in the NaOH is 54.4% (to maintain a concentration of 16 M) while the water in the Na_2SiO_3 is 65.5%. This results in a water content of 43.6 kg/m^3 in the NaOH solution and 78.6 kg/m^3 in the Na_2SiO_3 solution. The total water content is therefore 122 kg/m^3.

Step 6: Aggregate content

The total aggregate content is calculated by assuming a concrete volume of 1 m^3 and an entrapped volume of 2% of the total concrete (Equation 12).

$$Vol_{concrete} = Vol_{aggregates} + Vol_{fly\ ash} + Vol_{NaOH} + Vol_{\mathrm{Na2SiO3}} + Vol_{entrapped\ air} \quad (12)$$

where Vol $_{concrete}$ = volume of concrete = 1 cm^3

Vol $_{fly\ ash}$ = vol. of fly ash = mass of fly ash/ specific gravity = 400/2.2 = 181.8 m^3

Vol $_{NaOH}$ = vol. of sodium hydroxide = mass of NaOH / specific gravity = 80/1.4506 = 55.1 m^3

Vol $_{Na2SiO3}$ = vol. of sodium silicate = mass of Na_2SiO_3/ specific gravity = 120/1.35 = 88.9 m^3, and Vol $_{entrapped\ air}$ = 0.02 m^3 (assumption).
The aggregate volume is thus 0.654 m^3.

Step 7: Aggregate composition

Sieves of aperture sizes 6.3, 12.5 and 20 mm were used to determine the particle size distribution of the aggregates as seen in Table 15.
The mass of each of the aggregate sizes is determined using equation 13.

$$Mass_{\ i} = \%Passing_i \times Vol_{entrapped\ air} \times specific\ gravity_i \times 1\,000 \quad (13)$$

where $Mass_i$ = mass required for each aggregate, $Vol_{entrapped\ air}$ = volume of the entrapped air = 0.654 m^3 and $specific\ gravity_i$ = specific gravity of each aggregate = 2.73
The aggregate results are shown in Table 15.

Table 15: Aggregate properties – F6

Sieve size (mm)	% Passing	Specific gravity (g/cm^3)	Aggregate mass per m^3 of geopolymer (kg/m^3)
4.75	20	2.63	344
6.3	20	2.61	341
12.5	32	2.76	578
20	28	2.73	500

Step 8: Superplasticiser content

The superplasticiser added is 1% of the fly ash (Equation 14).

$$Mass_{Superplasticiser} = 1\% \times Mass_{fly\ ash} \quad (14)$$

where $Mass_{fly\ ash}$ = Mass of the fly ash = 400 kg/m^3 and $Mass_{superplasticiser}$ = Mass of superplasticiser required
The mass of the superplasticiser is thus 4 kg/m^3.

- The specimens were tested and a compressive strength of 45.95 MPa was achieved after 28 days of curing. This mix design therefore exceeds strength tests as the target strength was 37.69 MPa.
- Table 16 shows the results of a slump test. The degree of workability increases as the activator to fly ash ratio increases. When the ratio reaches 0.8, however, the slump collapses as the mix is too wet.

- Figure 23 illustrates that a lower activator to fly ash ratio results in a high compressive ratio.

Table 16: Activator to fly ash ration vs slump - F6

Activator to fly ash ratio	Slump (mm)	Degree of workability
0.4	35	Low
0.5	60	Medium
0.6	80	Medium
0.7	110	High
0.8	Collapse	-

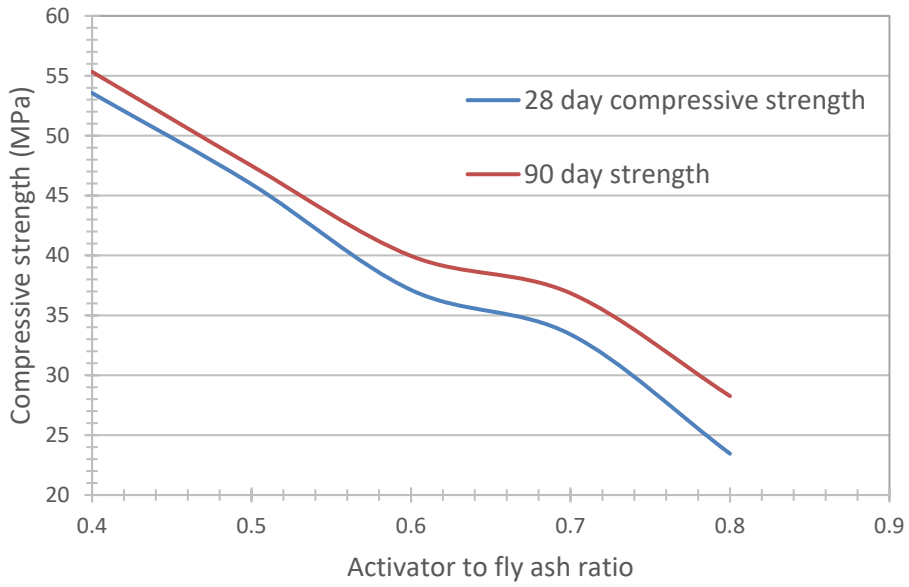

Figure 23: Activator to fly ash vs compressive strength - F6 (Pavithra, et al. 2016)

2.5 Geopolymer characterisation

In this section of the literature study, the Fourier-Transform Infrared Spectroscopy (FTIR), Thermogravimetric Analysis (TGA) and X-ray Diffraction (XRD), X-ray Fluorescence (XRF), drying shrinkage and soundness analyses of geopolymer products are reviewed. Several studies show that these analyses, in addition to mechanical strength testing, are key in understanding the behaviour of geopolymers (Rosas, et al. 2014).

2.5.1 XRD and XRF

Although geopolymers are primarily amorphous in nature, crystalline phases may form (Rosas, et al. 2014). XRD is therefore important to analyse to assess the degree to which the

geopolymer starting materials have reacted and the amorphicity of the final product. The intensity of the peaks may be ascribed to the curing time and molarity of the alkaline hydroxide used which influence the crystallization of the phases (Rosas, et al. 2014).

In a study where the geopolymer starting materials were fly ash and a sodium hydroxide solution at a solution to activator ratio of 0.4, the XRD analysis was examined in the range 5 º ≤ 2θ ≤ 90 º, The diffractogram illustrated that the geopolymer is amorphous by the hump seen between 20º ≤ 2θ ≤ 33º, which is typically seen in amorphous materials (Rosas, et al. 2014). The peaks in the diffractogram reveal the presence of quartz, hematite and various types of zeolites which are formed when the fly ash and sodium hydroxide react (Rosas, et al. 2014).

When the XRD results for fly ash and the fly ash based geopolymer are compared , the hump associated with amorphicity shifts from 14º ≤ 2θ ≤ 30º in the fly ash to 20º ≤ 2θ ≤ 40º in the geopolymer due to the formation of an alkaline aluminosilicate hydrate gel (Alehyen, Achouri and Taibi 2017). The quartz and mullite crystalline phases seen in the fly ash remain unchanged by the reaction and are seen in the geopolymer. Overall, the mineralogy of the fly ash and geopolymer are largely the same.

In another study, where the aluminosilicate source used was metakaolin, the halo indicating amorphicity is centred at 20º ≤ 2θ ≤ 33º. The peaks illustrate the presence of kaolinite, anatase and quartz (Ferone, et al. 2013). Metakaolin based geopolymers also have peaks of microline and illite (Hawa, Tonnayopas and Prachasaree 2013).

Table 17 illustrates the chemical composition of Moroccan Class F fly ash and the geopolymer manufactured from ash and an alkaline activator made of sodium silicate and sodium hydroxide (12 M). The results show a decrease in SiO_2 and Al_2O_3, which indicates the degree of geopolymerisation of the fly ash. The increase in Na_2O originates from the sodium silicate source in the activator which was made up of 18 % Na_2O and 63 % SiO_2 (Alehyen, Achouri and Taibi 2017).

Table 17: Fly ash vs Geopolymer XRF (Alehyen, Achouri and Taibi 2017)

	LOI	SiO_2	Al_2O_3	Fe_2O_3	CaO	K_2O	Na_2O	TiO_2	SO_3
Fly ash (%)	7.12	52.50	30.20	2.94	0.82	2.08	0.72	1.03	0.79
Geopolymer (%)	5.82	37.80	15.90	4.67	1.15	2.65	28.30	1.58	0.37

2.5.2 Thermogravimetric analysis (TGA)

TGA is an analysis that determines the thermal stability of a material by assessing the weight loss of the material as it is heated at a constant rate (Rajisha, et al. 2011).

Figure 24 illustrates the TGA graph of a metakaolin based geopolymer. According to Ferone et al (2013), the first weight loss, which occurs between 30 and 100ºC, is attributed to water molecule loss absorbed from the environment while loss up to 200ºC is from free water in the pores of the geopolymer. Finally, weight loss at temperatures between 200 and 500ºC are caused by the loss of structural and bound water in the nanopores of the geopolymer (Ferone, et al. 2013). The overall weight loss of 28% is related solely to water loss.

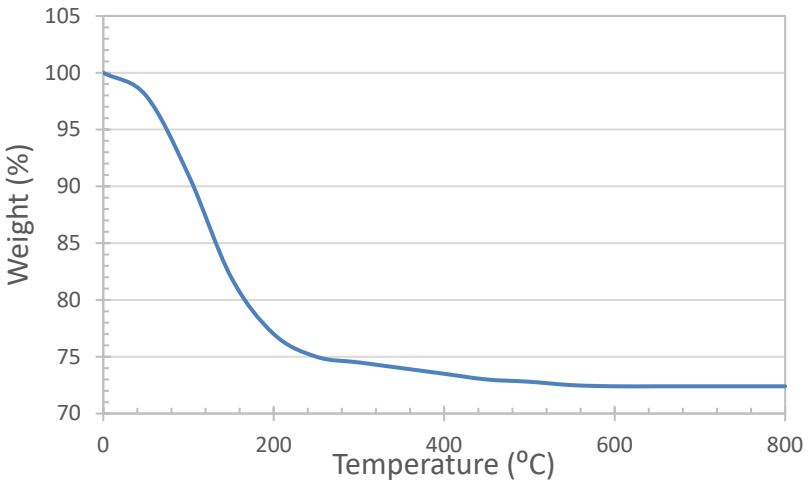

Figure 24: TGA 1 (Ferone, et al., 2013)

In a study by Rosas, et al (2014), the first major weight decline (0 – 120 ºC) in Figure 25 is said to be associated with a loss in absorbed water on the surface of the geopolymer and accounts for 10 % of the overall weight loss. The second weight loss (120 – 200 ºC) that occurs is associated with the loss of the NASH gel in the geopolymer and the final is in the carbonates range (450 – 800ºC) that are produced by external measures when geopolymerisation occurs (Rosas, et al. 2014).

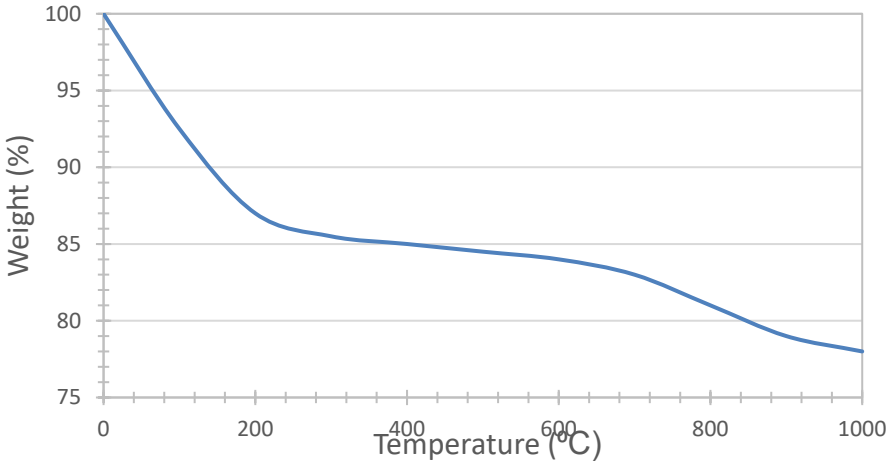

Figure 25: TGA 2 (Rosas, et al., 2014)

2.5.3 Fourier-transform infrared spectroscopy (FTIR)

The most characteristic band in the FTIR study by Rosas, et al., (2014) is located at 1 000 cm^{-1} and represents X-O bonds where X is either Si or Al. It is attributed to the hydrated sodium aluminosilicate gel that was formed and its magnitude is due to the amorphous nature of the geopolymer (Rosas, et al. 2014). Two more bands, one at 1625 cm^{-1} and the other at 3 500 cm^{-1}, correspond to water molecules in the NASH gel. Finally, smaller bands between at 625 cm^{-1} and 795 cm^{-1} are attributed to the quartz and mullite in the fly ash (Rosas, et al. 2014).

In the Alehyen et al., (2017) study, the most characteristic transmission bands are at 3 432, 997 and 444 cm^{-1}. The 3 432 band is attributed to the presence of O-H in silanol groups and the bonds between water molecules and the silanol groups. The 997 cm^{-1} band represents the Si-O-Si and Al-O-Si asymmetric stretching bonds in the geopolymer while the 444 cm^{-1} band is Si-O and Al-O bending vibration bonds in the geopolymers (Alehyen, Achouri and Taibi 2017).

The presence of siliceous material in the Samantasinghar & Singh., (2019) study is shown by the peak between of 1 024 cm^{-1} and 797 cm^{-1}. This is associated with the presence of mullite in the fly ash. Water molecules are observed at 1 877 cm^{-1} and 3 453 cm^{-1} due to the presence of water in the fly ash. Lastly, peaks at 463 and 1 092 cm^{-1} are attributed to Si-O which indicate the existence of silica in the fly ash (Samantasinghar and Singh 2019).

For the metakaolin based geopolymer in the Hawa, et al., (2013) study, major bands are seen at 1 000 and 446 cm^{-1} and reflect Si-O vibrations while the bands at 810 cm^{-1} represent Al-O

bonds. Bands at 3 453 are formed by O-H stretching vibration and 1 659 cm^{-1} by H-O-H bending vibrations (Hawa, Tonnayopas and Prachasaree 2013).

2.5.4 Drying shrinkage and soundness

Drying shrinkage is the decrease in volume and is caused primarily by the loss of water during drying (Wallah 2009). A high water to binder ratio results in an increase in shrinkage since paste strength and stiffness decrease because of the reduction of volume of restraining aggregates (Wallah 2009).

The drying shrinkage results shown in Figure 26 are for a geopolymer study with a sodium silicate to sodium hydroxide ratio of 2.5 (A and B) and 1.5 (C and D) (Deb, Nath and Sarker 2015). Slag makes up 10% of A and C and 20% B and D. The results show that the shrinkage ranges between 480 and 770 microstrain. In general, the addition of slag decreases the shrinkage and a higher silicate to hydroxide ratio increases the shrinkage.

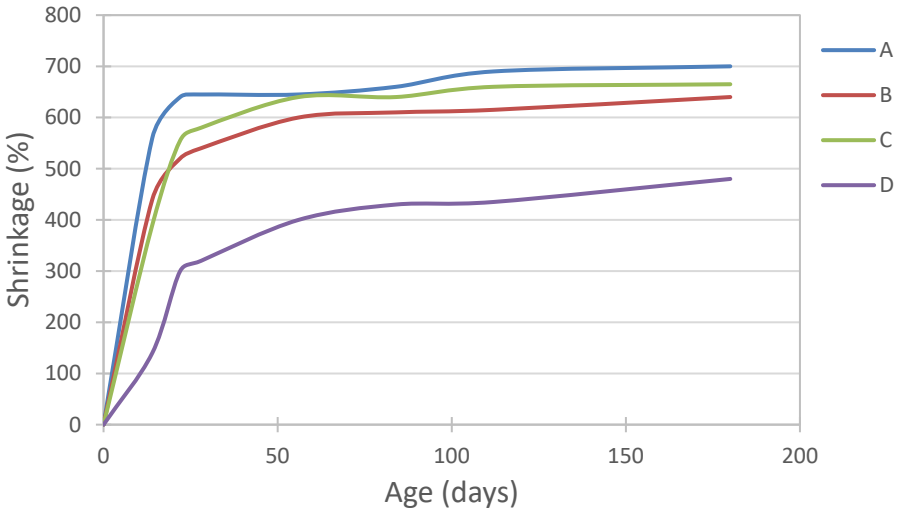

Figure 26: Drying shrinkage results (Deb, Nath and Sarker 2015)

Figure 27 shows the drying shrinkage results for geopolymers manufactured using fly ash from Lethabo power station in the Free State and were cured at 60 ºC in a dry oven for 24 hours (Shekhovtsova, Kovtun and Kearsley 2014). The drying shrinkage reaches about 360 microstrain after one year.

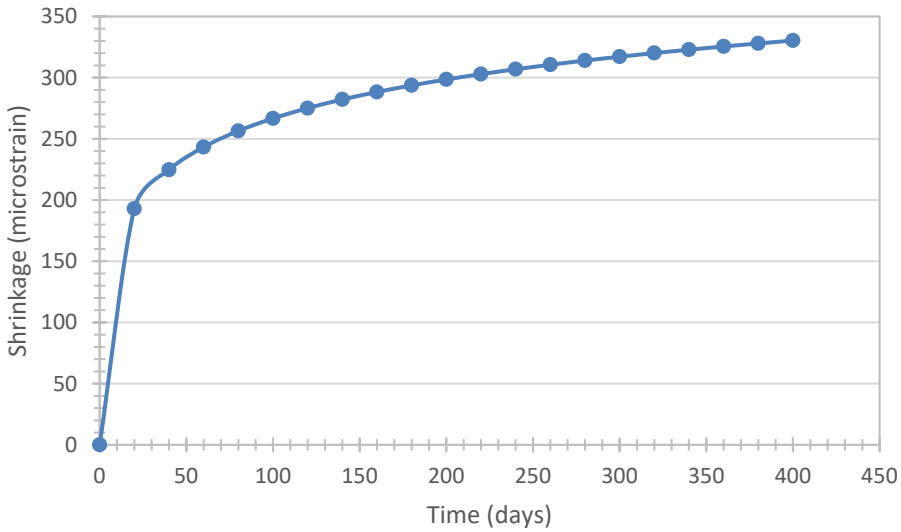

Figure 27: Drying shrinkage results (Shekhovtsova, Kovtun and Kearsley 2014)

Table 18 shows the drying shrinkage results of geopolymers manufactured with Indian fly ash using different concentrations of sodium hydroxide. It is found that a higher concentration of sodium hydroxide reduces the drying shrinkage. This occurs because there is more capillary water available in the geopolymers when a low molarity is used (Samantasinghar and Singh 2019).

Table 18: Drying shrinkage results (Samantasinghar and Singh 2019)

NaOH concentration (M)	Drying shrinkage (microstrain)
2	500
4	440
8	400
12	360
16	320

The soundness test determines the stability of change in volume when cement sets or hardens. If there is a significant change in volume, the concrete is prone to cracking (Zhang 2011). The existence of free lime and magnesia cause geopolymers to be unsound because they can potentially cause the cured geopolymer to expand (Samantasinghar and Singh 2019).

The Samantasinger & Singh (2019) study reveals that fly ash based geopolymers do not expand during soundness testing, while slag based geopolymers expand by 1 mm.

2.6 Conclusion

2.6.1 Starting materials

2.6.1.1 Fly ash

From Table 1 above, which describes the composition of fly ash from several South African coal power stations, it is observed that ash sample 1 from Mpumalanga has the highest Si: Al ratio but this fly ash also had the lowest calcium oxide content. The inverse is noted in sample 2, also from Mpumalanga, which has the lowest Si: Al ratio and the highest calcium content. Since the addition of the sodium silicate in the activator would increase the Si: Al ratio significantly, the calcium oxide content is prioritised when selecting the ash that will be used. Thus, fly ash from the power stations where sample 2 is produced will be considered in the study. Kriel power station is identified as the power station with the highest calcium content in ash. This fly ash will therefore be used in the study since it will result in a less porous geopolymer which ultimately creates a stronger product.

2.6.1.2 Alkaline activator

Sodium silicate and sodium hydroxide will be used to make the activator. The NaOH concentration in each set will be kept constant while the sodium silicate to sodium hydroxide ratio is to be varied.

Although Formulation 1 concludes that the optimal NaOH is 6 M, Formulation 2 and 5 conclude that a higher concentration results in a stronger geopolymer compressive strength. Thus, a NaOH solution with a 15 M molarity will be used in the first set of geopolymers. In the second set of geopolymers, the NaOH concentration will be decreased to 10 M.

2.6.2 Formulation

In general, the formulations show that curing at higher temperatures for a longer period of time will improve the performance of the geopolymer. Additionally, using a higher sodium hydroxide concentration and increasing the sodium silicate to hydroxide ratio also enhances the properties of the geopolymer produced.

Formulations 3 to 6 start off similarly in that a desired compressive strength is targeted. In Formulations 3, 5 and 6, an activator to fly ash versus compressive strength graph is used to determine the activator to fly ash ratio using the desired compressive strength. As illustrated in Figure 28, Formulation 5 (F5) and 6 (F6) have similar graphs despite the F5 graph being based on past geopolymer tests and F6 on the water to concrete ratio of Ordinary Portland Cement. F5 and 6 follow similar steps after the aggregate to fly ash ratio step.

This study will follow a methodology that meshes F5 and F6. The steps taken will be as follows:

Step 1: Activator basis

An activator basis of 200 g/dm^3 is assumed as this results in a geopolymer that is strong, workable and cost-efficient, according to F6.

Step 2: Activator to fly ash ratio

In this step, the activator to fly ash versus compressive strength of F5 will be used as this is based on previous geopolymer formulations. A target strength of 30 MPa, which was the strength selected in this formulation, corresponds to an activator to fly ash ratio of 0.5, as shown in Figure 28. The concentration of the NaOH was kept constant at 15 M for one set of samples and then 10 M for another.

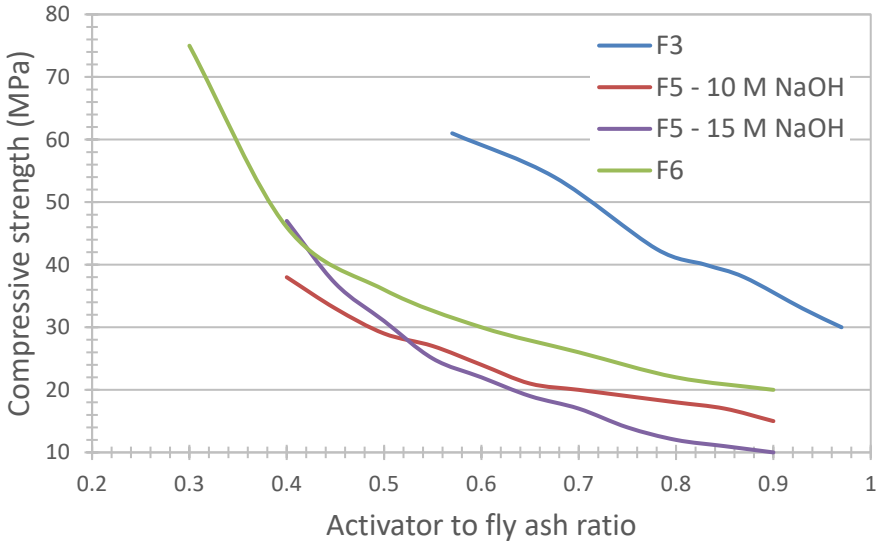

Figure 28: Activator to fly ash vs strength comparison

Step 3: Fly ash content

The ash content was determined using Equation 11 using the calculated values in step 1 and 2 above.

Step 4: Activator composition

The sodium silicate to sodium hydroxide ratio in the activator was varied: 1.5, 2 and 2.5, while the total activator to fly ash ratio was kept constant.

Step 5: Aggregate content

The aggregate content was calculated using Equation 12 in F6. The volume of entrapped air will be assumed to be 2 % as done in the formulation.

Step 6: Aggregate composition

The fine to coarse aggregate ratio was 30: 70 as seen in F5.

Step 7: Superplasticiser

No superplasticiser was added in the study.

2.6.3 Curing

Two sets of samples were manufactured: one where the geopolymers are cured at ambient temperature and the other when they are cured at 80ºC for 6 hours in order to assess the effect of curing temperature. The curing conditions were selected because the oven used was set to this temperature during this time and could not be varied. Samples were tested 3, 7 and 28 days apart from both the sets. In this respect, the curing time was investigated.

Upon completion, 18 samples of geopolymers, for each sodium silicate solution that was manufactured, were investigated as summarised in Table 19. In total, 36 samples were tested. Only one specimen is tested for each composition. The values in the table represent the Na_2SiO_3: NaOH ratio of the activator.

Table 19: Geopolymer test samples

Curing temperature	3 days curing time	7 days curing time	28 days curing time
Ambient temperature (Na_2SiO_3: NaOH)	1.5	1.5	1.5
	2	2	2
	2.5	2.5	2.5
80ºC for 6 hours (Na_2SiO_3: NaOH)	1.5	1.5	1.5
	2	2	2
	2.5	2.5	2.5

2.6.4 Geopolymer characterisation

It is expected that the XRD diffractogram will reflect that the geopolymer is amorphous in nature with a hump between 14 and 40º. Quartz, hematite and mullite from the aggregates used and the formation of zeolites in the geopolymerisation process are also expected to be seen in the

diffractogram. The XRF results should show a decrease in SiO_2 and Al_2O_3 and an increase in Na_2O reflecting the degree to which geopolymerisation occurred.

The TGA graph should depict a weight loss of up to 28 %, resulting primarily from surface and structural water loss. The loss of carbonates, which are formed from external measures in the process, is expected in the range of 450 and 1 000ºC.

For the FTIR analysis, as shown in Table 20, Si-O and Al-O are expected due to the presence of the NASH gel, silica from aggregates or mullite in the fly ash. O-H bonds between water molecules and silanol groups as well as from water molecules in the ash are expected.

Table 20: Expected FTIR bonds

Frequency (cm^{-1})	Bond type	Attribution	Reference
997 – 1 092	Si-O	Sodium aluminosilicate (NASH) gel Silica from fly ash and aggregates Mullite in fly ash	(Alehyen, Achouri and Taibi 2017). (Rosas, et al. 2014). (Samantasinghar and Singh 2019)
1 625 - 1 877	O-H	Water molecules in NASH gel Water molecules in the ash	(Rosas, et al. 2014). (Samantasinghar and Singh 2019)
3 432 -3 500	O-H	Water molecules in NASH gel Bond between water molecule and silanol group Water molecules in ash	(Alehyen, Achouri and Taibi 2017). (Rosas, et al. 2014). (Samantasinghar and Singh 2019)
625 - 797	Si-O	Mullite and quartz in the fly ash	(Rosas, et al. 2014). (Samantasinghar and Singh 2019)
444 - 463	Si-O or Al-O	Silica in the aggregates	(Samantasinghar and Singh 2019)

A drying shrinkage between 360 and 760 microstrain is expected and minimal expansion should be seen in the soundness test.

CHAPTER 3: METHODOLOGY

3.1 Overview

In Chapter 3 the materials and equipment used in the study are discussed along with the methodology used to conduct experiments.

3.2 Materials

3.2.1 Fly ash

The fly ash used was sourced form Kriel power station which is an Eskom owned power station located in Kriel, Mpumalanga as depicted in Figure 29. As mentioned in Section 2.6.1.1, this ash is selected as it typically has a high calcium source content. The XRD and XRF results of the ash are shown in Tables 29 and 30 respectively.

Figure 29: Kriel power station location

3.2.2 Aggregates

Two aggregates were used. Aggregate 1 was sourced from Balmoral Sandworks and made of crushed limestone. Aggregate 2 was river sand from sourced from PPC. The particle size distribution for these is illustrated in Figure 30. These aggregates were used because the relatively small particle size promotes geopolymers that will not be porous.

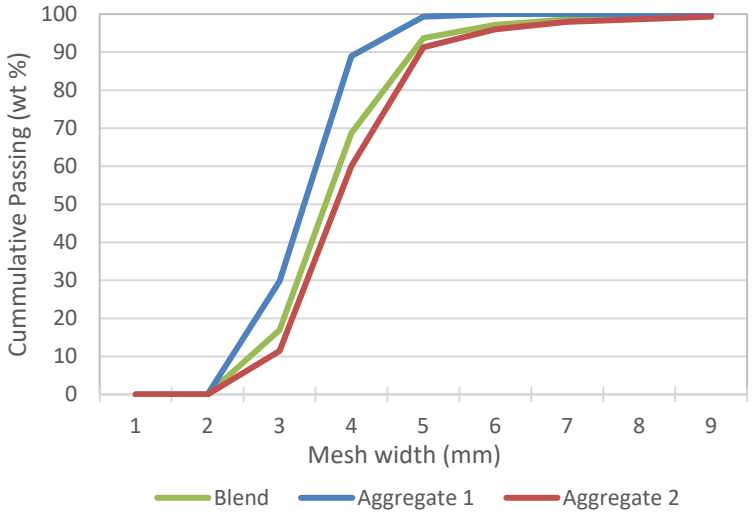

Figure 30: Aggregate particle size distribution

3.2.3 Sodium hydroxide

NaOH is the chosen alkaline hydroxide as it typically used for the geopolymer manufacture as opposed to KOH and generally leaches more Si^{4+} and Al^{3+} ions than KOH.

Two sodium hydroxide solutions were used in the study. One with a concentration of 15 M and the other a concentration of 10 M. The MSDS sheet for 100 % pure sodium hydroxide, supplied by LabChem, can be found in Appendix B.

3.2.4 Sodium silicate

Sodium silicate is the selected alkaline silicate as opposed to potassium silicate as it is typically paired with sodium hydroxide. The sodium silicate used is a 37.5% solution in water and is supplied by National Silicates, an affiliate of PQ Corporation. The MSDS sheet for this can be found in Appendix A.

3.2.5 Demoulding oil

Demoulding oil was applied on the moulds to prevent the geopolymer from sticking onto the mould when demoulding occurs. The oil, supplied by Viscol Oil, is made up of petroleum and naphthenic oil as shown in the MSDS sheet in Appendix C.

3.3 Moulds

The moulds used were tubes cut from a PVC pipe with an outer diameter of 50 mm and inner diameter of 45 mm. Plastic moulds were used after it was found that, despite using lubricating

oil, the geopolymer stuck onto steel cubes after curing which resulted in the geopolymer being deformed after removal.

A long PVC pipe was cut into smaller, 45 mm long tubes. The volume of the mould is therefore 71.6 cm^3. This is the theoretical volume of the geopolymer once manufactured. An example of the mould used is given in Figure 31. Although the moulds are non-standard, the study is comparative thus trends will not be affected.

Figure 31: Mould

3.4 Geopolymer manufacturing

The manufacturing process in completed according to the following steps as shown in Figure 32.

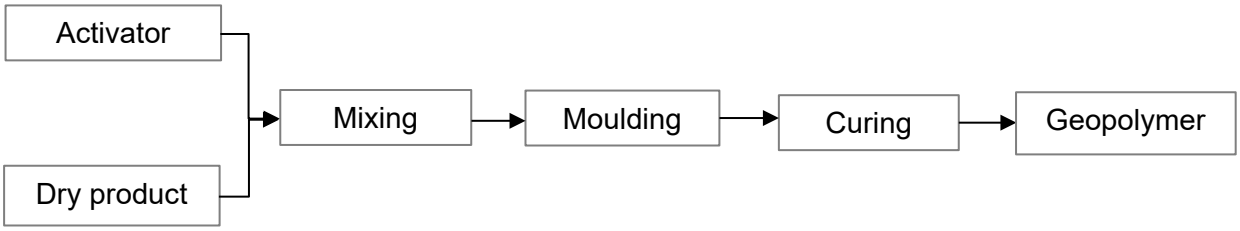

Figure 32: Overall geopolymer manufacture process

The activator is mixed according to the relevant composition depicted in Table 21.

Table 21: Activator composition

Na_2SiO_3: NaOH	Sodium silicate (g)	Sodium hydroxide (g)	Total (g)
1.5	8.60	5.7	14.3
2.0	9.50	4.8	14.3
2.5	10.2	4.1	14.3

The aggregates and fly ash are mixed in the amounts shown in Table 22 in a separate container. As mentioned above, the aggregates are mixed at a 70: 30 coarse to fine ratio.

Table 22: Dry product mixture

Product	Aggregate 1	Aggregate 2	Fly ash
Amount (g)	20.1	46.9	28.6

Once the activator and dry product are mixed individually, they are combined and 5 ml of water per specimen (42.9 g) is added for workability purposes. The moulds are oiled by wiping a paper towel soaked in the demoulding oil on the inside of the tube. The mix is then poured into the mould and cured.

3.5 Curing

One set of geopolymers is cured at 21 ºC until strength testing while the other set is oven cured at 80 ºC for 6 hours and then at 21 ºC until strength testing.

For 21 ºC curing, the geopolymers are placed in a room that is kept at that temperature through the use of an air conditioner (climate controlled). The samples are first wrapped in a plastic bag to prevent any contamination from occurring before curing as shown in Figure 33.

Figure 33: Geopolymers cured at 21°C

The oven used, pictured in Figure 34, is a ventilated oven set to a temperature of 80 ºC. The oven is a dry environment with a negligible humidity.

Figure 34: Curing oven

3.6 Compressive strength testing

For compressive strength testing, a manually operated press, pictured in Figure 35, was used. It is a Cube Press- Foote test manufactured by Concrete Testing Equipment. The press has a load of 150 kN. The samples were crushed at a rate of 15 kN/min which is the standard for concrete units.

The press requires for the samples to be parallel on both ends to ensure an even distribution of load on the sample. Typically, a concrete cube is the mould used to manufacture concrete samples. These cubes are optimal because if the top surface of the cube is uneven, the sides adjacent to the top can will be even and the press load can be tested on those sides. In this instance however, cylinders were used which mean that only the top and bottom flat surfaces could be tested. The samples were thus shaved down with a grinder to achieve the even and parallel surfaces required. Upon crushing, foams were placed on either side of the samples for further precaution for even load distribution.

The use of the grinder and foam are not the typical and accepted compressive strength testing methods however the unavailability of necessary equipment such as the cube moulds resulted in their use. Section 4.2.1 below shows that samples are repeatable and that the result of using these unconventional methods did not have a major effect on the compressive strength results.

Figure 35: Compressive strength press

Figure 36: Porcelain crusher

3.7 Crushing

In preparation for XRD, XRF, TGA and FTIR analyses, the samples must be crushed down to a particle size 150 µm. This is done by using the porcelain crusher illustrated in Figure 36. Following crushing, the geopolymer is sieved to ensure the correct particle size.

3.8 Thermo-gravimetric Analysis (TGA)

The TGA machine used is a SC-TGA Instrument- SDT Q600 supplied by TA Instruments. The following specifications were used:

- Gas type: Argon
- Gas flow rate: 100 ml/min
- Heating rate: 10.3 mW
- Temperature range: 15 – 900 ºC
- Mass of sample: ~ 18 mg
- Sample particle size: < 150 µm

The samples are cooled after the experiment is executed with compressed air introduced into the heating chamber, flushing the system until the temperature is below 50ºC.

3.9 X-Ray Diffraction Analysis (XRD)

The samples were scanned after the addition of 20 % silicon for quantitative determination of amorphous content and micronizing in a McCrone micronizing mill. The samples were prepared for XRD analysis using a back loading preparation method.

Diffractograms were obtained using a Malvern Panalytical Aeris diffractometer with PIXcel detector and fixed slits with Fe filtered Co-Kα radiation. The phases were identified using *X'Pert Highscore plus* software.
The relative phase amounts (weight %) were estimated using the Rietveld method.

3.10 X-Ray Fluorescence Analysis (XRF)

The instrument used for the XRF analysis is PANalytical Axios Max.

6 g of lithium tetraborate and lithium metaborate at a ratio of 66:33 was added to 0.3 mg of each sample and then fused in a Eagon Furnace at 1 100 ºC. The sample was thereafter read against a set of standards which include WROXI and AMIS standards with the Axios Max which was calibrated for the purpose of determining the elemental composition of the fused beads.

3.11 Fourier Transform Infrared Analysis (FTIR)

FTIR results were prepared using the IRAffinity -1 Fourier Transform Infrared Spectrophotometer manufactured by Shimadzu.
The sample was prepared by adding potassium bromide before analysis in the IRAffinity machine.

3.12 SANS tests

The drying shrinkage and expansion on rewetting of the samples were conducted according to SANS 608/5:2006 and the determination of soundness according to SANS 50196-3:2006.
The samples were manufactured in bulk with the mix design shown in Table 23.

Table 23: Drying shrinkage and expansion on rewetting formulation

Product	Amount (g)
Fly ash	6 000
Fine aggregates	3 688
Coarse aggregates	8 605
Sodium silicate	2 143
Sodium hydroxide	857
Water (workability)	1 048
Total	**21 293**

CHAPTER 4: RESULTS AND DISCUSSION

4.1 Overview

The compressive strength results are discussed first in this chapter. Compressive strength analysis includes a set of 10 geopolymers to assess the repeatability of the formulations, the 3-, 7- and 28-day core strength test results are also discussed followed by the XRD, XRF, TGA and FTIR chemical analyses. The XRD and XRF results give information on the phase of the geopolymers formed and the fly ash used. This is helpful in understanding the reactions that took place and the effect of altering the sodium silicate to sodium hydroxide ratio. The TGA results are useful in determining the purity and stability of the geopolymers. Lastly, the FTIR results reveal the compounds in the geopolymers.

4.2 Compressive strength results

Compressive strength is the ability of a material to withstand compressive stress. This is an important and useful property in construction material as these materials are intended to resist stress.

The samples were tested for 3-, 7- and 28-day compressive strength. There are two sets of samples: The first set was manufactured with a 15 M sodium hydroxide solution in the activator while the second set was manufactured with a 10 M sodium hydroxide solution.

4.2.1 Repeatability

Before manufacturing the core samples for the study, 10 samples were made in order to ensure that results were repeatable. The ambient condition cured samples were manufactured with a 15 M sodium hydroxide concentration and 1.5 silicate to hydroxide ratio. The 7-day compressive strength results are illustrated in Figure 37.

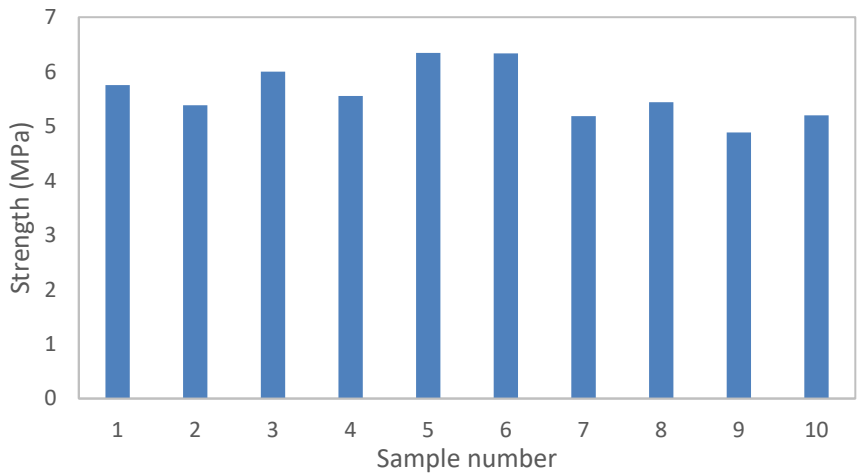

Figure 37: Compressive strength repeatability results

Statistical analysis on the compressive strength, density and mass of each of the samples is shown in Table 24. The following formulas were used to calculate the mean, standard deviation and coefficient of variance (Equations 15 – 17):

$$Mean = \frac{\sum x_i}{N} \quad (15)$$

where x_i = individual value, and N = number of samples = 10.

$$Standard\ deviation = \sqrt{\frac{\sum(x_i - \mu)}{N}} \quad (16)$$

where x_i = individual value, μ = mean value, and N = number of samples = 10.

$$Coefficient\ of\ variance = \frac{Standard\ deviation}{Mean} \quad (17)$$

Table 24: Compressive strength repeatability statistics

	Strength (MPa)	Density (kg/m^3)	Mass (g)
Mean	5.61	2008	104
Standard deviation	0.490	18.2	1.20
Coefficient of variance	0.088	0.009	0.012
Variance	Low	Low	Low

The variance is determined to be low if the coefficient of variance is lower than 1. The results show that there is low variance between the samples indicating that the formulation is repeatable. Since the average strength was 5.61 MPa, the characteristic strength is 4.8 MPa. All the samples are above this strength further indicating that the samples are repeatable.

4.2.2 Core compressive strength results

Table 25 depicts a sample guide that specifies the sodium silicate to sodium hydroxide ratio and curing conditions of each sample. Samples A, B and C were cured in an oven at 80°C for 6 hours and thereafter were stored at 21°C until compressive strength testing, while samples D, E and F were cured at 21°C throughout until testing.

Table 25: Sample guide

Sample name	Na_2SiO_3 : NaOH	Curing conditions
A	1.5	80°C, 6 hours
B	2.0	80°C, 6 hours
C	2.5	80°C, 6 hours
D	1.5	21°C
E	2.0	21°C
F	2.5	21°C

4.2.2.1 15 M sodium hydroxide concentration results

The compressive strength results for the samples that were manufactured with a 15 M sodium hydroxide solution in the activator are discussed here.

The compressive strength results of the first set are shown in Figure 38. Sample C is the best performing geopolymer, reaching a 28-day compressive strength of 23 MPa. Sample C has the highest sodium silicate to sodium hydroxide ratio (2.5) and was cured in the oven for 6 hours at 80 °C.

Sample F, which had the same sodium silicate to hydroxide ratio as Sample C but was not oven cured, had a 28-day compressive strength of 14 MPa. The effect of oven curing for this activator composition (2.5) therefore increases the compressive strength by 40%.

Sample B has the closest compressive strength to Sample C, 21 MPa. The effect of reducing the silicate to hydroxide ratio to 2 while keeping curing conditions the same reduced the strength by 11% while reducing the ratio from 2.5 to 1.5 reduced the strength by 31%.

Sample D is the poorest performing geopolymer. This sample has the lowest silicate to hydroxide ratio (1.5) and was not oven cured. The resulting 28-day compressive strength of 10.8 MPa, 1.38 MPa less than Sample A, which was oven cured. This corresponds to a 11%

difference. This difference indicates that the effect of the silicate to hydroxide ratio has a large impact on the compressive strength.

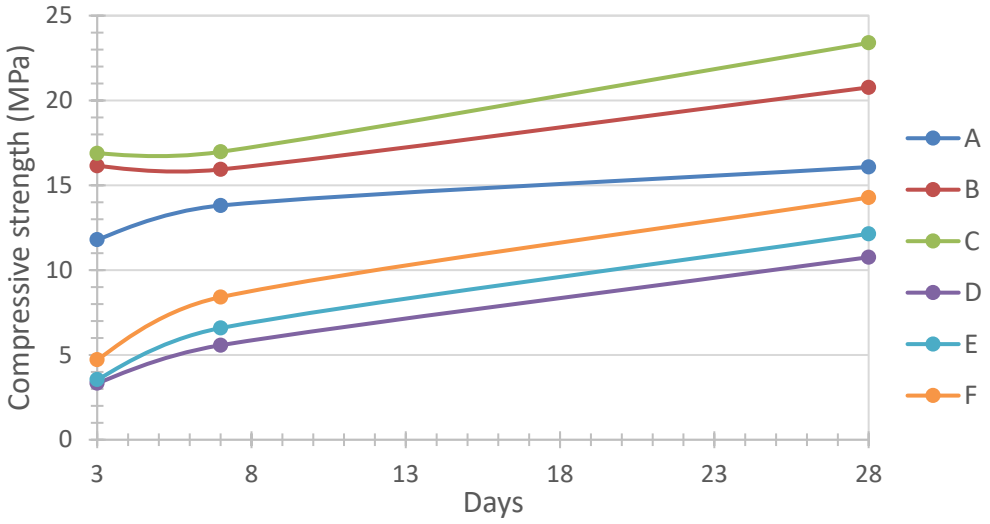

Figure 38: Compressive strength – 15 M sodium hydroxide concentration

4.2.2.2 10 M sodium hydroxide concentration results

Similar trends are seen in the sample set with a 10 M sodium hydroxide solution in the activator (Figure 39). Sample C achieved the highest 28-day compressive strength results with 15.9 MPa. This is equivalent to 66% of Sample C in the 15 M sodium hydroxide solution results. A notable difference in this set to the previous is Sample F, which was not oven cured, outperforming Sample A.

The best performing geopolymer in this set is also Sample C. This sample reaches a 28-day compressive strength result of 16 MPa. This is 30 % lower than Sample C in Set 1. The poorest performing geopolymer is Sample D again, further demonstrating that elevated curing conditions and a higher silicate to hydroxide ratio in the activator results in higher compressive strength results.

Unlike in Set 1, Sample F, which is not oven cured, has a higher compressive strength than Sample A. Sample F and A have 28-day compressive strength results of 12.2 MPa and 12 MPa respectively. This demonstrates that the effect of an increased silicate to hydroxide ratio results in comparable compressive strength values as samples that are oven cured but have a low silicate to hydroxide ratio.

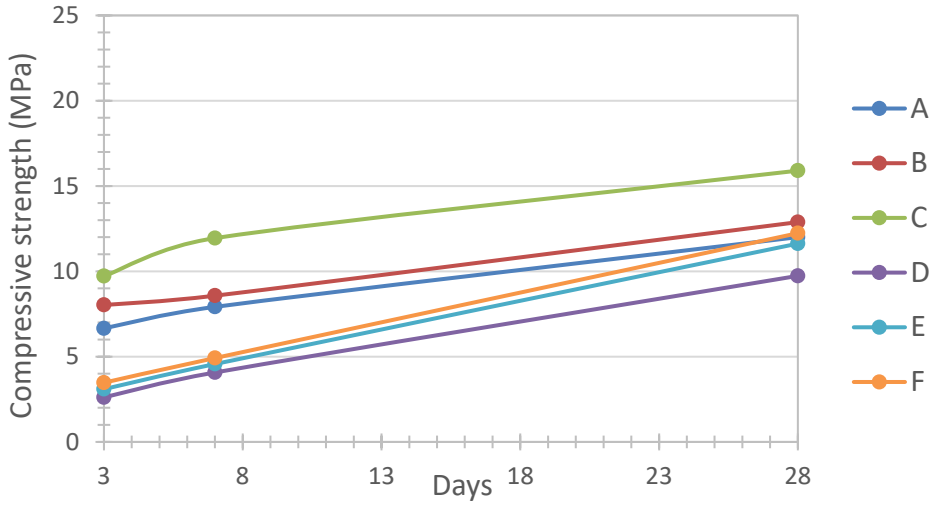

Figure 39: Compressive strength – 10 M sodium hydroxide concentration

4.2.2.3 Sodium hydroxide concentration

The concentration of the sodium hydroxide affects the amount of Al^{3+} and Si^{4+} ions released from the decomposition of the fly ash. The more ions are released, the more the process of geopolymerisation occurs resulting in a stronger geopolymer (Mustafa Al Bakri, et al. 2011).

Set 1, which has a sodium hydroxide concentration of 15 M, results in higher compressive strengths than Set 2 with a sodium hydroxide concentration of 10 M. Figure 40 compares the compressive strength of the samples manufactured in the same conditions but with different sodium hydroxide concentrations. It is seen that samples A, B and C, which were oven cured, show a larger strength difference than D, E and F. The effect of curing at elevated conditions therefore impacts the ability of the sodium hydroxide to dissolve the fly ash.

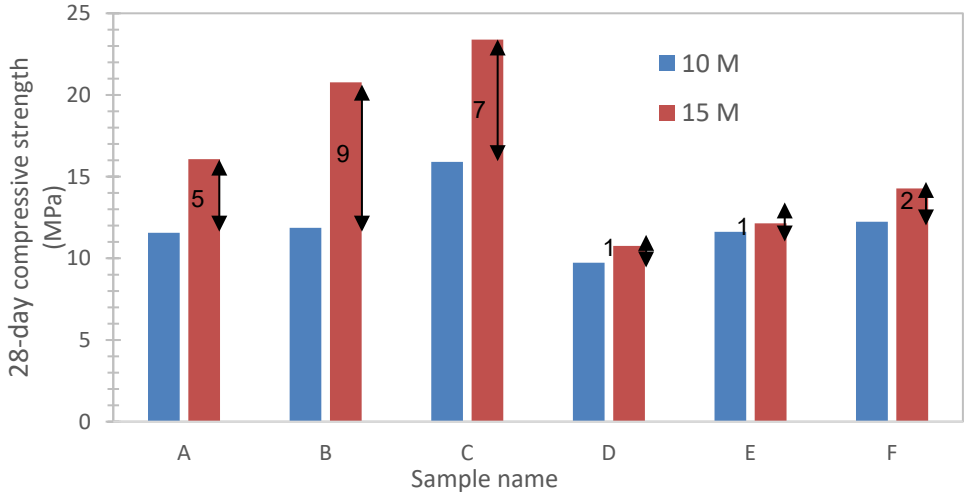

Figure 40: Sodium hydroxide concentration comparison

4.2.2.4 Sodium silicate to sodium hydroxide ratio

The addition of sodium silicate to the activator increases the number of silicon ions in the geopolymer which in turn increases the ratio of silicon to aluminium ions. A higher Si: Al ratio increases the number of -Si-O-Si- bonds which are stronger bonds compared to the -Si-O-Al- and -Al-O-Al- bonds that can be formed (Zhuang, et al. 2016). The stronger bonds therefore result in a higher compressive strength in the geopolymer. In addition to this, a high Si: Al ratio also causes a lower porosity and finer pore system (Zhuang, et al. 2016). A denser geopolymer therefore increases the amount of stress that it can withstand.

Figures 41 and 42 show the relationship between the sodium silicate to hydroxide ratio and the compressive strength of the cured and uncured samples respectively. The blue, red and green graphs grouped together were all subjected to the same curing conditions and hydroxide concentration but with different silicate to hydroxide ratios. The results confirm that the compressive strength increases as the silicate to hydroxide concentration increases.

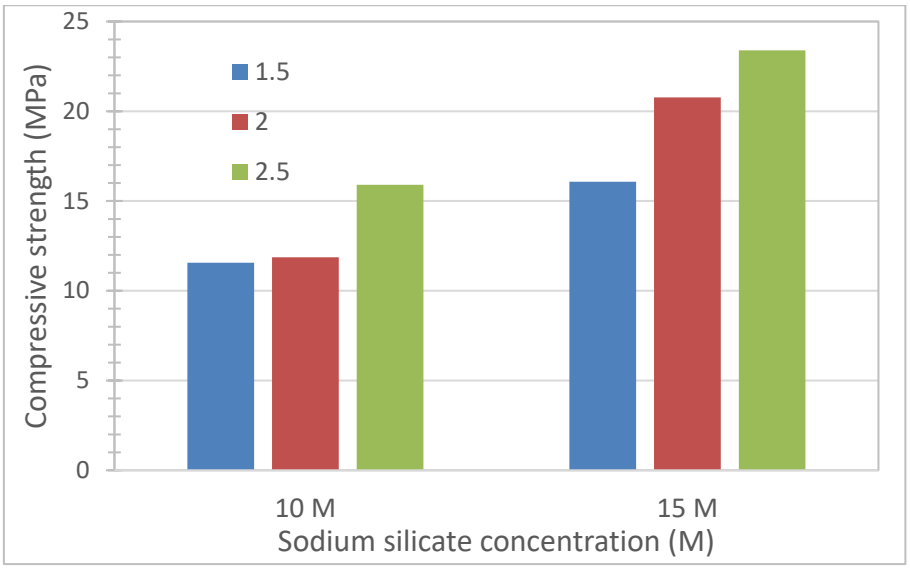

Figure 41: Effect of activator composition on oven cured samples

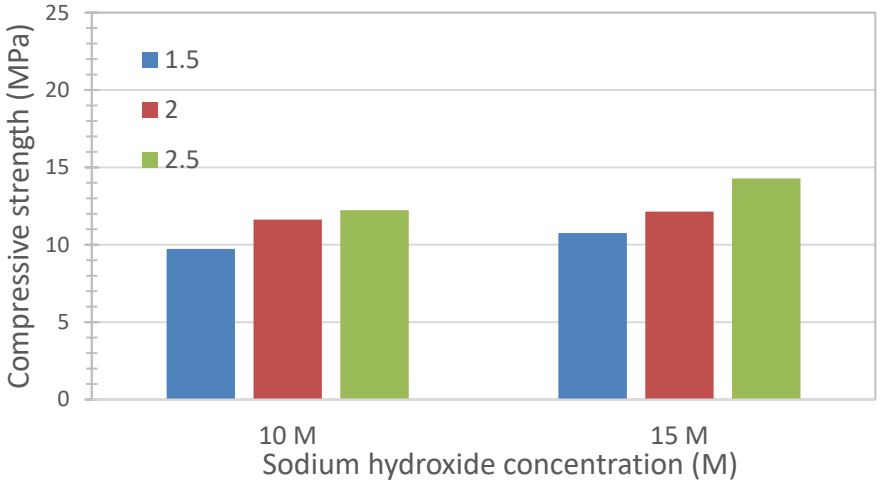

Figure 42: Effect of activator composition on uncured samples

The activator composition effect on compressive strength is quantified in Table 26 by assessing the increase in compressive strength between samples that were manufactured with a ratio of 1.5 and 2.5. The samples underwent the same conditions except for the difference in silicate to hydroxide ratio.

It can be observed that the oven cured samples result in an average increase of 5.5 MPa difference which translates to a 29 % increase, while the ambient cured samples average a 23 % increase. The results illustrate that the effect of curing affects the performance of the silicate to hydroxide ratio.

Table 26: Effect of silicate to hydroxide ratio

Curing conditions	Sodium hydroxide concentration (M)	Actual increase (MPa)	Percent increase (%)
Oven cured	10	4	27
	15	7	31
Ambient cured	10	2	20
	15	3	25

4.2.2.5 Curing conditions

Curing allows for the more reactivity in the fly ash which causes more dissolution of the ash and more Al^{3+} and Si^{4+} ions available to form a stronger geopolymer. Elevated curing temperatures directly after manufacturing the geopolymer also allows for the release of water which causes a less porous and denser geopolymer. This results in a product that is able to withstand greater compressive stress.

Figures 43 and 44 illustrate the difference in compressive strength for samples under the same conditions but with different curing conditions. There is a greater increase in compressive strength for samples that were manufactured with a 15 M sodium hydroxide concentration than 10 M. This is because the combination of curing at elevated temperatures and using a more concentrated sodium hydroxide solution allows for a greater dissolution of the fly ash which aids in the geopolymerisation process.

The average impact of oven curing samples for the first set (sodium hydroxide concentration of 15 M) increases the compressive strength by 38% while the second set averages a 14% increase in strength.

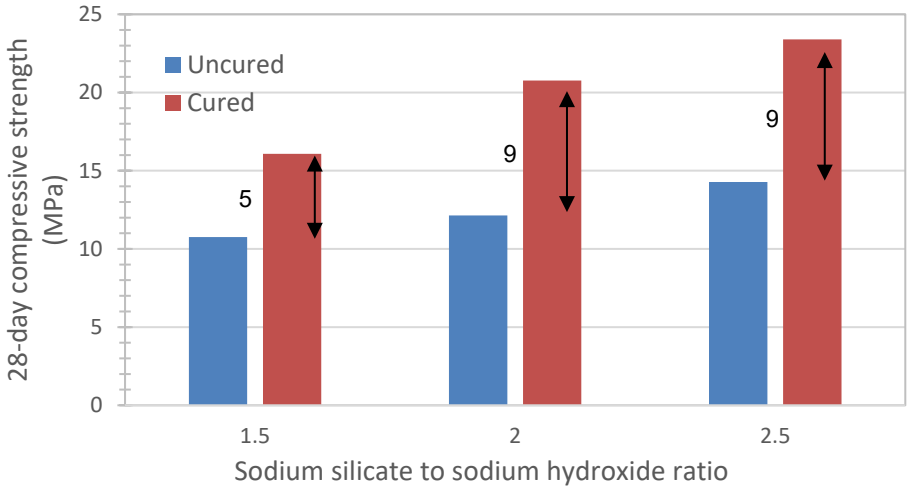

Figure 43: Oven cured vs uncured samples (Concentration$_{NaOH}$ = 15 M)

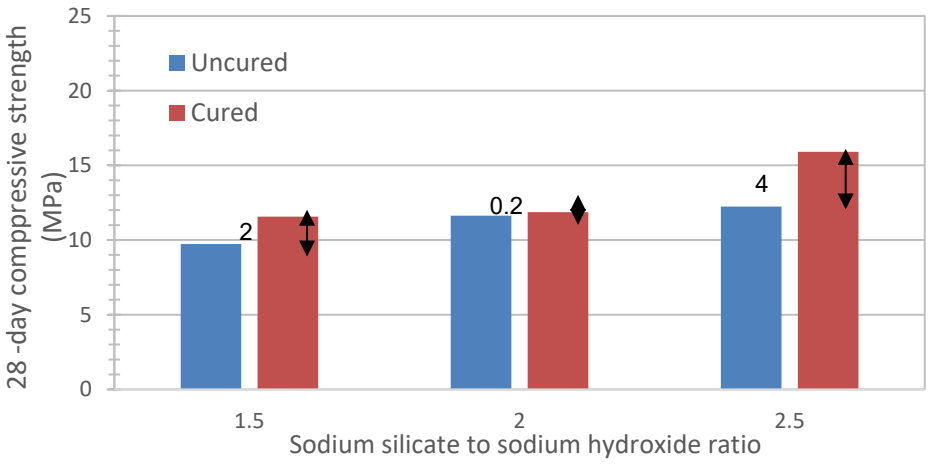

Figure 44: Oven cured vs uncured samples (Concentration $_{NaOH}$ = 10 M)

4.2.3 Confirmation samples

Samples of the best performing geopolymer, Sample C, which was manufactured using a sodium hydroxide concentration of 15 M and was oven cured, were evaluated to confirm the original compressive strength results. The strength results and statistical analysis are illustrated in Figures 45 and Table 26 respectively. The blue bars represent the original strength results while the green bars depict the confirmation sample results. The results show a low variance (coefficient of variance <1). The most variance is noted in the 28-day strength results where the confirmation samples on this day are notably higher than the original sample, averaging 27 MPa while the original sample reached 24 MPa.

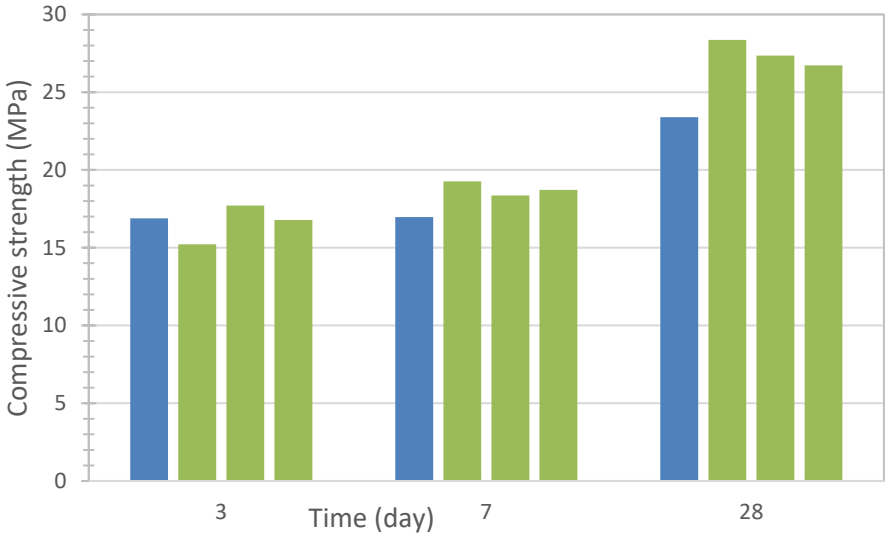

Figure 45. Strength confirmation results for best performing geopolymer.

Table 27: Statistical analysis of strength results for confirmation samples

	3-day	7-day	28-day
Mean (MPa)	16.6	18.8	27.5
Std. Dev.	1.04	0.97	2.15
Coef. Var.	0.063	0.052	0.078
Variance	Low	Low	Low
Characteristic Strength (MPa)	14.9	17.2	24

4.2.4 Compressive strength conclusion

The minimum 28-day curing compressive strength for concrete blocks, according to The Masonry Advisory Council, is 13 MPa, however, the average concrete block has a strength of 24 MPa (Turnbull Masonry 2019). Table 28 shows the samples that achieved a compressive strength higher than 13 MPa.

Five of the twelve samples that were manufactured have a compressive strength higher than 13 MPa however four more have a compressive strength of 12 MPa. It is evident from Figures 38 and 39 that the strength has not plateaued yet, indicating that a longer curing time would result in an increase in the geopolymer strengths.

Table 28: Conforming samples

Sample name	NaOH concentration (M)	Na_2SiO_3 : NaOH	Curing conditions	Compressive strength (MPa)
A	15	1.5	80°C, 6 hours	16
B	15	2.0	80°C, 6 hours	21
C	15	2.5	80°C, 6 hours	23
F	15	2.5	21°C	14
C	10	2.5	80°C, 6 hours	16

4.3 XRD and XRF results

The XRD and XRF results are shown in Tables 29 and 30 respectively. The samples were all manufactured with a sodium hydroxide concentration of 15 M. The sample guide in Table 25 gives more information on the conditions of manufacturing for each sample.

4.3.1 XRD

The XRD results show a decrease in mullite from the fly ash to the geopolymer. This is because mullite is the aluminosilicate source in the fly ash that is dissolved by the sodium hydroxide. The geopolymers have a consistent mullite content between 10 and 11 wt%. Sample B and C however have the lowest mullite content indicating that there was more mullite that dissolved by reaction. These two samples underwent oven curing, which as previously stated, aids the process of geopolymerisation and results in stronger geopolymers. As such, Samples B and C also have the highest 28-day compressive strengths at 21 and 23 MPa respectively.

The quartz content increase from 12 % in the fly ash to an average of 25 % in the geopolymers. The increase in quartz is associated with the increase in the sodium silicate added in the

activator and the addition of the fine and coarse aggregates. The aggregates constitute 61 % of the starting materials of which 70 % of that is river sand.

Paragonite and albite were not found in the fly ash however are formed in the geopolymers at low percentages. Paragonite is a derivative of muscovite while albite is a derivative of feldspar. These minerals are formed due to the excess silicon during manufacturing of the geopolymers when the sodium silicate is added and the mullite is broken down.

The amorphous phase decreases from 60 % in the fly to an average of 52 %. There is less amorphous phase in samples A and D at 45 and 49 % respectively. These two samples were manufactured with a silicate to hydroxide ratio of 1.5, the lowest ratio. A low ratio means that there was more sodium hydroxide and less sodium silicate used in the formation. The excess sodium hydroxide made way for zeolite crystal formation as opposed to geopolymers. Zeolite are hydrated aluminosilicate minerals (Gjyli, et al. 2021) that form when the fly ash is dissolved by the hydroxide ions, in the absence of sodium silicate, to form silicate and aluminium ions which precipitate to form the crystals (Rosas, et al. 2014).

The opposite is true for sample C which has the highest amorphous content. This sample was manufactured with a high silicate to hydroxide ratio (2.5) and was oven cured resulting in less crystal formulation and more amorphous polysialates which polymerise to form the geopolymer (Zhuang, et al. 2016).

Table 29: XRD results

	Fly ash	A	B	C	D	E	F
Mullite	26	11	10	10	11	12	11
Quartz	12	28	25	23	27	23	23
Hematite	2	1	1	1	1	1	1
Paragonite	-	6	3	4	4	5	5
Albite	-	9	7	7	9	4	7
Amorphous	60	45	55	56	49	55	53
Total	100	100	100	100	100	100	100

4.3.2 XRF

XRF results reveal two important factors in geopolymers: The Si: Al ratio and the calcium source content in the fly ash. These parameters affect the compressive strength of the geopolymers formed as well as the potential application of the geopolymer.

A higher Si: Al results in the formation of more Si-O-Si bonds as opposed to weaker Si-O-Al or Al-O-Al bonds (Zhuang, et al. 2016). These stronger bonds result in a stronger geopolymer. Accordingly, Sample C has the highest a Si: Al ratio and achieves the highest compressive strength (23 MPa). Conversely, Sample D has the lowest Si: Al ratio and had the lowest compressive strength (11 MPa). The Si: Al ratio also indicate the application that the geopolymer can be used for. The ratio averages 8.1 for all the samples, meaning that the geopolymers could potentially be used for bricks, fire protection, toxic waste confinement, heat resistance, foundry equipment, sealants from 200 ºC to 1 000 ºC and aeronautics tooling (Mustafa Al Bakri, et al. 2011).

The calcium source content in the fly ash promotes the formation of the $CaO\text{-}Al_2OH\text{-}SiO_2\text{-}H_2O$ gel. This gel causes a shorter setting time which decreases the porosity of the geopolymer formed, increasing the strength (Zhuang, et al. 2016). The expected calcium source content was 10 % because it was sourced from Kriel power station in Mpumalanga. The relatively low calcium content means that a longer setting time occurred, increasing the porosity of the geopolymers.

Table 30: XRF results

Sample name	A	B	C	D	E	F	Fly ash
SiO_2	62	63	64	61	61	63	62
Al_2O_3	20	20	19	21	21	21	24
Na_2O	6	6	6	7	6	6	1
CaO	5	5	5	5	5	5	6
Fe_2O_3	3	3	2	3	3	2	3
K_2O	1	1	1	1	1	1	1
MgO	1	1	1	1	1	1	2
TiO_2	1	1	1	1	1	1	1
Total	100	100	100	100	100	100	100
Si: Al	8.4	8.3	9.0	7.8	7.8	8.3	7.1

4.4 Thermogravimetric analysis

Thermogravimetric analysis is conducted on the samples in order to gauge the thermal stability of the samples. Figures 46 to 51 show the TGA graphs for each of the samples (A to F) that were manufactured with a sodium hydroxide concentration of 15 M. Each graph shows the percentage weight loss and the derivative thereof.

The weight loss occurring for the samples ranges between 8 and 10 % and is primarily associated with water loss. The samples that were oven cured (A – C) show a smaller weight loss. These samples each lost less than 8 % of the original weight. This is because of the evaporation of water that occurs when temperatures are elevated (Rosas, et al. 2014).

The first weight loss, which occurs between 30 and 100 ºC, is attributed to water molecule loss absorbed from the environment (Rosas, et al. 2014). Loss up to 200 ºC is from free water in the pores of the geopolymer (Ferone, et al. 2013). Finally, weight loss at temperatures between 200 and 500 ºC are caused by the loss of structural and bound water in the nanopores of the geopolymer (Ferone, et al. 2013).

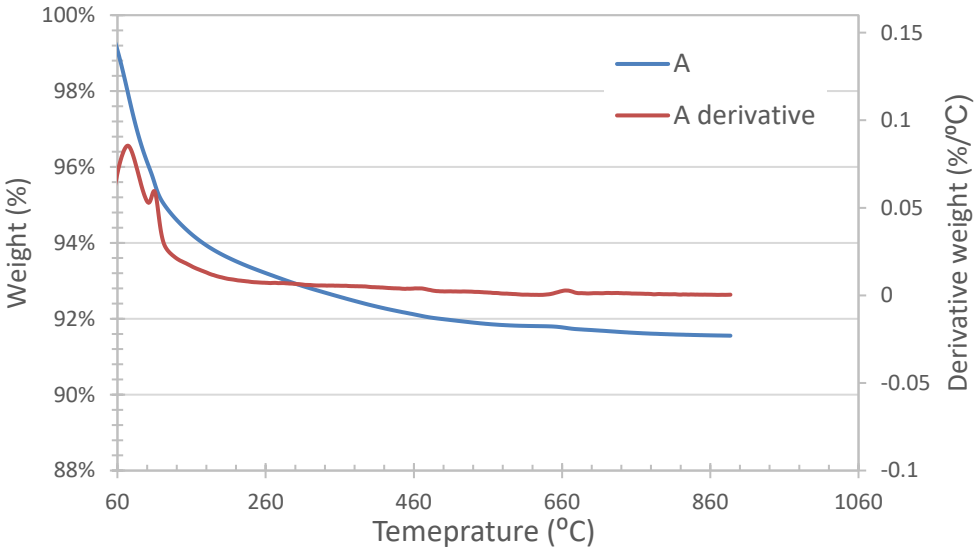

Figure 46: TGA - Sample A

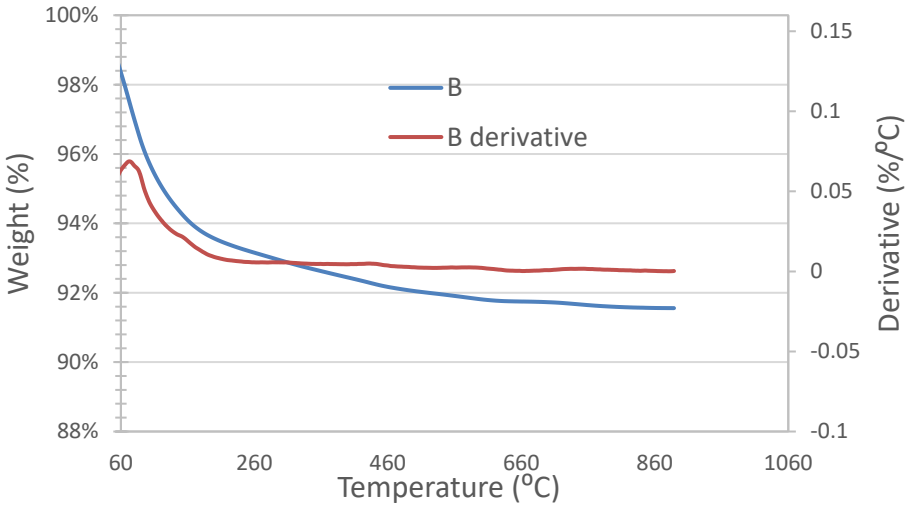

Figure 47: TGA - Sample B

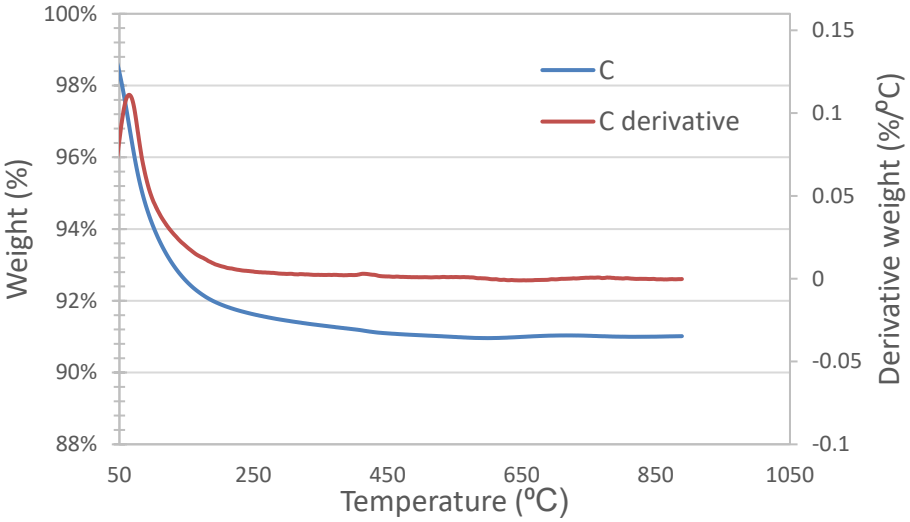

Figure 48: TGA - Sample C

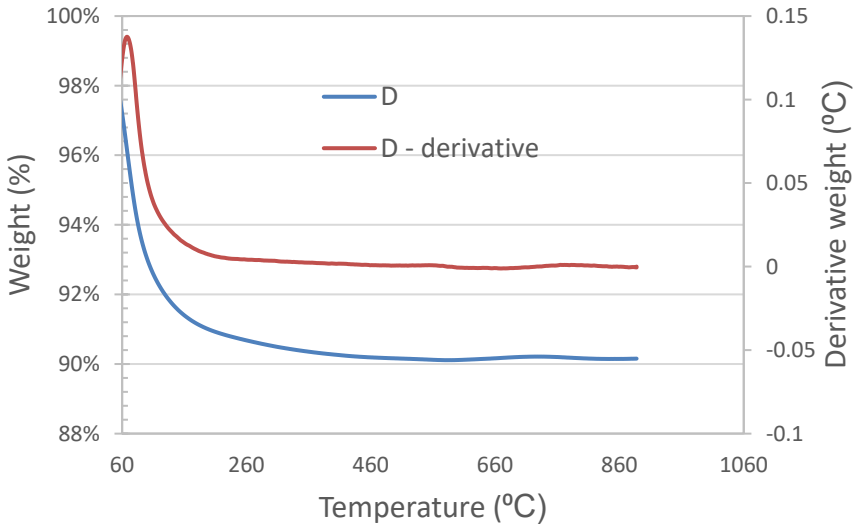

Figure 49: TGA - Sample D

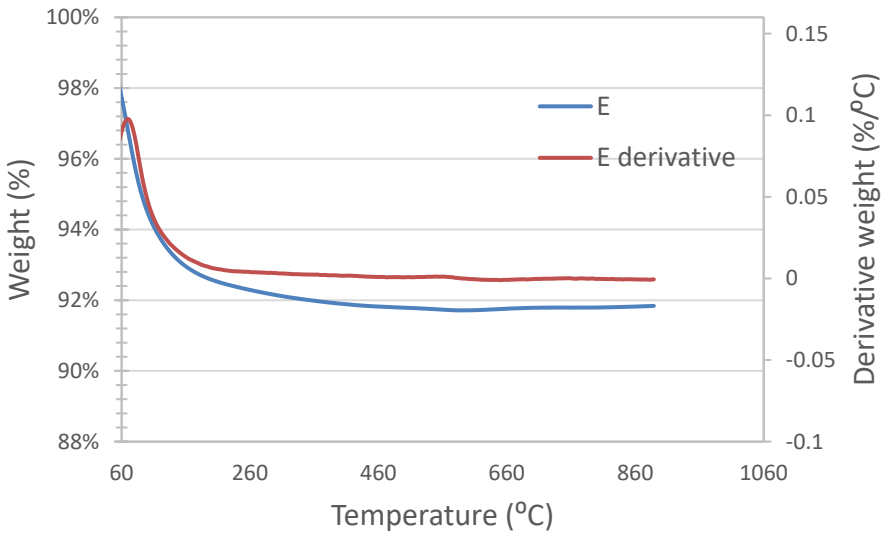

Figure 50: TGA - Sample E

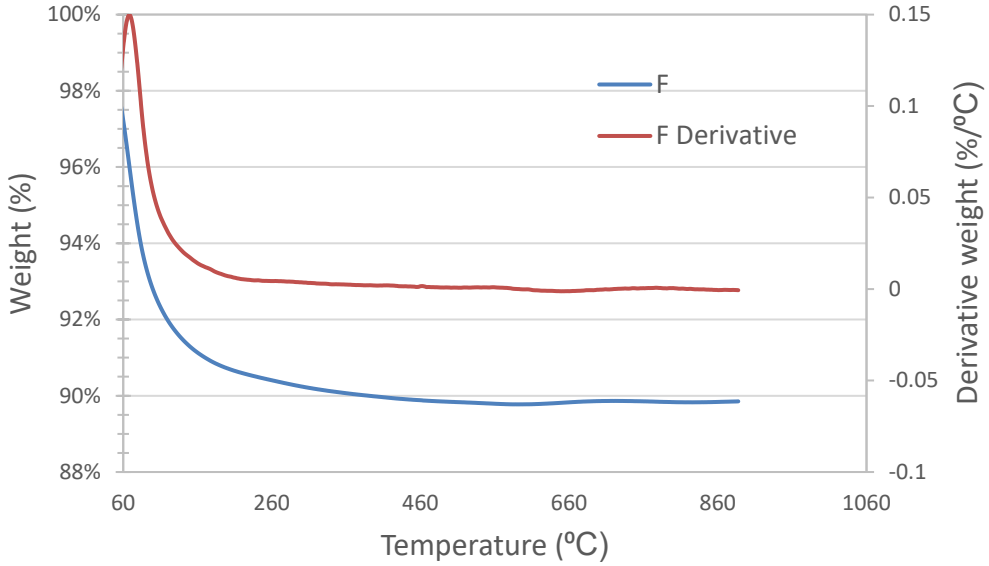

Figure 51: TGA - Sample F

4.5 Fourier-transform infrared spectroscopy

FTIR analysis assists in identifying the composition of the geopolymers. Table 31 shows the compounds found in the geopolymers. The graphs for each sample can be found in Appendix C.

Bands at 3 200 cm^{-1} are attributed to O-H bonds in the water molecules in the NASH gel that are formed (Alehyen, Achouri and Taibi 2017), bonds between water molecules and silanol groups (Rosas, et al. 2014) and water molecules in the ash (Samantasinghar and Singh 2019).

The bands at a frequency of 1 875, 1 650 and 1 425 cm^{-1} represent the presence of O-H bonds from water molecules and the NASH gel (Rosas, et al. 2014) (Samantasinghar and Singh 2019).

Finally, bands at a frequency of 1 000 cm^{-1} represent Si-O bonds found in the silica and from the aggregates as well as the mullite in the fly ash (Alehyen, Achouri and Taibi 2017) (Rosas, et al. 2014) (Samantasinghar and Singh 2019).

Table 31: FTIR results

Frequency (cm^{-1})	Frequency range (cm^{-1})	Bond type
3 200	3 000 – 3 400	O-H stretching
1 875	1 850 – 1 900	O-H stretching
1 650	1 600 – 1 700	O-H stretching
1 425	1 350 – 1 500	O-H bending
1 000	950 – 1 050	Si-O

4.6 Drying shrinkage, expansion on rewetting and soundness

Drying shrinkage, expansion on rewetting and soundness tests are required (SANS 1215) for concrete masonry units, in addition to compressive strength. Table 32 shows the limits for each of the tests conducted. Drying shrinkage should not exceed 600 microstrain and expansion on rewetting should not exceed the value of the drying shrinkage plus 200 microstrain. For soundness tests, there should not be an expansion greater than 2 – 5 mm.

Table 32: SANS 1215 limits

Test	Limit
Drying shrinkage	< 600 microstrain
Expansion on rewetting	< Drying shrinkage + 200 microstrain
Soundness	< two pop-outs of diameter 2 – 5 mm

The drying shrinkage and expansion on rewetting results are shown in Table 33 and 34 respectively. The tests were conducted on the three identical samples. Expansion on rewetting tests were conducted on the same samples that were used in the drying shrinkage testing.

Drying shrinkage results average a shrinkage of 6100 microstrain. The test results are unrealistic and fail the shrinkage test according to SANS 1215 by a factor of ten. The most

probable reason for this is a high water content in the samples (Wallah 2009). An increase in water content in a concrete paste by one percent will potentially cause an increase in shrinkage by 3% (Koratich 2021). This is because more capillary water is held in the pores and evaporates once the geopolymer cures, which causes more shrinkage (Wallah 2009).

Table 33: Drying shrinkage results

Day	Sample 1 (microstrain)	Sample 2 (microstrain)	Sample 3 (microstrain)
0	0	0	0
7	6 170	6 260	5 850
8	6 170	6 270	5 860

The expansion on rewetting results are significantly less than the drying shrinkage results. The average expansion on rewetting for the samples is 796 microstrain. These results correspond more to the SANS 1215 limits where the expansion should not exceed 200 microstrain of the shrinking limit of 600 microstrain, thus the maximum expansion should be ~ 800 microstrain, which corresponds to the value achieved.

Since the drying shrinkage results are out of specification, it is recommended that this test should be retested. Not only are the results out of specification, they also do not correspond to the expansion on rewetting results shown in Table 34.

Table 34: Expansion on rewetting results

Day	Sample 1 (microstrain)	Sample 2 (microstrain)	Sample 3 (microstrain)
0	767	844	759
2	770	848	770
3	770	848	770

The soundness test results reveal that there was an expansion of 2.5 mm on the samples with no pop-outs. This means that the geopolymers meet the specification stipulated by SANS 1215 for soundness testing.

CHAPTER 5: COST EVALUATION

5.1 Overview

A cost evaluation of the geopolymers is conducted in order to compare the cost of manufacturing with the price of cement bricks. The full calculations for each geopolymers can be found in Appendix D.

5.2 Assumptions

The following assumptions were made in the calculation of the cost for each geopolymer:

- The capital expenditure was not accounted for, only the cost of the raw materials per brick was considered.
- It is assumed that the oven can take samples to the capacity of 80 % of its volume.
- The unit cost of electricity and water in Isando, an industrial area in the south-west of Kempton Park, are assumed.

5.3 Results

The unit costs for each of the materials used is shown in Table 35. The table shows that the sodium silicate and sodium hydroxide, which make up the activator, have the highest unit cost.

Table 35: Unit costs of materials

Product	Unit cost (R/kg)
Fly ash	0.08
Sodium silicate	4.20
Sodium hydroxide	3.90
Fine aggregates	0.18
Coarse aggregates	0.20
Water	0.036

The oven curing cost calculations, which make up the electricity cost, are summarised in Table 36. The oven used 18 kWh of electricity to cure the samples A, B and C over 6 hours. This corresponds to R54.00. The oven allows for 188 bricks with a volume of 1.7 l (220 X 70 X 110 cm) to cure at the same time. The total cost of electricity for running the oven is therefore divided by the number of samples and the total cost of oven curing each brick is found to be 29 cents.

Table 36: Electricity calculations – oven curing

Unit	Amount
Power (kW)	3
Time (hrs)	6
Energy (kWh)	18
Cost (ZAR)	3
Electricity cost	54
Oven volume (L)	400
Sample volume (L)	1.7
Samples in oven	188
Electricity cost per sample (ZAR)	0.29

The price of concrete bricks ranges between R1.50 and R2.50 (Reynolds-Clausen 2021). Figure 52 shows the relationship between the compressive strength and the cost of manufacturing for each of the samples. The cost range for the samples that have a compressive strength higher than 13 MPa (above the black line) is R1.50 and R1.79. At a compressive strength higher than 13 MPa, these samples meet the minimum strength requirement for concrete bricks (Turnbull Masonry 2019).

On average, the activator (sodium silicate and sodium hydroxide) accounts for 70 % of the cost of manufacturing. The sodium silicate alone accounts for 60 % of the total manufacturing cost. The impact of increasing the amount of sodium silicate, i.e. increasing the sodium silicate to hydroxide ratio from 1.5 to 2.5, causes an average cost increase of 5.9 % while increasing the strength by 28 %.

When the sodium hydroxide concentration is increased, the total manufacturing cost increases by an average of 4 %, which translates to approximately R0.06, while the strength increases by an average of 29 %. Curing, the cost of electricity, accounts for R0.29 per sample, which is on average 27% of the cost of manufacturing. On the other hand, curing increases the strength by an average of 41%. These results show that increasing the parameters mentioned translates to a larger performance increase than the cost increase.

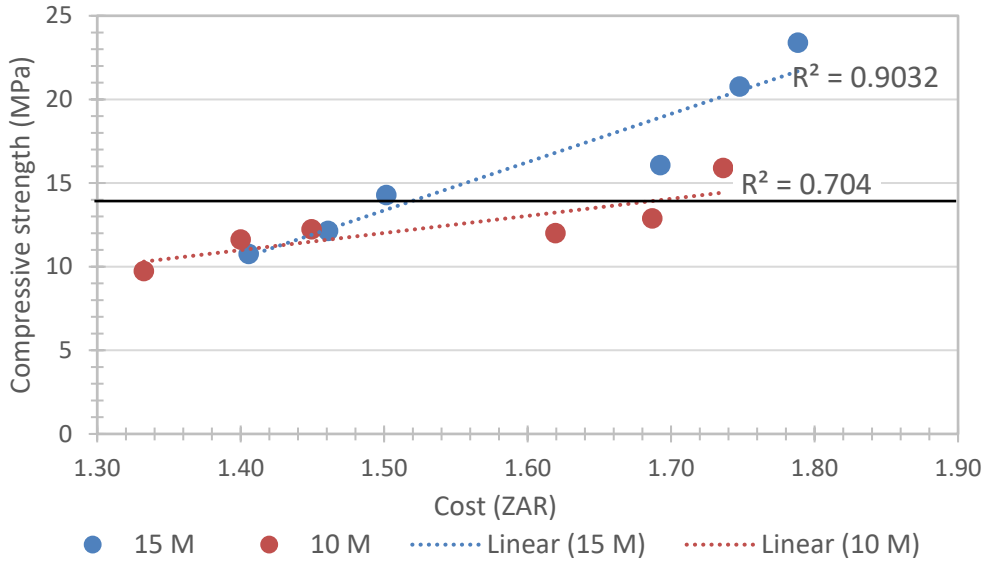

Figure 52: Cost of manufacturing vs 28-day compressive strength

CHAPTER 6: CONCLUSIONS AND RECOMMENDATIONS

6.1 CONCLUSIONS

The formulation used produces repeatable geopolymer that perform with similarly in terms of compressive strength, density and mass. The strongest geopolymer reaches a 28-day compressive strength of 23 MPa. This was manufactured with a sodium hydroxide concentration of 15 M and a sodium silicate to sodium hydroxide ratio of 2.5. The geopolymer was also cured at 80 ºC for 6 hours and thereafter 21 ºC until strength testing.

As expected from literature, an increase in sodium hydroxide concentration, sodium silicate to hydroxide ratio and curing conditions all increases the performance of the geopolymer. When the sodium hydroxide concentration in the activator is increased, the overall compressive strength increases by an average of 28% since a higher concentration assists in the decomposition of the fly ash. An increased sodium silicate to sodium hydroxide ratio results in more silicon ions involved in the geopolymerisation process which cause more Si-O-Si bonds in the geopolymer and therefore a higher compressive strength. The effect of curing increases the compressive strength by 38 % in samples that are manufactured with a 15 M sodium hydroxide concentration and 14 % in the set manufactured with a sodium hydroxide concentration of 10 M.

The XRD and XRF results show that the best performing geopolymer has the highest amorphous content and the highest Si: Al while the opposite is true for the geopolymer that achieved the lowest compressive strength. TGA results show an 8 to 10 % weight loss in the samples when constant heat is applied. The weight loss (between 0 and 200 ºC) is attributed primarily to the loss of water in the geopolymers. The samples that were oven cured show a smaller weight loss to the samples cured at 21 ºC throughout. The FTIR results show O-H bonds related to water molecules in the gel formed and the fly ash. The Si-O bonds are from the silica in the fly ash and the aggregates. The geopolymers failed the drying shrinkage tests according to SANS 1215 for concrete masonry units likely due to a high water content however the geopolymers passed the expansion on rewetting and the soundness tests.

The economic evaluation, which was based on material and electricity requirements of the geopolymers, showed that the cost of manufacturing a geopolymer was between R1.50 to R1.79. This is comparable to concrete brick prices which ranges between R1.50 and R2.50 per brick. The activator accounts for ~70 % of the cost of manufacturing, with sodium silicate alone accounting for 60 % of the manufacturing cost.

Overall, it can be concluded that the geopolymers produced are a viable way to make use of fly as an underutilised resource. Geopolymers can be utilised as replacements for concrete bricks since the compressive strength performance and cost for production are comparable to concrete bricks.

6.2 RECOMMENDATIONS

Since none of the samples achieved the target strength of 30 MPa, it is recommended that oven curing at increased temperatures and for longer periods it explored further. The effect of curing has a large impact on the compressive strength so there is potential for an increase in strength.

Fly ash composition varies significantly in different power stations. It is therefore recommended that different ash samples be used in geopolymer manufacture to assess the effects of the Si: Al ratio and calcium content on the performance of the geopolymer.

The most probable cause for the geopolymers failing the drying shrinkage test is excessive moisture in the samples. The amount of water added into the geopolymer for workability purposes in conjunction with slump test should therefore be investigated further.

Compressive strength was the only mechanical strength test conducted. It is recommended that the tensile and flexural strength tests also be conducted in order to get a broader understanding of the geopolymer strength performance.

The Si: Al ratio decreases the porosity of the geopolymers and therefore increases the compressive strength. Porosity of surface area measurements of the geopolymers such as BET (Brunauer, Emmett and Teller) tests should be conducted to confirm this.

REFERENCES

Alehyen, S, M EL Achouri, and M Taibi. 2017. “Characterization, Microstructure and Properties of Fly Ash based Geopolymer.” *Journal of Materials and Environmental Sciences* 8 (5): 1783-1796.

Bellum, Ramamohana Reddy, Ruben Nerella, Sri Rama Chand Madduru, and Chandra Sekhar Reddy Indukuri. 2019. “Mix Design and Mechanical Properties of Fly Ash and GGBFS-Synthesized Alkali-Activated Concrete (AAC).” *Infrastructures* 4 (20): 1 - 11.

Chandler, David L. 2019. “Researchers have created emissions-free cement.” 18 September. Accessed May 29, 2020. https://www.weforum.org/agenda/2019/09/cement-production-country-world-third-largest-emitter/.

Chemguide. 2020. *Acid-base behaviour of the period 3 oxides.* Accessed September 1, 2020. https://www.chemguide.co.uk/inorganic/period3/oxidesh2o.html#:~:text=Silicon%20dioxide%20reacts%20with%20sodium,of%20sodium%20silicate%20is%20formed.&text=This%20is%20also%20an%20example,dioxide%20reacting%20with%20a%20base.

Choi, Sung, and Kwang-Myong Lee. 2019. “Influence of Na2O content and Ms (SiO2/Na2O) of alkline activator on the workability and setting of alkali-activated slag paste.” *Materials* 2 (2072): 1-13.

Collins, A. C. 2019. *Extraction of K, Al and Ti containing compounds from ash produced by low temperature combustion.* MSc(Eng) dissertation, North West University (Potchefstroom).

Davidovits, Joseph. 2008. *Geopolymer Chemistry and Applications.* 5th. Saint-Quentin: Institut Geopolymere.

Deb, Partha Sarathi, Pradip Nath, and Prabir Kumar Sarker. 2015. “Drying shrinkage of slag based fly ash geopolymer concrete cured at room temperature.” *Procedia Engineering* 125: 594-600.

Department of Energy. 2020. *Coal Resources.* Accessed March 28, 2020. http://www.energy.gov.za/files/coal_frame.html.

Department of Environmental Affairs. 2018. *South Africa State of Waste Report.* Pretoria: Department of Environmental Affairs.

Department of Mineral Resources and Energy (DMRE). 2019. *Integrated Resource Plan 2019.* Pretoria: Department of Mineral Resources and Energy.

Department of National Treasury. 2014. *Carbon Offset Paper.* Pretoria: Department of National Treasury.

Dhadse, Sharda, P. Kumari, and L. J. Bhagia. 2008. “Fly ash characterization, utilization and Government initiatives in India - A review.” *Journal of Scientific and Industrial Research* 67: 11-18.

Eskom. 2021. *Ash Utilisation.* Accessed June 22, 2021. https://www.rotekindustries.co.za/productsandservices/EskomASH/Pages/default.aspx.

—. 2016. *Electricity Technologies.* Accessed March 28, 2020. http://www.eskom.co.za/AboutElectricity/ElectricityTechnologies/Pages/Coal_Power.aspx.

—. 2016. *Eskom and ash management.* Accessed March 10, 2020. http://www.eskom.co.za/news/Pages/Feb20.aspx.

Fakir, Saliem. 2018. “The Just Transition debate in South Africa.” 18 May. Accessed May 29, 2020. https://www.engineeringnews.co.za/article/the-just-transition-debate-in-south-africa-2018-05-18/rep_id:4136.

Federal Highway Administration. 2017. *Pavements.* Accessed March 29, 2020. https://www.fhwa.dot.gov/pavement/recycling/fach01.cfm.

Ferdous, M.W., O. Kayali, and A. Khennane. 2013. “A detailed procedure of mix desin for fly ash based geopolymer concrete.” *Fourth Asia-Pacific Conference on FRP in Structures (APFIS 2013).* Melbourne: International Institute for FRP in Construction.

Ferone, Claudio, Laura Ricciotti, Giuseppina Roviello, and Francecse Colangelo. 2013. “Synthesis and characterisation of novel epoxy geopolymer hybrid composites.” *Materials* 6(9): 3943-3962.

Garside, M. 2020. *South Africa's proved coal reserves 2011-2019.* Accessed September 3, 2020. https://www.statista.com/statistics/265445/proved-coal-reserves-in-south-africa/#:~:text=Its%20largest%20coal%20deposits%20are,two%20thirds%20of%20the%20country.

GroundUp. 2017. *Everything you need to know about government housing.* Accessed May 8, 2020. https://www.groundup.org.za/article/everything-you-need-know-about-government-housing/.

S. Gjyli, A. Korpa, V. Teneqja, D. Siliqi, C. Belviso. 2021. "Siliceous Fly Ash Utilization Conditions for Zeolite Synthesis." *Environmental Sciences Proceedings* 6(1): 1-8.

Hawa, Abideng, Danupon Tonnayopas, and Woraphot Prachasaree. 2013. “Performance Evaluation and Microstructure Characterization of Metakaolin-Based Geopolymer Containing Oil Palm Ash.” *The Scientific World Journal* 2013: ID 857586, 9 pp. doi: doi.org/10.1155/2013/857586.

Index Mundi. 2020. *Coal consumption by country.* Accessed March 15, 2020. https://www.indexmundi.com/energy/?product=coal&graph=consumption&display=rank.

International Energy Agency. 2019. *Data and statistics.* Accessed May 29, 2020. https://www.iea.org/data-and-statistics?country=WORLD&fuel=Energy%20supply&indicator=Electricity%20generation%20by%20source.

International Energy Agency. 2017. *IEA Atlas of energy.* International Energy Agency.

International Energy Agency. 2016. *Key World Eneergy Statistics.* International Energy Agency.

Jha, Vinay Kumar, and Gautam Prasad Budhamagar. 2012. “Synthesis of geopolymer from coal fly ash.” *Journal of Nepal Society* 30: 24-28.

Koratich, David. 2021. *Drying shrinkage.* Accessed November 1, 2021. https://www.engr.psu.edu/ce/courses/ce584/concrete/library/cracking/dryshrinkage/dryingshrinkage.html.

McSweeney, Robert, and Jocelyn Timperley. 2018. *The carbon brief profile: South Africa.* Accessed May 29, 2020. https://www.carbonbrief.org/the-carbon-brief-profile-south-africa.

Meyer, Winroe. 2020. *The evalution of coal pellets as alternative fuel for a semi-continuous coal stove.* Potchefstroom: North West University.

Mustafa Al Bakri, M. A., H. Kamarudin, M. Bnhussain, I. Khairul Nizar, and W. I. W. Mastura. 2011. “Mechanism and chemical reaction of fly ash geopolymer cement - a review.” *Journal of Asian Scientific Research* 1 (5): 247-253.

Nevada Ready Mix. 2021. *Flexural strength concrete - what, why, & how?* Accessed July 5, 2021. https://www.nevadareadymix.com/concrete-tips/flexural-strength-concrete/#.

Patankar, Subhash V, Yuwaraj M Ghugal, and Sanjay S Jamkar. 2014. “Mix design of fly ash based geopolymer concrete .” Kopargaon: Research Gate.

Patankar, Subhash V., Yuwaraj M. Ghugal, and Sanjay S. Jamkar. 2015. “Mix Design of Fly Ash Based Geopolymer Concrete.” *Advances in Structural Engineering.* New Dehli: Springer, New Delhi. 1619-1634.

Pavithra, P, M Srinivasula Reddy, Pasla Dinakar, B Hanumantha Rao, BK Satpathy, and AN Mohanty. 2016. “A mix design procedure for geopolymer concrete with fly ash.” *Journal of Cleaner Production* 113: 117-125.

Phoo-ngernkham, Tanakprn, Chattarika Phianghimai, Nattapong Damrongwiriyanupa, Sakowan Hanjitsuwan, Jaksada Thumrongvut, and Prinya Chindaprasirt. 2018. “A mix design procedure for alkali-activated high-calcium fly ash concrete cured at ambient temperature.” *Hindawi* 2018: 1-13.

Rajisha, KR, B Deepa, LA Pothan, and S Thomas. 2011. “Thermomechanical and spectroscopic characterization of natural fibre composites.” *Interface Engineering of Natural Fibre Composites for Maximum Performance* 241-274.

Ratshomo, Keneilwe, and Ramaano Nembahe. 2015. *Soith African Coal Sector Report.* Pretoria: Department of Energy.

Reynolds-Clausen, Kelley. 2021. *Optimisation of 3D printing of coal ash geopolymers.* Johannesburg: Eskom Holdings Limited.

Ribberink, JA. 2018. *Influence of moisture on the resistivity of selected South Africa fly ashes.* Potchefstroom: North West University.

Rodgers, Lucy. 2018. “Climate change: The massive CO2 emitter you may not know about.” 17 December. Accessed May 29, 2020. https://www.bbc.com/news/science-environment-46455844.

Rosas, Carlos Antonio, Jose Manuel Gomez-Soberon, Susana Paola Arredondo-Rea, and Jorge Almaral. 2014. “Experimental study of XRD, FTIR and TGA techniques.” *Internal Journal for Housing Science and its Applications* 221-226.

Rycroft, Mike. 2017. *EE Publishers.* Accessed March 30, 2020. https://www.ee.co.za/article/exploring-many-uses-fly-ash.html.

Sacramento State. 2019. *Waste and wastewater terms beginning A.* Accessed July 5, 2021. https://www.owp.csus.edu/glossary/absorption-capacity.php.

Samantasinghar, Subhashree, and Suresh Prasad Singh. 2019. “Fresh and hardened properties of fly ash-slag blended geopolymer paste and mortar.” *International Journal of Concrete Structures and Materials* 13 (47): 1-12.

Shekhovtsova, Julia, Maxim Kovtun, and Elsabe Kearsley. 2014. *Evaluation of short- and long-term properties of heat cured alkali-activated fly ash concrete.* Pretoria: Depratment of Civil Engineering, University of Pretoria.

Singh, Nakshatra B. 2018. “Fly-ash based geopolymer binder: a futire construction material.” *Minerals* 8 (7): 299.

Socio-Economic Rights Institute of South Africa. 2018. *Informal Settlements and Human Rights in South Africa.* May. https://www.ohchr.org/Documents/Issues/Housing/InformalSettlements/SERI.pdf.

Staden, AJ. 2019. *Influence of coal grade on the emissions performance of a semi-continuous coal stove.* Potchefstroom: North West University.

Statistics South Africa. 2016. *General Household Survey.* Pretoria: Statistics South Africa.

Turnbull Masonry. 2019. *Which is stronger - concrete blocks or conventional bricks?* 22 April. Accessed August 18, 2021. https://www.turnbullmasonry.com/stronger-concrete-blocks-conventional-bricks/.

Wallah, Steenie Edwrad. 2009. “Drying shrinkage of heat-cured flyash-based geopolymer conrete.” *Modern Applied Science* 3 (12): 14-21.

Wang, Hao, Thiry Aravinthan, and Tawfg Omar Omar. 2009. “Energy and emissions analysis of fly ash based geopolymers.” *SSEE 2009: Solutions for a Sustainable Planet.* Brisabane: Engineers Australia. 311-321.

We civil engineers. 2018. *What is slump and its types, values for various construction work.* Accessed September 3, 2020. https://wecivilengineers.wordpress.com/2018/04/05/what-is-slump-its-types-values-for-various-construction-work/.

Zhang, Haimei. 2011. “Cement.” In *Building materials in civil engineering*, edited by Haimei Zhang, 46-80. Woodhead Publishing.

Zhuang, Xiao Yu, Liang Chen, Sridhar Komareni, Chun Hui Zhou, Dong Shen Tong, Hui Min Yang, Wei Hua Yu, and Hao Wang. 2016. “Fly ash-based geopolymer: clean production, properties and application.” *Journal of Cleaner Production* 125: 253-267.

Zierold, Kristina M, and Chisom Odoh. 2020. “A review on fly ash from coal-fired power plants: chemical composition, regulations and health evidence.” *Rehabilitation and Health Services* 35 (4): 401-418.

Appendix A: Sodium silicate MSDS sheet

National Silicates
an affiliate of PQ Corporation

MSDS

MATERIAL SAFETY DATA SHEET

Trade Name: **N® Sodium Silicate Solution**
Date Prepared: **April 5, 2012** *Page:* **1 of 5**

1. CHEMICAL PRODUCT AND COMPANY IDENTIFICATION

Product name: **N® Sodium silicate solution**
Product description: **A 3.22 weight ratio sodium silicate, 37.5% solution in water**
Product Use: **Adhesive, binder, pulp & paper, water treatment, catalysts & gels**
Manufacturer: **National Silicates**
429 Kipling Ave
Etobicoke, ON M8Z 5C7
Phone number: 416-255-7771
Fax number: 416-201-4347
In case of emergency call: **1 416-255-7771**

2. COMPOSITION/INFORMATION ON INGREDIENTS

Chemical and Common Name	*CAS Registry Number*	*Wt. %*	*OSHA PEL*	*ACGIH TLV*
Water	**7732-18-5**	**62.5%**	**Not Established**	**Not Established**
Silicic acid, Sodium salt; Sodium silicate	**1344-09-8**	**37.5%**	**Not Established**	**Not Established**

3. HAZARDS IDENTIFICATION

Emergency Overview: **Clear to hazy, colorless, odorless, thick liquid. Causes moderate eye, skin, and digestive tract irritation. Spray mist causes irritation to respiratory tract. Due to high pH of product, release into surface water is harmful to aquatic life. Noncombustible. Spills are slippery. Reacts with acids, ammonium salts, reactive metals and some organics.**
Eye contact: **Causes moderate irritation to the eyes.**
Skin contact: **Causes moderate irritation to the skin.**
Inhalation: **Spray mist is irritating to respiratory system.**
Ingestion: **May cause irritation to mouth, esophagus, and stomach.**
Chronic hazards: **No known chronic hazards. Not listed by NTP, IARC or OSHA as a carcinogen.**
Physical hazards: **Dries to form glass film which can easily cut skin. Spilled material is very slippery. Can etch glass if not promptly removed.**

Appendix B: Sodium hydroxide MSDS sheet

LabChem
performance through chemistry

Sodium Hydroxide

Safety Data Sheet

according to Federal Register / Vol. 77, No. 58 / Monday, March 26, 2012 / Rules and Regulations

Date of issue: 07/06/1998 Revision date: 02/21/2018 Supersedes: 10/14/2013 Version: 1.1

SECTION 1: Identification

1.1. Identification

Product form	:	Substance
Substance name	:	Sodium Hydroxide
CAS-No.	:	1310-73-2
Product code	:	LC23900
Formula	:	NaOH
Synonyms	:	anhydrous caustic soda / caustic alkali / caustic flake / caustic soda, solid / caustic white / caustic, flaked / hydrate of soda / hydroxide of soda / LEWIS red devil lye / soda lye / sodium hydrate / sodium hydroxide, pellets

1.2. Recommended use and restrictions on use

Use of the substance/mixture	:	Industrial use
Recommended use	:	Laboratory chemicals
Restrictions on use	:	Not for food, drug or household use

1.3. Supplier

LabChem Inc
Jackson's Pointe Commerce Park Building 1000, 1010 Jackson's Pointe Court
Zelienople, PA 16063 - USA
T 412-826-5230 - F 724-473-0647
info@labchem.com - www.labchem.com

1.4. Emergency telephone number

Emergency number	:	CHEMTREC: 1-800-424-9300 or 011-703-527-3887

SECTION 2: Hazard(s) identification

2.1. Classification of the substance or mixture

GHS-US classification

Skin corrosion/irritation, Category 1A	H314	Causes severe skin burns and eye damage.
Serious eye damage/eye irritation, Category 1	H318	Causes serious eye damage.
Hazardous to the aquatic environment — Acute Hazard, Category 3	H402	Harmful to aquatic life

Full text of H statements : see section 16

2.2. GHS Label elements, including precautionary statements

GHS-US labelling

Hazard pictograms (GHS-US) :

GHS05

Signal word (GHS-US) : Danger

Hazard statements (GHS-US) : H314 - Causes severe skin burns and eye damage.
H402 - Harmful to aquatic life

Precautionary statements (GHS-US) : P260 - Do not breathe dust, vapours.
P264 - Wash exposed skin thoroughly after handling.
P273 - Avoid release to the environment.
P280 - Wear eye protection, face protection, protective clothing, protective gloves.
P301+P330+P331 - IF SWALLOWED: rinse mouth. Do NOT induce vomiting.
P303+P361+P353 - IF ON SKIN (or hair): Take off immediately all contaminated clothing. Rinse skin with water/shower.
P304+P340 - IF INHALED: Remove person to fresh air and keep comfortable for breathing.
P305+P351+P338 - IF IN EYES: Rinse cautiously with water for several minutes. Remove contact lenses, if present and easy to do. Continue rinsing.
P310 - Immediately call a POISON CENTER/doctor

Appendix D: FTIR graphs

Appendix C: Demoulding oil MSDS sheet

Viscol cc
Reg No: 1987/028096/23
Vat Reg: 4380103046

P.O Box 7182, Centurion, 0046
130 Sarelbaard Crescent
Gateway Industrial Park
Rooihuiskraal

Tel: (012) 661 9888
Fax: (012) 661 9882
E-mail: viscol@iafrica.com
Website: www.viscol.co.za

Document Number:

SDS 147

SUBJECT: SAFETY DATA SHEET

ENVIRONMENTAL & QUALITY MANUAL
(in accordance with ISO 9001 & 14001)

Viscol Nosol (VOC free Cement Tile Release Agent)

1. IDENTIFICATION OF THE SUBSTANCE/PREPARATION AND OF THE COMPANY/UNDERTAKING

Identification of substance/preparation
Viscol Nosol

Application
Base oil for blending lubricants
For specific application advice see appropriate Technical Data Sheet

Company Identification
Viscol cc, Reg.: 1987/028096/23
130 Sarel Baard Crescent
Gateway Industrial Park
Rooihuiskraal
Centurion
0167

Emergency Telephone Number
(012) 661 9888 (O/H)
(011) 331 2947

2. COMPOSITION/INFORMATION ON INGREDIENTS

Chemical name	CAS-No.	Weight%	EINECS No.
Distillates (petroleum), hydrotreated light naphthenic	64742-53-6	100.00	265-156-6

3. HAZARDS IDENTIFICATION

Classification: No classification needed according to 67/548/EC and 1999/45/EC.

Human Health: Inhalation of vapours and/or mists might irritate respiratory tract.
Prolonged skin contact will cause defatting and possible irritation.
Eye contact might cause irritation.

Appendix D: FTIR graphs

Appendix D: FTIR graphs

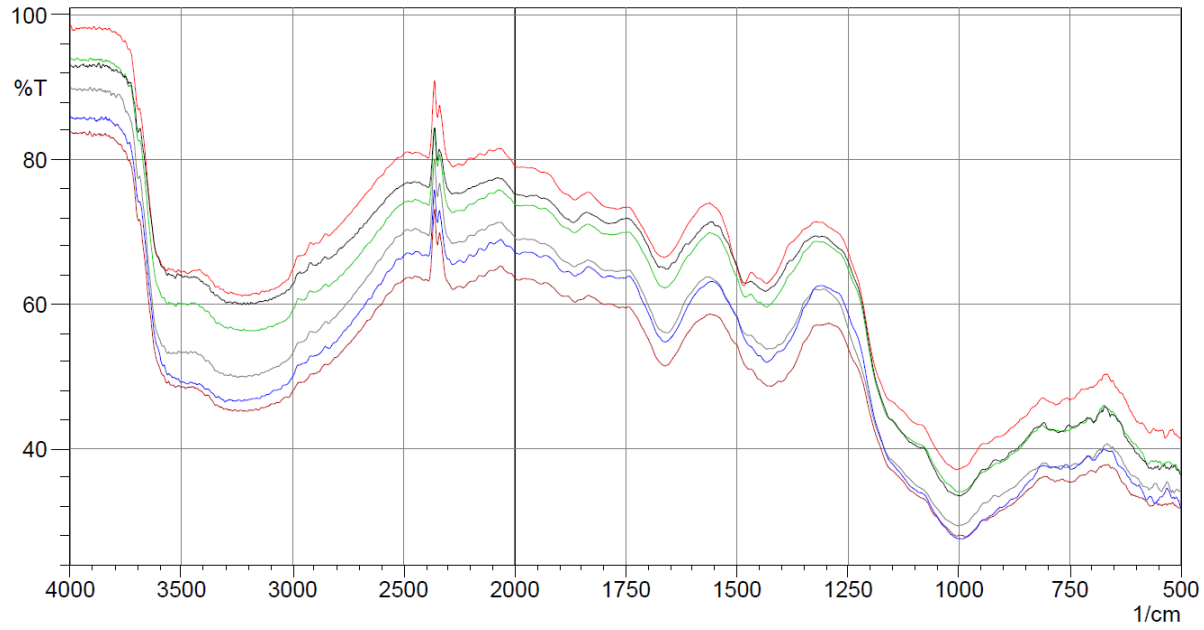

Figure 53: FTIR results - overlay

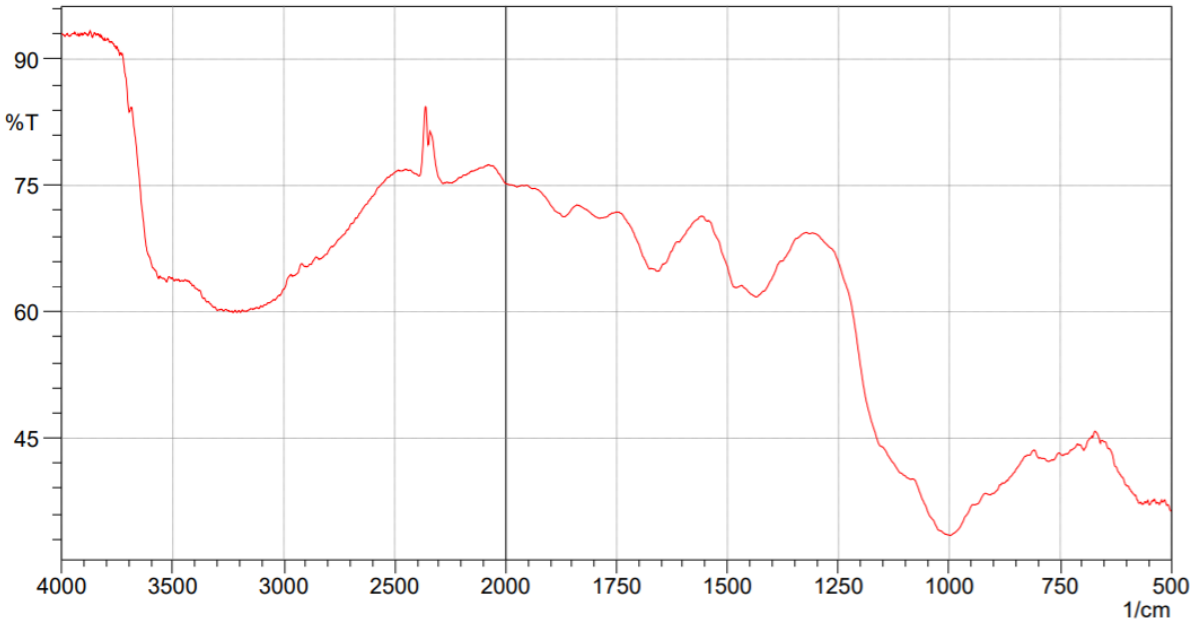

Figure 54: FTIR - Sample A

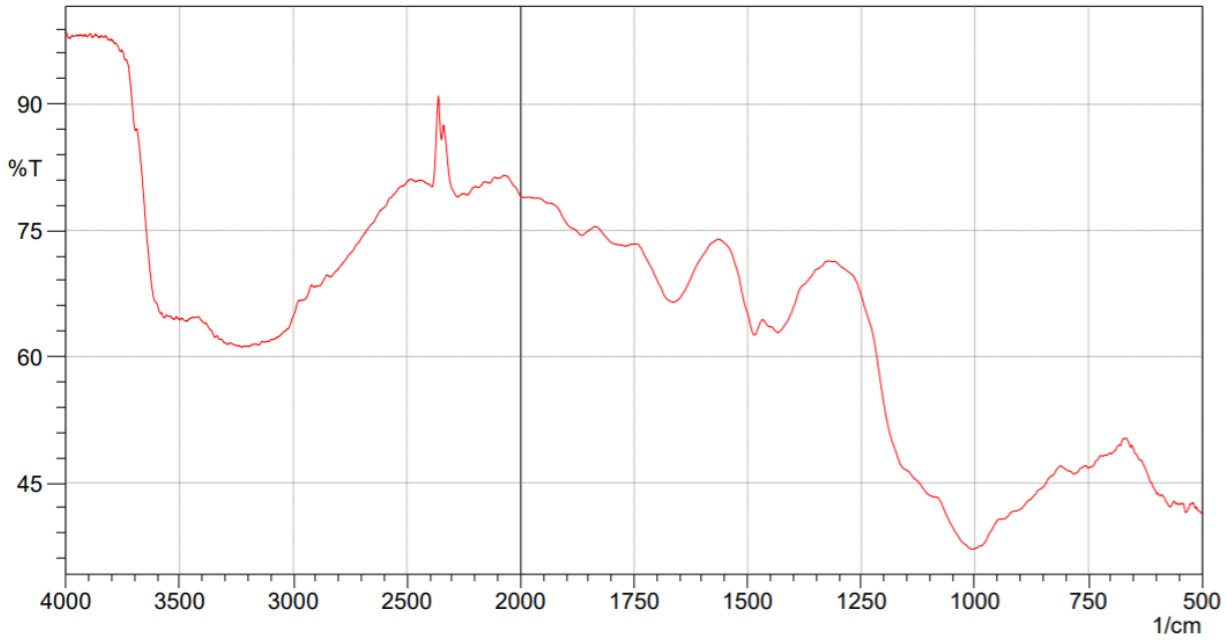

Figure 55: FTIR - Sample B

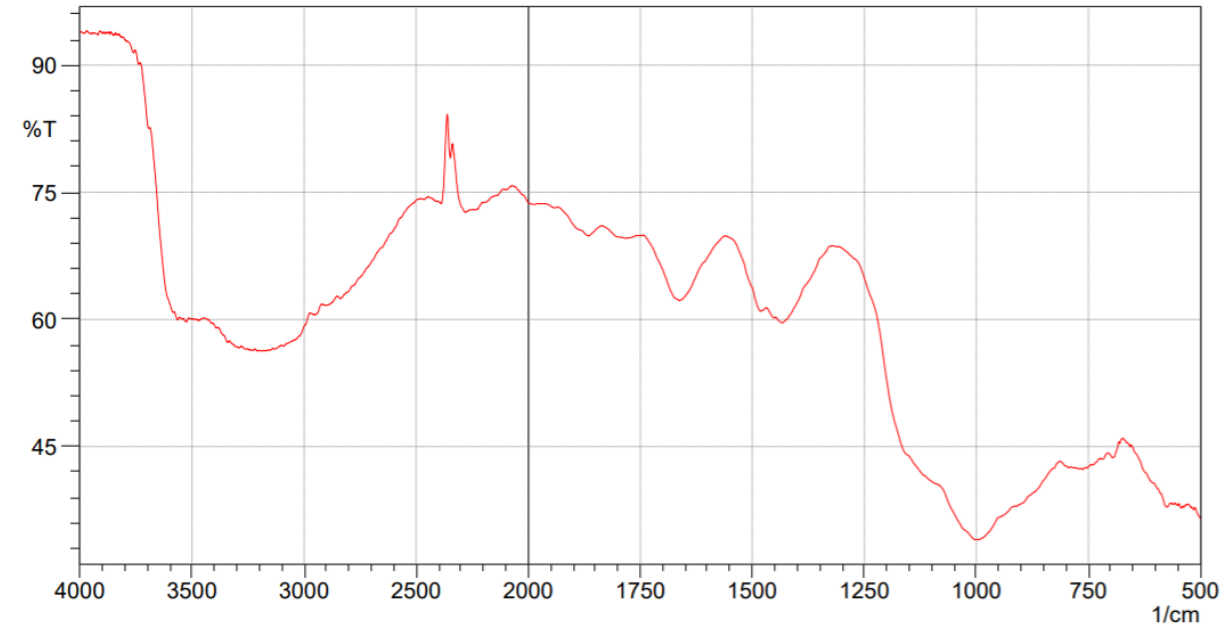

Figure 56: FTIR - Sample C

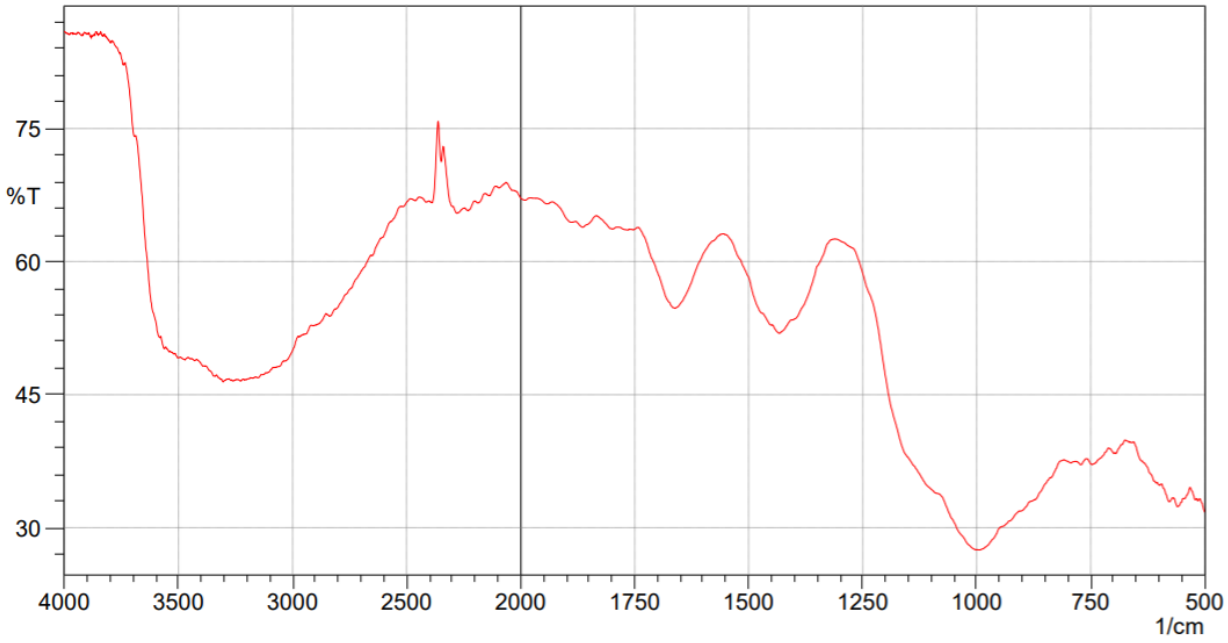

Figure 57: FTIR - Sample D

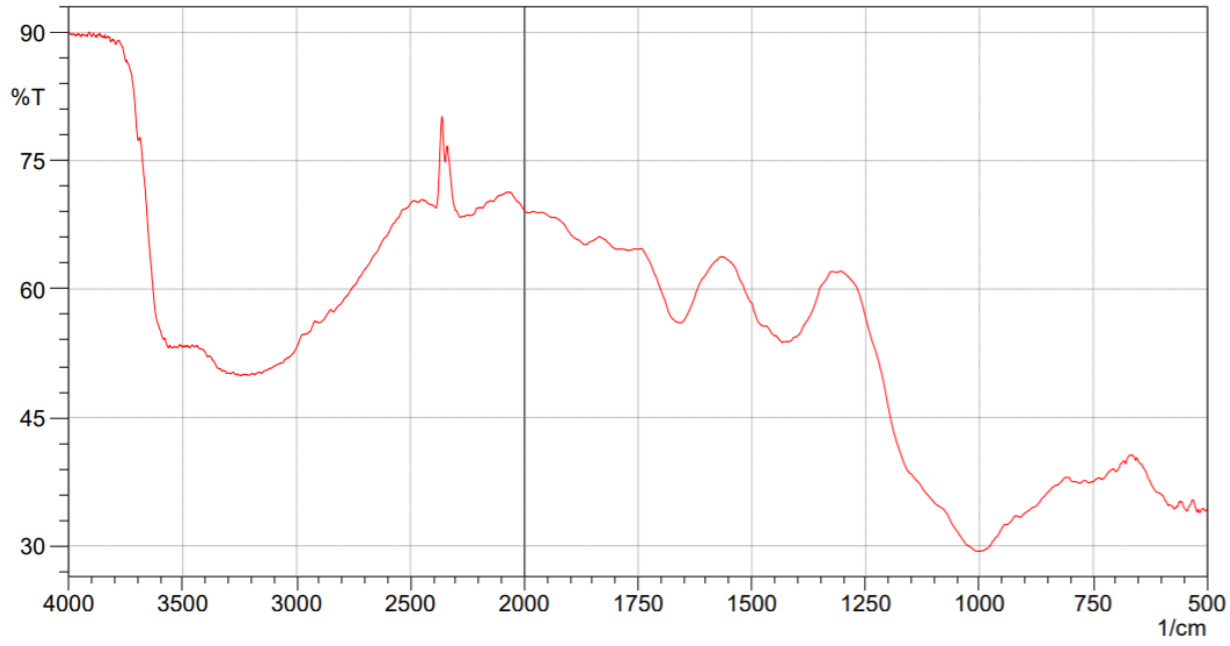

Figure 58: FTIR - Sample E

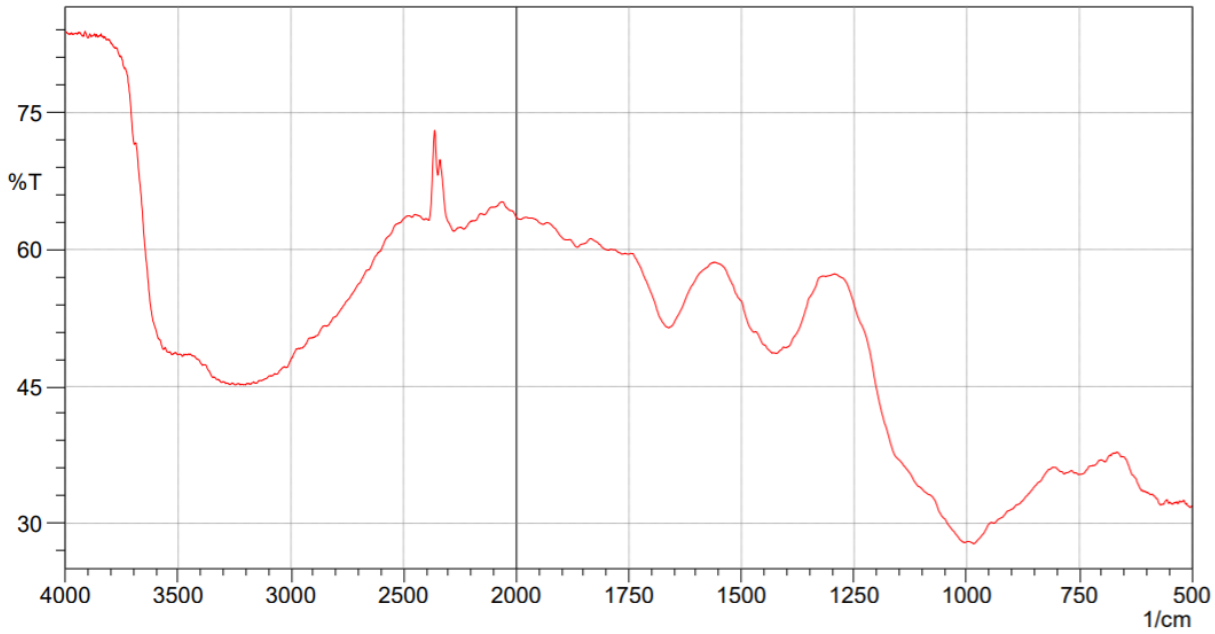

Figure 59: FTIR - Sample F

Appendix E: Drying shrinkage and soundness report

Beton-Lab cc

Tel: 011-979-1422 | Fax: 011-979-1430
e-mail: betonlab@absamail.co.za
32a Third Road, Bredell
PO Box 10583, Aston Manor, 1630

Tshiamo Geneke
1 Sydney Road
Boksburg

Report No: BLM3468 (final)
Date: 13th September 2021

TEST REPORT

1. **Sample description:**
   The following samples was received at the lab on the 16th August 2021 for testing as per client requirements.
   - Fly Ash
   - River Sand
   - Coarse aggregate
   - Sodium Hydroxide
   - Sodium Silocate

   The samples were received in sealed plastic bags and deemed suitable for testing.

2. **Test required and test method:**
   Initial drying shrinkage and wetting expansion of concrete – SANS 608/5:2006
   Determination of soundness – SANS 50196-3:2006

3. **Results:**
   The results are tabulated below:

   3.1 Initial drying shrinkage and wetting expansion of concrete – SANS 6085:2006

Shrinkage Measurement:	Expansion Measurement:
Individual values %	Individual values %
0.617	0.077
0.627	0.085
0.586	0.077
Mean = 0.610	Mean = 0.085
Range = 0.041	Range = 0.008

Note: Mix design not known to the lab. Mixes were done in the lab by the student.

3.2 Determination of soundness – SANS 50196-3:2006
Fly Ash = 2.5

A.D.R de Kock
Member

R de Lange
Report compiled by:

Appendix F: Cost evaluation calculations

Tables 37 and 38 represent the cost (ZAR) of each material to manufacture a geopolymer with the dimensions 220 X 110 X 75 mm.

Table 37: Cost evaluation (concentration $_{NaOH}$ = 15 M)

15 M	A	B	C	D	E	F
Fly ash (R)	0.05	0.05	0.05	0.05	0.05	0.05
Fine aggregates (R)	0.08	0.08	0.08	0.08	0.08	0.08
Coarse aggregates (R)	0.19	0.19	0.19	0.19	0.19	0.19
Sodium silicate (R)	0.86	0.95	1.02	0.86	0.95	1.02
Sodium hydroxide (R)	0.22	0.18	0.16	0.22	0.18	0.16
Water for NaOH solution (R)	0.003	0.003	0.002	0.003	0.003	0.002
Water for workability (R)	0.004	0.004	0.004	0.004	0.004	0.004
Electricity (R)	0.29	0.29	0.29			
TOTAL (R)	**1.69**	**1.75**	**1.79**	**1.41**	**1.46**	**1.50**

Table 38: Cost evaluation (concentration $_{NaOH}$ = 10 M)

10 M	A	B	C	D	E	F
Fly ash (R)	0.05	0.05	0.05	0.05	0.05	0.05
Fine aggregates (R)	0.08	0.08	0.08	0.08	0.08	0.08
Coarse aggregates (R)	0.19	0.19	0.19	0.19	0.19	0.19
Sodium silicate (R)	0.86	0.95	1.02	0.86	0.95	1.02
Sodium hydroxide (R)	0.15	0.12	0.10	0.15	0.12	0.10
Water for NaOH solution (R)	0.003	0.003	0.002	0.003	0.003	0.002
Water for workability (R)	0.004	0.004	0.004	0.004	0.004	0.004
Electricity (R)	0.29	0.29	0.29			
TOTAL (R)	**1.62**	**1.69**	**1.74**	**1.33**	**1.40**	**1.45**